The Standard Model to the Planck scale

Kyle Allison
Balliol College
University of Oxford

A thesis submitted for the degree of
Doctor of Philosophy
Trinity 2014

The Standard Model to the Planck scale

Kyle Allison, Balliol College

A thesis submitted for the degree of *Doctor of Philosophy*, Trinity 2014

Abstract

The lack of direct evidence for physics beyond the SM at the LHC has led some to reevaluate the need for such physics to solve the hierarchy problem. Instead, the notion that the SM, or something like it, is valid up to the Planck scale and that technical naturalness is sufficient for solving the hierarchy problem has been suggested. This thesis examines minimal extensions of the SM that address its phenomenological and theoretical shortcomings while avoiding new physics between the electroweak and Planck scales that introduces a hierarchy problem.

This thesis first studies two issues with the νMSM — an extension of the SM by three right-handed neutrinos — and their possible solutions. The first issue is the tension between dark matter production in the νMSM and constraints from the Lyman-α forest data. To avoid this tension, the νMSM is extended by a Higgs singlet ϕ and neutrino dark matter is produced through the decays of ϕ rather than through left-right neutrino mixing. It is shown that the hierarchical parameters of this model can arise from symmetries broken at or near the Planck scale for two specific examples: one in which ϕ stabilizes the electroweak vacuum and one in which ϕ is a light inflaton.

The second issue pertains to Higgs ξ-inflation. In the νMSM, a large non-minimal coupling ξ of the Higgs to gravity gives inflation but leads to a possible violation of perturbative unitarity below the inflationary scale. A study of Higgs ξ-inflation with $M_h \simeq 125$–126 GeV, for which the Higgs self-coupling λ runs to small values near the Planck scale, is carried out. It is shown that small λ can significantly reduce ξ required for inflation, but ξ cannot be small enough to address the possible unitarity issue. For small λ, a new region of Higgs ξ-inflation with a large tensor-to-scalar ratio r that is consistent with BICEP2 is discovered.

This thesis then studies the technical naturalness and cosmology of a model that addresses the strong CP problem. It is shown that a classically scale invariant DFSZ invisible axion model with a Peccei-Quinn scalar S, whose couplings to the SM are ultra-weak, can solve the strong CP problem and generate electroweak symmetry breaking via the Coleman-Weinberg mechanism. The ultra-weak couplings of S are natural due to an underlying approximate shift symmetry. The model contains a light pseudo-Goldstone dilaton that can be consistent with cosmological bounds while the axion can be the dark matter of the universe.

Finally, a summary of the thesis is presented and future research topics are suggested.

I would like to dedicate this thesis to my family, who have always been there for me, to my teachers and supervisors, who have opened my mind to new ideas, and to my friends, who have given me more experiences than I could have imagined.

Acknowledgements

First of all, I would like to thank my supervisors Graham Ross and Subir Sarkar for their invaluable contributions to this work. From suggesting areas of research to giving input on presentations to reviewing written papers, I have benefited greatly from their experience. Their guidance has made this possible.

I would also like to thank the fellow D.Phil. students and postdoctoral researchers in the department for the many conversations we have had. They have shown true patience in answering my many questions about physics, and the working environment in Oxford would not have been as inspiring or productive without them.

As an early stage researcher in the Marie Curie Initial Training Network ("Unification in the LHC era", PITN-GA-2009-237920), I would like to acknowledge the generous financial support of the European Commission. The funding has enabled me to pursue this degree and to travel to many conferences and summer schools over the last four years.

Finally, I am immensely grateful to my family for their complete support during my time away from home and to the friends I have made in the UK and around the world. Together they have made this experience an exceptional one.

Contents

List of Figures

List of Tables

Chapter 1

Introduction

The Standard Model (SM) — defined as the renormalizable quantum field theory (QFT) based on the SU(3)×SU(2)×U(1) gauge group with three generations of chiral fermions (excluding right-handed neutrinos) and one Higgs doublet — does remarkably well in fitting the large collection of precision measurements in high energy physics. Other than a small number of discrepancies at the few-σ level [1–3] and, in a strict sense, the observation of neutrino oscillations, results from the Large Hadron Collider (LHC) and other direct experimental tests of the SM are in excellent agreement with the predictions of the SM. Moreover, no direct evidence for supersymmetry (SUSY), technicolour, large extra dimensions, or any of the other well-motivated beyond the SM (BSM) theories has been observed up to the energy scales probed to date.

1.1 Evidence for BSM physics

That is not to say there is no indirect evidence for BSM physics. There are a number of issues that the SM cannot explain in a satisfactory way and for which new physics is likely required. It is useful to distinguish between two types of evidence for BSM physics: phenomenological evidence, which encompasses results that cannot be explained within the SM, and theoretical considerations, which vary from the desire to explain fine-tuned parameters in the SM to the aesthetic appeal of certain underlying symmetries of nature.

1.1.1 Phenomenological evidence

From a phenomenological point of view, several results suggest that the SM is incomplete. The strongest evidence for BSM physics includes:

Neutrino oscillations

Many reactor-based and atmospheric neutrino experiments have confirmed that oscillations of the three neutrino flavours take place (see [4] and references therein). Neutrino oscillations imply that neutrinos are massive with a misalignment of their weak and mass eigenbases [5]. A recent fit to the oscillation parameters gives [6]

$$\Delta m^2_{\rm sol} \simeq 7.5 \times 10^{-5}\ {\rm eV}^2, \qquad \left|\Delta m^2_{\rm atm}\right| \simeq 2.4 \times 10^{-3}\ {\rm eV}^2, \tag{1.1}$$

where the sign of $\Delta m^2_{\rm atm}$ is not yet known and is related to whether the neutrino mass spectrum is normal or inverted. The physics that is responsible for generating neutrino masses is, in a strict sense, BSM physics if one assumes the SM is defined with massless neutrinos. It is also argued that neutrino masses cannot come from Planck-scale physics since the lowest Planck-suppressed operator that is capable of generating neutrino masses,

$$\mathcal{O}_5 = A_{\alpha\beta}\left(\bar{L}_\alpha \tilde{H}\right)\left(H^\dagger L^c_\beta\right), \qquad \mathcal{L} = \mathcal{L}_{\rm SM} + \sum_{n=5}^{\infty} \frac{\mathcal{O}_n}{M_{\rm Pl}^{n-4}}, \tag{1.2}$$

leads to neutrino masses on the order of $m_\nu \sim v^2/M_{\rm Pl} \sim 10^{-6}$ eV [7]. This is much smaller than the mass scale $m_\nu \gtrsim \sqrt{\Delta m^2_{\rm sol}} \sim 10^{-2}$ eV required by neutrino oscillation experiments.

Dark matter

Numerous cosmological results indicate that a sizable component of the universe's energy density is in the form of non-baryonic dark matter (see [8] and references therein). Evidence for dark matter can be found in the rotation curves of spiral galaxies [9], gravitational lensing in galaxy clusters [10], and structure formation inferred from the cosmic microwave background (CMB) [11, 12]. The *Planck* 2013 fit of the cosmological parameters gives a value for $\Omega_{\rm DM}$, the dark matter abundance as a fraction of the total energy density today, of [12]

$$\Omega_{\rm DM} h^2 \simeq 0.12, \tag{1.3}$$

where $h \equiv H_0/(100\ ({\rm km/s})/{\rm Mpc}) \simeq 0.7$. Although the existence of dark matter is well established, the SM does not contain a particle candidate that satisfies the properties of dark matter,[1] and it is generally agreed that cosmological objects such as primordial black

[1] Massive neutrinos behave as hot dark matter (HDM), but the energy density in left-handed (active) neutrinos is too small to be all of the dark matter [13, 14]. Observations of small scale structure and numerical simulations of structure formation also disfavour an entirely HDM scenario.

holes are disfavoured as dark matter candidates [15]. The majority of proposed dark matter candidates are new particles that appear in BSM physics,[2] with examples including neutralinos [19, 20] and other weakly-interacting massive particles (WIMPs), singlet scalar dark matter [21, 22], axions [23–25], and right-handed neutrinos [26]. Whatever dark matter is, its origin likely involves BSM physics.

Baryon asymmetry

The observed abundance of baryonic matter in the universe is about 10^9 times larger than the relic abundance expected for a state in thermal equilibrium [27]. It is therefore necessary to have a large primordial asymmetry between baryons to anti-baryons to prevent their mutual annihilation. This in turn requires some out-of-equilibrium process that violates baryon number (B), charge conjugation (C), and charge parity (CP) — conditions that are collectively known as the Sakharov conditions [28] — to dynamically generate the baryon asymmetry. In the SM, processes during a first-order electroweak (EW) phase transition involving CP-violating scattering and baryon number violating sphalerons satisfy the Sakharov conditions and can, in principle, produce a sufficiently large baryon asymmetry [29–31]. However, the lack of a first-order EW phase transition for the measured Higgs mass [32, 33] prevents the realization of such a scenario [34].[3] Therefore some BSM physics must be responsible for producing the primordial baryon asymmetry of order [4]

$$\eta \equiv \frac{n_{\rm b}}{n_\gamma} \simeq 6 \times 10^{10}, \tag{1.4}$$

where $n_{\rm b}$ and n_γ are the number densities of baryons and photons, respectively. Proposed models for the baryon asymmetry production include Grand Unified Theory (GUT) baryogenesis [38],[4] Affleck-Dine baryogenesis [42], EW baryogenesis from the decay of heavy right-handed neutrinos [43] or neutrino oscillations [44], and many others.

[2] Interestingly, modified Newtonian dynamics (MOND) [16] offers an empirical solution to the dark matter puzzle that does not involve new particles. Instead, it proposes a modification of the classical $1/r^2$ gravitational interaction at very small accelerations $a \lesssim 10^{-8}$ cm/s^2. MOND does quite well in reproducing the rotation curves of galaxies but fails on the level of galaxy clusters [17]. It has also proven difficult to formulate a underlying relativistic theory for MOND [18].

[3] Moreover, CP violation in the SM may not be sufficiently large to produce the required baryon asymmetry even with a first-order EW phase transition [35–37].

[4] If the GUT is supersymmetric, GUT baryogenesis faces a problem with the overproduction of relic gravitinos for the large reheat temperature $T_{\rm reh} \gtrsim \Lambda_{\rm GUT}$ required by the model [39]. However, a stage of pre-heating after inflation may rescue the scenario [40, 41].

Inflation

A period of inflation in the early universe provides an elegant explanation for the flatness, isotropy, and homogeneity of the universe today [45–49]. Moreover, it provides a very plausible mechanism for generating the nearly scale invariant spectrum of primordial density fluctuations that are inferred through the CMB [11, 50].[5] Although many details of inflation are unknown, a period of inflation is generally assumed to have occurred. A large number of inflationary models that extend the scalar degrees of freedom in the SM have been proposed (see [52, 53] for an overview), and for some time it was thought that no scalar field in the SM could be the inflaton. Recently, though, there have been a number of proposals in which the Higgs boson may be the inflaton [54–63]. Most of these models involve specific forms of Higgs couplings to gravity, which rely heavily on assumptions about the ultraviolet (UV) completion of gravity, or have other issues that require some BSM physics for their resolution. If there is no viable scenario in which the SM Higgs boson alone can be the inflaton, inflation provides a strong indication of BSM physics.

1.1.2 Theoretical considerations

From a theoretical point of view, the clearest evidence of the need for BSM physics is arguably that the SM does not include gravity. Gravity inevitably affects particle physics at the reduced Planck scale $M_{\rm Pl}/\sqrt{8\pi} \simeq 2.44 \times 10^{18}$ GeV or below, but since gravity is non-renormalizable it is not a valid QFT in the usual sense. Some fundamentally new physics is therefore necessary to reconcile gravity with particle physics.

One may suppose that the UV completion of the SM that includes gravity does not invalidate the predictions of the SM up to the Planck scale. However, even in this case there are several theoretical problems with the SM that may require solutions in BSM physics.

U(1) Landau pole problem

If there was no expectation of new physics at the Planck scale from gravity, there would still be reason to believe the SM is inconsistent as a QFT up to arbitrarily large energy scales because the $\mathrm{U}(1)_Y$ gauge coupling g' suffers from a Landau-pole; a naive renormalization

[5] Specifically, during inflation quantum fluctuations of the nearly massless inflaton result in inflation lasting different amounts of time in different regions. Each region undergoes the same history (post-inflation oscillations, reheating, etc.) but at a slightly different time, thereby leading to density perturbations [51].

group (RG) running of g' gives an infinite value for the coupling at some finite scale. Some non-perturbative physics or UV completion of the SM would therefore be required at a scale below the Landau pole to keep the coupling finite and produce sensible results.[6]

Since the Landau pole occurs above the Planck scale, however, the problem is often ignored under the assumption that the complete theory of quantum gravity also resolves the Landau pole problem [64]. In a discussion of BSM physics, though, it is important to note that if an extension of the SM introduces a Landau pole below the Planck scale then it is typically assumed that the UV completion of gravity is unrelated to the solution of the Landau pole problem; that is, a Landau pole problem exists and additional BSM physics is required for its resolution.

Gauge hierarchy problem

The often-cited gauge hierarchy problem is related to the fact that heavy states with sufficiently strong couplings to the Higgs induce radiative corrections to the bare Higgs mass parameter m_0^2 that are much larger than the measured sum

$$m^2 \equiv m_0^2 + \delta m^2 = \frac{m_h^2}{2} \simeq -(89\ \text{GeV})^2 \tag{1.5}$$

that is needed for successful EW symmetry breaking. In the cutoff regularization scheme with a high momentum cutoff Λ, the radiative correction δm^2 has the form [65, 66]

$$\begin{aligned}\delta m^2 = &\sum_{\text{gauge bosons}} \frac{N_g g_g^2}{16\pi^2}\left(\Lambda^2 + M_g^2 \ln\frac{M_g^2}{\Lambda^2} + \dots\right) - \sum_{\text{fermions}} \frac{N_f g_f^2}{16\pi^2}\left(\Lambda^2 + M_f^2 \ln\frac{M_f^2}{\Lambda^2} + \dots\right) \\ &+ \sum_{\text{scalars}} \frac{N_s g_s^2}{16\pi^2}\left(\Lambda^2 + M_s^2 \ln\frac{M_s^2}{\Lambda^2} + \dots\right),\end{aligned} \tag{1.6}$$

where each N_i is some $\mathcal{O}(1)$ factor that counts the number of degrees of freedom of the particle, g_i is the coupling strength of the particle to the Higgs, and M_i is the mass of the particle. The gauge hierarchy problem is often mistakenly associated with the quadratic divergences $\propto \Lambda^2$ in (1.6); in a renormalizable field theory such as the SM, these divergences are unphysical and absorbed into the definition of the physically measurable parameter m^2

[6] For the former case, it is possible that a non-perturbative g' leads to confinement and new bound states at the non-perturbative scale (as in quantum chromodynamics (QCD)) that prevent g' from becoming infinite. Since the Higgs doublet is charged under $\mathrm{U}(1)_Y$, however, these very heavy states would couple to the Higgs and introduce a gauge hierarchy problem, again suggesting the need for new physics.

in the renormalization procedure.[7] The renormalization procedure also replaces Λ^2 in the logarithmic terms with the renormalization scale μ^2, and so the logarithmic corrections from the SM particles, which are physical, are under control. The actual hierarchy problem occurs if one introduces a new particle with mass $M_i^2 \gg m^2$ that couples to the Higgs with strength $g_i \sim 1$,[8] which is the case for many well-motivated BSM theories. In this case, the logarithmic term in (1.6) that is proportional to M_i^2 induces a large correction $\delta m^2 \gg m^2$. The gauge hierarchy problem is therefore the question of why m^2 is so light *if the BSM physics at some high scale contains heavy states that are sufficiently strongly coupled to the Higgs.*

A number of models including SUSY, technicolour, and extra dimensions are able to address the hierarchy problem and accommodate heavy states with new physics at the EW scale. Alternatively, if there is no sufficiently strongly coupled BSM physics then there may be no hierarchy problem. With regards to the latter case, note that the UV completion of gravity is expected to introduce states with masses at or near the Planck scale. However, it is possible that there is some symmetry of the underlying UV theory, for instance a classical scale invariance, that sets m^2 to some small value at the Planck scale. Then, without sufficiently strongly coupled new physics between the EW and Planck scales, the RG running preserves the small value of m^2 down to the EW scale and ensures that small m^2 is technically natural.

Strong CP problem

Another fine-tuning problem in the SM is related to the quark sector and known as the strong CP problem. In general, the symmetries of the SM allow a term in the Lagrangian of the form [67]

$$\mathcal{L}_\theta = \frac{\theta g_s^2}{32\pi^2} G^a_{\mu\nu} \tilde{G}_{a\mu\nu}, \tag{1.7}$$

where $G^a_{\mu\nu}$ are the QCD field strengths, g_s is the strong coupling constant, and θ is an angular parameter related to the QCD vacuum structure. An anomalous chiral transformation of the quarks, which is performed in diagonalizing the quark mass matrix M_q, also induces a

[7] This result is seen more clearly by using the dimensional regularization scheme instead of the cutoff regularization scheme, in which case the quadratic divergences never appear.

[8] More precisely, if the coupling g_i is large enough that $(N_i g_i^2/16\pi^2) M_i^2 \ln(M_i^2/M_Z^2) \gtrsim (100 \text{ GeV})^2$ then some level of fine-tuning is necessary to get $m^2 \simeq -(89 \text{ GeV})^2$.

term of the form (1.7) and shifts θ to give the physically measurable angle

$$\bar{\theta} = \theta + \arg\det M_q. \tag{1.8}$$

Thus $\bar{\theta}$, whose deviation from zero measures the strength of CP violation in strong interactions, is a sum of two unrelated and presumably $\mathcal{O}(1)$ terms: the bare Lagrangian parameter θ and the quark mass matrix. However, bounds on the neutron electric dipole moment [68, 69]

$$|d_{\mathrm{n}}| \simeq 5 \times 10^{-16} \bar{\theta}\ e\ \mathrm{cm} \tag{1.9}$$

$$\lesssim 3 \times 10^{-26}\ e\ \mathrm{cm} \tag{1.10}$$

give the constraint $\left|\bar{\theta}\right| \lesssim 10^{-10}$. The strong CP problem is the question of why the CP-violating angle $\bar{\theta}$ is so small, particularly since CP is violated elsewhere in the SM [70]. Moreover, unlike the hierarchy problem, the strong CP problem is a low-energy one; a symmetry that sets θ to zero at some high scale does not prevent $\bar{\theta}$ from being generated at the EW scale due to the contribution from the quark mass matrix.

Possible solutions to the strong CP problem that do not require new physics include having a massless up quark, which is currently disfavoured [4], and employing special boundary conditions, which some have argued is not well motivated [67]. Barring these possibilities, some form of BSM physics is required to solve the strong CP problem. The most appealing solution is to introduce a global chiral U(1) symmetry in the SM known as a Peccei-Quinn (PQ) symmetry [71, 72]. Doing so leads to a new light pseudo-scalar axion field in the SM spectrum and, depending on the implementation of the PQ symmetry, additional quarks or Higgs doublets.

Origin of flavour

While the gauge sector of the SM Lagrangian is uniquely determined by the choice of the SU(3)×SU(2)×U(1) gauge group, the flavour sector of the SM contains many parameters that can only be measured experimentally and then must be set by hand. For instance, the SM does not provide an explanation for the masses of the fermions, the quark mixing angles, or even why there are three generations or "flavours" of fermions.[9] The issue is particularly

[9] One might argue that at least three generations of fermions are required to have a CP-violating phase in the Cabibbo-Kobayashi-Maskawa (CKM) quark mixing matrix and that CP violation is necessary to produce the observed baryon asymmetry. However, since the CP violation in the SM is insufficient for producing the baryon asymmetry [35–37], arguing for three generations of fermions along these lines lacks some appeal.

vexing since the three generations exhibit a fairly regular hierarchy in their masses [4] and since the quark mixing angles appear to have an underlying pattern or structure to their values (made clear, for instance, by the Wolfenstein parametrization of the CKM matrix [73]). If one does not believe that these parameters are accidental, then an explanation of their values requires going beyond the SM. It has been supposed for a long time that some underlying flavour symmetry with an origin in BSM physics may be responsible for generating the pattern of masses and couplings in the quark sector. With the discovery of neutrino oscillations and an analogous set of mixing angles in the lepton sector, though with a very different values, there has been a renewed interest in the ideas of flavour symmetries and BSM physics (see [74] and references therein).

Cosmological constant problem

Although inextricably linked with the UV completion of gravity, the cosmological constant problem is worth mentioning on its own to put other fine-tuning problems into perspective. Without gravity, shifting the Lagrangian by a constant term $\mathcal{L} \to \mathcal{L} + \Lambda$ does not have any physical effect; it simply introduces an overall multiplicative factor in the functional integral

$$Z = \int D\phi e^{i\int d^4x \mathcal{L}(x)}, \tag{1.11}$$

which ultimately drops out of calculations in elementary particle physics.[10] In cosmology, however, Λ does have an observable effect since it represents a constant energy density that permeates the universe and couples to gravity. Current estimates of Λ from the CMB through its effect on the cosmological expansion give [12]

$$\Omega_\Lambda \simeq 0.69 \implies \Lambda \simeq \left(2.3 \times 10^{-3}\ \text{eV}\right)^4. \tag{1.12}$$

When studying EW symmetry breaking in the SM, constant terms in the potential V of order $(100\ \text{GeV})^4$ are ignored because they are assumed to cancel with the bare cosmological constant to give the value of Λ in (1.12). This represents a fine-tuned cancellation to about one part in 10^{55} and is referred to as the cosmological constant problem.[11] A number of unsuccessful solutions have been put forth (see [75] for a review), and it is assumed that the

[10] For fermionic path integrals, rescalings of measure can have physical effects through anomalies.

[11] If one suspects contributions to the potential energy from Planck-scale physics of order $V \sim M_{\text{Pl}}^4$, then the fine-tuning is to an astonishing one part in 10^{122}.

solution to the cosmological constant problem is contained in the correct theory of quantum gravity, other BSM physics, or is due to anthropic selection.

1.2 Approaches to BSM physics

For the past few decades, it has been widely assumed that there is some new physics between the EW and Planck scales with coupling strengths that are comparable to those of the SM gauge couplings; that is, coupling strengths that are $\mathcal{O}(1)$. A classic example is the embedding of the SM into a GUT based on the group SU(5) [76] or SO(10) [77] at the scale $\Lambda_{\rm GUT} \sim 10^{16}$ GeV — a theoretically appealing scenario suggested by the approximate unification of the SM gauge couplings around this scale. The resulting gauge hierarchy problem and the idea that the SM is somehow "natural" in the presence of this new physics has dominated much of the theoretical effort over the last few decades. In particular, it has led to many proposals of BSM physics at or near the EW scale designed to stabilize the bare Higgs mass parameter and preserve the experimentally successful predictions of EW symmetry breaking.

The LHC has, in some respects, brought this line of reasoning into question. With roughly 5 fb^{-1} of data taken at $\sqrt{s} = 7$ TeV and 20 fb^{-1} taken at $\sqrt{s} = 8$ TeV [32, 33], the LHC results are remarkably consistent with the predictions of the SM; the LHC indicates that EW symmetry breaking is due to an elementary weakly coupled scalar field and has not seen any evidence for SUSY, technicolour, extra dimensions, or other BSM physics. The LHC now places bounds on the simplest versions of these BSM physics models that push them into regions of parameter space with a fine-tuning of about 1% or more [78, 79]. Since the primary purpose of many of these models is to solve the hierarchy problem in a natural way, some of their appeal has been lost and the principle of naturalness has been brought into question [80, 81].

At the same time, the LHC measurement of the Higgs mass $M_h \simeq 125$–126 GeV [32, 33], which allows an accurate determination of the Higgs self-coupling λ in the SM, suggests something interesting: the SM lies in a special region of parameter space in which both λ and its beta function β_λ vanish near the Planck scale for a top quark mass that is a few σ above its central value [82]. This result may be a simple coincidence or it may be, as some

have argued, an indication of some deeper underlying physics [83]. For instance, an infrared (IR) fixed point in an asymptotically safe theory of gravity may ensure very small values of $\lambda(\mu)$ near the Planck scale [64]. Since new physics that is introduced around the EW scale to solve the hierarchy problem typically modifies the running of λ and spoils this result, Higgs measurements further suggest that perhaps there is no new physics to be found at the LHC and that the SM running is valid up to the Planck scale.

It is then tempting to consider a different approach to BSM physics in which naturalness through the presence of new EW scale physics is not the guiding principle. After all, Grand Unification is not a necessary feature of the UV completion of the SM but an aesthetic requirement that is placed upon such a theory. One approach, which is along the lines of [84], is the following: suppose that there are no intermediate scales of new physics between the EW and Planck scales — or, more precisely, that there are no intermediate scales of new physics that are sufficiently strongly coupled to the Higgs to introduce a hierarchy problem.[12] This is an example of the principle of technical naturalness, which allows small parameters in a model so long as they are stable in the presence of radiative or quantum corrections. With the principle of technical naturalness in mind for addressing the hierarchy problem, put aside for the moment other fine-tuning problems such as the strong CP problem.[13] Instead, focus on addressing the phenomenological shortcomings of the SM with the minimal extension required. A very simple extension of the SM that explains neutrino oscillations is then the Type I seesaw, which introduces right-handed neutrinos that are singlets under the SM gauge group. At least two right-handed neutrinos are needed to explain the (at least) two massive neutrinos implied by oscillation data. Adding the fewest number of additional right-handed neutrinos that are also needed to explain dark matter and the baryon asymmetry gives the neutrino minimal Standard Model (νMSM) [87, 88] — an extension of the SM by three right-handed neutrinos[14] with no intermediate scales of new physics.

Such an approach, though still suffering from fine-tuning problems such as the strong CP problem, is appealing from a practical point of view. Much work can be carried out on

[12] As discussed in section 1.1.2, an underlying symmetry that gives a small value of m^2 at the Planck scale would then ensure that small m^2 is natural even with heavy states from the UV completion of gravity.

[13] Some proposals to solve the strong CP problem with extra dimensions claim to avoid introducing an intermediate scale of new physics [85, 86] but seem to reintroduce the hierarchy problem.

[14] From a theoretical point of view, introducing three right-handed neutrinos is also attractive because it completes the left/right partnering of fermions in the SM.

the phenomenology of the νMSM, including examining how extensions of the νMSM may be required to solve some of its phenomenological issues and how the model of Higgs inflation in the νMSM behaves for the measured Higgs mass.

With no intermediate scale of new physics that couples significantly to the Higgs, all values of m^2, including small ones, are technically natural [89]. Since there is no *a priori* reason for nature to prefer a value of $m^2 \simeq -(89\text{ GeV})^2$ over any other value,[15] it is also interesting to consider the possibility that the renormalized m^2 is zero; this is the only intrinsically special value for m^2 and corresponds to a scale invariance in the SM at the Lagrangian or "classical" level. One can then take the approach that classical scale invariance is a fundamental principle of physics, including BSM physics, or suppose that it is an emergent symmetry arising from the RG evolution of mass parameters in UV physics down to the Planck scale (at which point BSM models are defined). In either case, the Higgs mass parameter must be generated by quantum corrections through the Coleman-Weinberg (CW) potential [90], which places non-trivial constraints on BSM physics.

Now, in the context of a classical scale invariance, return to one of the major SM fine-tuning problems: the strong CP problem. The most attractive solution to the strong CP problem is that of the invisible axion. In its original formulations, the invisible axion solution introduces a global chiral $\mathrm{U}(1)_{\mathrm{PQ}}$ symmetry and a complex scalar field to the SM as well as either an additional quark or Higgs doublet. The complex scalar field is a singlet under the SM gauge group but charged under the $\mathrm{U}(1)_{\mathrm{PQ}}$ symmetry. Due to experimental and cosmological constraints, the PQ scalar must develop a very large vev that breaks the $\mathrm{U}(1)_{\mathrm{PQ}}$ symmetry [67, 68]. In a classically scale invariant model, this spontaneous symmetry breaking must occur radiatively through the CW mechanism rather than through a large negative mass term for the PQ scalar. It is important to show that the ultra-weak couplings of PQ scalar to the Higgs sector, which are necessary to prevent a large tree-level contribution to the Higgs mass from the vev of the PQ scalar, are technically natural and hence do not result in a hierarchy problem. The invisible axion model with a classical scale invariance also has interesting phenomenological consequences, particularly with regards to the additional light state associated with the PQ scalar and its possible influences on cosmology.

[15] The size of the negative m^2 drives EW symmetry breaking and sets the Higgs vacuum expectation value (vev), so a larger or smaller value of m^2 just produces a different scale of EW symmetry breaking.

1.3 Overview of the thesis

This thesis is comprised of several self-contained topics that are connected by the general approach to BSM physics outlined above. Note that a complete and self-consistent picture of BSM physics that uses the principle of technical naturalness, together with a classical scale invariance, to address all phenomenological and theoretical issues with the SM is not provided here.[16] If such a picture exists, the details go beyond the scope of this thesis.

The topics of this thesis are organized as follows. Motivated by tension in the νMSM with the Lyman-α forest data and other small scale structure bounds, chapter 2 considers an extension of the νMSM in which the Majorana masses for the right-handed neutrinos originate from the vev of a Higgs singlet ϕ and dark matter is produced through the decays of ϕ rather than through active-sterile neutrino mixing. Like the νMSM, though, the neutrino next-to-minimal Standard Model (νNMSM) requires a specific hierarchy of Majorana masses and Yukawa couplings without an obvious origin. In chapter 2, it is shown that the hierarchical parameters of the νNMSM can arise from Planck-scale symmetries for two specific examples of this model: one in which ϕ helps stabilize the EW vacuum through a scalar threshold effect and one in which ϕ is a light inflaton. Both examples require a complex ϕ and have several experimental signatures that are distinct from the νMSM, including additional dark radiation and, for the former, a possibly large invisible branching ratio of the Higgs.

Chapter 3 focuses on the model of Higgs inflation that is used by the νMSM and its close extensions. In particular, a non-minimal coupling ξ of the SM Higgs field to gravity can give rise to inflation, but it is usually argued that large ξ is required. A naive estimate for the scale of perturbative unitarity violation, $M_{\rm Pl}/\xi$, is then well below the inflationary scale $M_{\rm Pl}/\sqrt{\xi}$ and therefore spoils the self-consistency of the model and its predictions. Chapter 3 re-examines this claim for a Higgs mass in the range 125–126 GeV for which the Higgs self-coupling λ runs to very small values near the Planck scale. A small self-coupling λ near the Planck scale, which may be due to some underlying physics, can significantly reduce the value of ξ required for inflation. Using the two-loop RG equations and effective potential for Higgs ξ-inflation, it is found that familiar inflationary solutions can have a non-minimal

[16] For instance, no serious attempt is made to solve the cosmological constant problem or provide a complete model for the origin of flavour.

coupling as small as $\xi \sim 400$ without the potential developing a second minimum. A new observationally allowed region of Higgs ξ-inflation with $\xi \sim 90$ and distinct inflationary predictions, including an observable level of the tensor-to-scalar ratio r, is also found.

Chapter 4 moves away from issues related specifically to the νMSM and develops the ideas of classical scale invariance and technical naturalness within the invisible axion solution to the strong CP problem. In particular, chapter 4 shows that a Dine-Fischler-Srednicki-Zhitnitsky-like (DFSZ-like) axion model with an ultra-weakly coupled PQ scalar can solve the strong CP problem and give rise to successful EW symmetry breaking through the CW mechanism. Due to an approximate underlying shift symmetry, the ultra-weak couplings of the PQ scalar are technically natural and hence the model does not contain a hierarchy problem for the Higgs mass parameter. It does, however, contain a light pseudo-Goldstone dilaton that can be consistent with cosmological bounds while the axion can be the dark matter of the universe.

Finally, chapter 5 summarizes the thesis and discusses how the ideas of classical scale invariance and radiative EW symmetry breaking in the DFSZ-like axion model may be combined with the νMSM. Future research topics along these lines are suggested.

1.3.1 Novel work

The novel work presented in this thesis is as follows. In chapter 2, the most important original contribution is the study of flavour symmetries that can produce the hierarchical parameters of the νNMSM, either in general or for the two examples of the scalar sector provided. To realize such symmetries, it is necessary to consider a complex singlet ϕ rather than the real singlet that is typically considered for adequate dark matter production through the decays of ϕ. Though the details of dark matter production for the complex and real singlet cases are similar, a minor discussion of the distinguishing experimental signatures for the complex singlet case, which include an increase in the effective number of neutrino species N_{eff} and a possibly large invisible branching ratio of the Higgs, is also new.

In chapter 3, the model of Higgs ξ-inflation is not original. However, the detailed two-loop study of the inflationary model in the region of small λ_{eff} is the first of its kind following the measurement of the Higgs boson mass. The analysis demonstrates clearly how small ξ can be in this region, which is important for the discussion of the self-consistency of the model,

and discovers a new region of Higgs ξ-inflation with large tensor-to-scalar ratio. The latter result has become particularly important for proponents of the νMSM after the BICEP2 collaboration hinted at the observation of a large tensor-to-scalar ratio.

In chapter 4, the study of invisible axion models with a classical scale invariance and CW symmetry breaking is also original. The demonstration that one such invisible axion model can solve the strong CP problem without introducing a hierarchy problem for the Higgs mass is an important conceptual result for the approach to BSM physics that is guided by classical scale invariance and technical naturalness. Unlike the usual implementation of the invisible axion, the classical scale invariance in this model results in a light pseduo-dilaton state with non-trivial cosmological implications. The technical discussion of the cosmology of the light pseudo-dilaton state, specifically how the energy density of the state is efficiently dissipated after inflation, is new.

Chapter 2

Dark matter, singlet extensions of the νMSM, and symmetries

The first topic of the thesis addresses the question of the origin of flavour in an extension of the SM that can explain most if not all of the phenomenological evidence for BSM physics with right-handed neutrinos. The aim is to show how underlying flavour symmetries can be used to reproduce the necessary pattern of Majorana masses and Yukawa couplings for the right-handed neutrinos, so the small parameters in the scalar sector (and in some instances the hierarchy problem introduced by new scalar fields) are generally left unexplained. These issues might be resolved with ultra-weakly coupled sectors that are technically natural, as discussed in chapter 4, but here the choices of scalar sector parameters are motivated primarily by phenomenological issues with the νMSM.

Disclaimer: This chapter contains a nearly identical copy of my work in ref. [91] plus a discussion of recent developments that have occurred since publication.

2.1 Introduction

The νMSM [7] is an extension of the SM that attempts to explain all observed phenomena beyond the SM using only three sterile neutrinos with Majorana masses below the EW scale. In the νMSM, one sterile neutrino, N_1, is responsible for dark matter [87] while two additional sterile neutrinos, N_2 and N_3, are responsible for baryon asymmetry production [88]. Moreover, the Higgs boson with a non-minimal coupling to gravity is responsible for inflation [54].

Although a detailed study of the νMSM (see [92] for a recent update) shows that this minimal model can explain most of the observed phenomena beyond the SM, there are several

indications that an extension of the νMSM, such as by a Higgs singlet, may be necessary:

- *Lyman-α forest bound*: The Lyman-α forest [93] — a series of absorption lines in the spectra of distant quasars caused by interstellar clouds of hydrogen gas — and other observations of small scale structure [94, 95] impose strong constraints on the non-resonant production of warm dark matter in the νMSM when combined with X/γ-ray limits [96]. Several solutions to this problem have been proposed, including a resonant production of dark matter from a large lepton asymmetry [97] and a dilution of dark matter from a late entropy release [98–101]. Generating a sufficiently large lepton asymmetry requires an inverted neutrino hierarchy as well as a high level of fine-tuning or the use of an approximate Planck-scale symmetry and non-renormalizable operators [102], while generating a sufficiently large entropy dilution requires some new physics beyond the νMSM [98–101]. An attractive alternative to these scenarios uses the decays of a Higgs singlet, whose vacuum expectation value provides an origin for the Majorana masses of the sterile neutrinos, to give a primordial production of dark matter [103–107].

- *Electroweak vacuum stability*: For a Higgs mass in the range $m_h \simeq 125$–126 GeV [108, 109], the Higgs potential develops an instability below the Planck scale unless the top mass is about 2σ below its central value; for its central value, an instability develops at 10^{11} GeV [110]. While more precise measurements of the top mass may lower its central value and relieve this tension, it has been shown that, if necessary, the addition of a Higgs singlet below the instability scale can stabilize the potential through its contribution to the RG evolution of the Higgs quartic coupling [111, 112] or through a tree-level scalar threshold effect [112, 113].

- *Higgs inflation*: There has been some discussion about unitarity violation and the self-consistency of Higgs inflation with a non-minimal coupling $\xi H^\dagger H \mathcal{R}$, where $\mathcal{R}$ is the scalar curvature and $\xi \sim 10^4$ (see [114] and references therein). In brief, this model of Higgs inflation violates unitarity at the scale $\Lambda_0 \sim M_{\rm Pl}/\xi$ when expanding about a small background Higgs field. Although the scale of unitarity violation is raised to $M_{\rm Pl}/\sqrt{\xi}$ when expanding about the large background Higgs field during inflation [114], if the theory is eventually embedded into a more complete one that is valid up to the

Planck scale then new physics is expected to appear at $M_{\rm Pl}/\xi$ [115]. Several solutions that do not abandon the minimality of the model have been proposed, including non-renormalizable Higgs interactions that accompany the non-minimal coupling and restore unitarity [116] as well as strong coupling in graviton exchange processes that only break unitarity perturbatively [117]. However, it has not yet been shown that these scenarios can actually be realized [117]. Alternatively, an extension of the νMSM by a Higgs singlet can "unitarize" Higgs inflation [115][1] or provide a workable scenario with the singlet as the inflaton [103–105].

The fact that a Higgs singlet can both provide an origin for the Majorana masses of the sterile neutrinos and allow a simple dark matter production mechanism that, unlike the non-resonant production of dark matter in the νMSM, is consistent with the Lyman-α forest bound is a strong motivation for considering singlet extensions of the νMSM (e.g. [103–107]). It is then natural to ask whether such extensions can also address the issues with Higgs inflation, as in [103–105], or help stabilize the EW vacuum, if necessary.

These singlet extensions of the νMSM, like the original model, require a particular hierarchy of Majorana masses and Yukawa couplings without an obvious origin. An important open question for these extensions is whether it is possible for such structure to come from an underlying symmetry. In the context of the νMSM, models employing a U(1) flavour symmetry [118, 119], discrete flavour symmetries [120], the split seesaw mechanism [121, 122], and the Froggatt-Nielsen mechanism [123–125] have been suggested for producing a hierarchical pattern of Majorana masses and Yukawa couplings. Similar techniques should also be able to produce the necessary pattern of masses and couplings in singlet extensions, but this has not been demonstrated explicitly.

In this chapter, we consider extensions of the νMSM by a Higgs singlet ϕ that address some of the model's possible phenomenological problems and demonstrate how underlying symmetries can give the necessary pattern of Majorana masses and Yukawa couplings in these extensions. In particular, our starting point is a generic model in which the decays of ϕ allow for primordial dark matter production that is consistent with the Lyman-α forest bound and in which the vev of ϕ provides an origin for the Majorana masses of the sterile neutrinos. We

[1] In [117], it is argued that this is not a true completion of Higgs inflation but rather an induced gravity inflation model added onto the SM.

then construct symmetries broken at or near the Planck scale that can produce the hierarchy of parameters for two specific examples of this model: one in which ϕ helps stabilize the EW vacuum through a scalar threshold effect [113] and one in which ϕ is the inflaton [103–105]. Both examples require a complex ϕ to be realized with underlying symmetries and have several experimental signatures that are distinct from the νMSM.

The chapter is organized as follows. In section 2.2, we review the constraints on the νMSM and primordial dark matter production from a Higgs singlet. In section 2.3, we develop symmetries broken at or near the Planck scale that can produce the required pattern of Majorana masses and Yukawa couplings for two examples of this model. Section 2.4 gives the conclusions.

2.2 The νMSM and dark matter production from a Higgs singlet

In this section, we first review the constraints on the νMSM and motivate the scenario of dark matter production from a Higgs singlet. We then discuss the constraints on dark matter production from a Higgs singlet.

2.2.1 The νMSM

The Lagrangian of the νMSM is given by

$$\mathcal{L} = \mathcal{L}_{\rm SM} + \bar{N}_I i\partial_\mu \gamma^\mu N_I - F_{\alpha I}\bar{L}_\alpha N_I H - \frac{M_{IJ}}{2}\bar{N}_I^c N_J + \text{h.c.}, \tag{2.1}$$

where $\mathcal{L}_{\rm SM}$ is the SM Lagrangian, N_I $(I = 1, 2, 3)$ are the sterile neutrinos, L_α $(\alpha = e, \mu, \tau)$ are the lepton doublets, H is the Higgs doublet, $F_{\alpha I}$ are the Yukawa couplings for neutrinos, and M_{IJ} are the Majorana masses for the sterile neutrinos. One of the striking features of the νMSM is the highly constrained and hierarchical pattern of parameters required for successful baryogenesis and dark matter production. These constraints are often best expressed not in the basis N_I of (2.1) but in the basis of the *physical* mass eigenstates N_I^m with masses M_I and Yukawa couplings $\tilde{F}_{\alpha I}$. The two bases are related by the unitary transformation given in [118].

First, consider the constraints on N_2^m and N_3^m. The oscillations between N_2^m and N_3^m above $T_{\rm EW}$ produce a lepton asymmetry in the active neutrinos that is converted into a

baryon asymmetry by sphalerons [88].[2] N_2^m and N_3^m cannot enter thermal equilibrium at temperatures much above $T_{\rm EW}$ or else the lepton asymmetry produced in their oscillations is wiped out, giving the constraint [118]

$$F_2 \lesssim 1.2 \times 10^{-6}, \tag{2.2}$$

where $F_I^2 \equiv \left(F^\dagger F\right)_{II}$ and, by convention, F_2 is taken to be larger than F_3 with $\epsilon \equiv F_3/F_2 \leq 1$. Similarly, masses $M_2, M_3 \ll T_{\rm EW}$ are required so that lepton number violating processes are negligible for $T \gtrsim T_{\rm EW}$; masses satisfying

$$M_2, M_3 \lesssim 20 \text{ GeV} \tag{2.3}$$

are generally considered acceptable [88, 126]. Meanwhile, effective baryon asymmetry production requires $M_2, M_3 \simeq M$ to be highly degenerate with a mass difference $\Delta M \equiv M_3 - M_2 \ll M$ [88]. The baryon asymmetry produced can be expressed as a function of $F_2, \epsilon, M, \Delta M$, and the neutrino hierarchy. Since active neutrino masses are generated via the seesaw mechanism, one of F_2, ϵ, and M (typically F_2) can be expressed in terms of the others with the relation [118]

$$\Delta m_{\rm atm} \simeq \frac{\kappa v^2 \epsilon F_2^2}{2M}, \tag{2.4}$$

where $\Delta m_{\rm atm} \simeq 0.05$ eV, $v = 246$ GeV, and $\kappa = 1(2)$ for the inverted (normal) hierarchy. Analytic expressions for the baryon asymmetry are given in [88, 127] while a numerical study has been carried out in [126]. The allowed range of each parameter individually is [126]

$$M \gtrsim 140 \text{ MeV}, \tag{2.5}$$

$$10^{-3} \text{ eV} \lesssim \Delta M \lesssim \text{MeV}, \tag{2.6}$$

$$10^{-4} \lesssim \epsilon \leq 1, \tag{2.7}$$

though the combination must produce the observed asymmetry $n_B/s \simeq (8.4\text{–}8.9)\times 10^{-11}$ [128]. Note that the lower bound (2.5) comes from demanding that N_2^m and N_3^m decay before Big Bang nucleosynthesis (BBN) [129, 130][3] and that a significant amount of parameter space for $M \lesssim 500$ MeV is ruled out by the CERN PS191 experiment and other accelerator

[2] $T_{\rm EW} \simeq 140$ GeV for a Higgs mass $m_h \simeq 125$ GeV [126].

[3] Recent work [131, 132] suggests this bound can been strengthened to $M \gtrsim 1.4$ GeV in the RP scenario, discussed later.

bounds [126, 130].[4] For the parameter space allowed by (2.5)–(2.7), a lower bound on F_2 is approximately

$$F_2 \gtrsim 3 \times 10^{-8}. \tag{2.8}$$

Now consider the constraints on the dark matter candidate N_1^m. Mixing with active neutrinos below $T_{\rm EW}$ allows the 1-loop decay $N_1^m \to \nu^m \gamma$ with width [7, 133]

$$\begin{aligned} \Gamma_{N_1^m \to \nu^m \gamma} &= \frac{9\alpha G_F^2}{1024\pi^4} \sin^2(2\theta_1)\, M_1^5 \\ &\simeq 5.5 \times 10^{-22} \theta_1^2 \left(\frac{M_1}{\rm keV}\right)^5 {\rm s}^{-1}, \end{aligned} \tag{2.9}$$

where $\theta_1^2 = v^2 \tilde{F}_1^2 / (2M_1^2)$ and $\tilde{F}_1^2$ is evaluated with [118]

$$\tilde{F}_{\alpha 1} \sim F_{\alpha 1} + \frac{M_{12}}{M} F_{\alpha 2} + \frac{M_{13}}{M} F_{\alpha 3}. \tag{2.10}$$

The second and third terms on the right hand side of (2.10) are contributions to $\tilde{F}_{\alpha 1}$ induced by the mixing of N_1 with N_2 and N_3 to form the mass eigenstate N_1^m. Direct searches for the X/γ-ray line corresponding to this decay provide the strongest limits on θ_1 (as a function of M_1) for the mass range relevant to the νMSM. A summary of these limits is given in [96]. In general,

$$\theta_1^2 \lesssim 3 \times 10^{-5} \left(\frac{\rm keV}{M_1}\right)^5 \tag{2.11}$$

must be satisfied for 0.5 keV $\lesssim M_1 \lesssim$ 14 MeV, though the constraint is typically 100 times stronger than (2.11) for masses outside the 12–40 keV range [96]. For N_1^m produced entirely from active-sterile neutrino mixing, M_1 can be bounded above by combining the X-ray constraints with the requirement of sufficient dark matter production ($\propto \theta_1^2$). The bound obtained depends on the lepton asymmetry at the time of N_1^m production: a negligible lepton asymmetry is called the non-resonant production (NRP) scenario while a large lepton asymmetry is called the resonant production (RP) scenario. The bounds for these two scenarios are [96, 97, 99]

$$M_1^{\rm NRP} \lesssim 2.2 \text{ keV}, \quad M_1^{\rm RP} \lesssim 40 \text{ keV}. \tag{2.12}$$

Meanwhile, M_1 can be bounded below by phase-space density arguments for dwarf spheroidal galaxies [134, 135], the Lyman-α forest data [93, 136], studies of gravitationally lensed

[4] The fixed target CERN PS191 experiment looked for heavy neutrinos in the decays of charged mesons $\pi^+/K^+ \to e^+ N$, where the heavy neutrino decays as $N \to e^+ e^- \nu_\alpha$. Bounds on these processes constrain regions of the mass-mixing plane of N_2^m and N_3^m for $M < m_{K^+} \simeq 493.7$ MeV.

QSOs [94], and N-body simulations of the Milky Way [95]. The bounds from the Lyman-α forest data and N-body simulations of the Milky Way are the strongest and give[5]

$$M_1^{\rm NRP} \gtrsim 13 \text{ keV}, \quad M_1^{\rm RP} \gtrsim 2 \text{ keV}. \tag{2.13}$$

Combining (2.12) and (2.13) rules out the simpler NRP scenario, even with a possibly large entropy dilution from the decays of N_2^m and N_3^m [99]. The RP scenario is still allowed for a range of M_1; it requires an even larger degeneracy than (2.6), on the order $\Delta M \lesssim 10^{-7}$ eV, to produce the required lepton asymmetry for enhanced dark matter production [102]. This level of degeneracy is unstable in the presence of radiative corrections and must be achieved with either fine-tuning or an extension of the model by a Planck-scale symmetry and non-renormalizable operators [102].

2.2.2 Dark matter production from a Higgs singlet

An alternative dark matter production scenario that is capable of satisfying the Lyman-α forest bound for warm dark matter (or allows for heavier cold dark matter) uses a real Higgs singlet ϕ and its decays to N_1^m [103]. This scenario is arguably simpler than the RP scenario and has the advantage that Majorana masses originate from the vev of ϕ rather than as bare mass terms. This extension of the νMSM, which we will call the *neutrino Next-to-Minimal Standard Model* (νNMSM), is the basis of this chapter.

In the νNMSM, the Majorana mass term in the Lagrangian (2.1) is modified to

$$\Delta\mathcal{L} = -\frac{\lambda_{IJ}}{2}\phi\bar{N}_I^c N_J, \tag{2.14}$$

where $M_{IJ} = \lambda_{IJ}\langle\phi\rangle$ once ϕ acquires a vev. In the mass basis N_I^m, $\lambda_{IJ} \to \lambda_I$ where $M_I = \lambda_I\langle\phi\rangle$. The mixing angle θ_1^2 is assumed small enough that dark matter production from active-sterile neutrino mixing is negligible and the X/γ-ray constraint (2.11) is satisfied.[6] Assuming no miraculous cancellations of terms in (2.10), this requires

$$F_{\alpha 1}, \frac{M_{12}}{M}F_{\alpha 2}, \frac{M_{13}}{M}F_{\alpha 3} \lesssim 10^{-13}. \tag{2.15}$$

[5]These are the (Bayesian) 2σ bounds. Although [95] quotes a stronger bound for $M_1^{\rm RP}$, it is based on a simple mass rescaling argument that is shown to be insufficient for a more rigorous analysis of the Lyman-α forest bound in the RP scenario [136].

[6]Since the NRP and RP bounds (2.12) no longer apply, M_1 may exceed the range in which (2.11) is valid. In this case, γ-ray constraints from EGRET [137] and FERMI [138] give $\tau \gtrsim 10^{26}$ s, or equivalently $\theta_1^2 \lesssim 2\times 10^{-20}\,(\text{MeV}/M_1)^5$, for masses up to 30 TeV.

With (2.15), one can show that the induced contributions to M_1 from M_{12} and M_{13} are small [118] and hence $\lambda_1 \simeq \lambda_{11}$. Dark matter production then proceeds via the decays $\phi^m \to N_1^m N_1^m$ with the partial width [103]

$$\Gamma = \frac{\lambda_1^2}{16\pi} m_\phi \simeq \frac{\lambda_{11}^2}{16\pi} m_\phi, \tag{2.16}$$

where $m_\phi > 2M_1$ is the mass of the physical mass eigenstate ϕ^m.[7] This production depends on the thermal history of ϕ^m, specifically the ratio of its mass to its freeze-out temperature, $r_f \equiv m_\phi / T_f$ [107]. For the case that ϕ^m is in thermal equilibrium down to temperatures $T \ll m_\phi$ (i.e. $r_f \gg 1$), the dark matter abundance is given by [103]

$$\Omega_{N_1^m} \simeq \frac{0.2 f(m_\phi)}{S} \left(\frac{\lambda_{11}}{10^{-10}}\right)^2 \left(\frac{M_1}{4 \text{ keV}}\right) \left(\frac{\text{GeV}}{m_\phi}\right), \tag{2.17}$$

where $f(m_\phi) \simeq (10.75/g_*(m_\phi/3))^{3/2}$ and $1 \leq S \lesssim 2$ is a factor that accounts for entropy production from the decays of N_2^m and N_3^m after N_1^m is produced.[8] Using $M_1 \simeq \lambda_{11} \langle\phi\rangle$ in (2.17), the appropriate dark matter abundance $\Omega_{N_1^m} \simeq 0.23$ is generated when

$$\lambda_{11} \simeq 4 \times 10^{-9} \left(\frac{S}{f(m_\phi)}\right)^{1/3} \left(\frac{m_\phi}{\langle\phi\rangle}\right)^{1/3}. \tag{2.18}$$

For the case that ϕ^m is a thermal relic decaying out of equilibrium (i.e. $r_f \ll 1$), the dark matter abundance is given by [107]

$$\Omega_{N_1^m} \simeq \frac{0.3}{S} \left(\frac{M_1}{\text{keV}}\right) \left(\frac{10.75}{g_*(T_f)}\right) \left(\frac{B}{0.01}\right), \tag{2.19}$$

where $B \equiv \Gamma/\Gamma_\phi^{\text{tot}}$ is the branching ratio of $\phi^m \to N_1^m N_1^m$.[9] Analytic expressions relevant to the intermediate case $r_f \sim 1$ can be found in [107], and the result is a combination of (2.17) and (2.19).

The Lyman-α forest bound for this dark matter production mechanism can be estimated by rescaling the NRP bound, giving [99, 107]

$$M_1^{\text{Higgs}} \gtrsim 10 \left(\frac{10.75}{g_*(T_{\text{prod}})}\right)^{1/3} \text{ keV}, \tag{2.20}$$

where T_{prod} is the temperature at which N_1^m is produced. Further constraints come from the requirement that the interactions $\phi^m \leftrightarrow N_2^m N_2^m$ and $\phi^m \leftrightarrow N_3^m N_3^m$ (and any interactions

[7] We have assumed a small mixing angle $\theta_{h\phi}$ between the Higgs boson h and ϕ so that $\phi^m \simeq \phi$, $h^m \simeq h$, and the decays $h^m \to N_1^m N_1^m$ are negligible compared to $\phi^m \to N_1^m N_1^m$ [107]. This is a good approximation for both models considered in section 2.3.

[8] Since N_1^m production peaks at $T_{\text{prod}} \equiv m_\phi/2.3$, (2.17) is a good approximation for $r_f \gtrsim 3$ [107].

[9] As in [107], we neglect any $\phi\phi$ annihilations that could reduce (2.19) by up to a factor of 2.

SM $\leftrightarrow N_2^m N_2^m$ and SM $\leftrightarrow N_3^m N_3^m$ mediated by ϕ^m) do not bring N_2^m and N_3^m into thermal equilibrium at the characteristic temperature of leptogenesis [139]

$$T_L \sim \left(\frac{M\Delta M M_0}{3}\right)^{1/3}, \tag{2.21}$$

where $M_0 \simeq 7 \times 10^{17}$ GeV, and spoil baryogenesis.[10] Moreover, the addition of ϕ must not open an invisible branching ratio of the Higgs greater than 30% at 2σ [140]. These constraints are discussed further in section 2.3 for specific models of the scalar sector.

Although we have assumed ϕ is real in the discussion above, it is also possible (with some restrictions) to have a complex ϕ. (We parametrize $\phi = (\rho + i\chi)/\sqrt{2}$ for a complex ϕ but continue to use m_ϕ and ϕ^m instead of m_ρ and ρ^m to maintain consistency with the notation for a real ϕ.) In previous studies of the νNMSM, which do not attempt to explain the origin of its parameters, ϕ is typically assumed real to avoid a massless Goldstone boson χ and hence the unsuitably fast decay channel $N_1^m \to \nu^m \chi$ for dark matter [103–107]. We have found it difficult, however, to explain the parameters of the νNMSM with an underlying symmetry if ϕ is real and hence uncharged. To construct such a symmetry, we must therefore consider a complex ϕ and address the problems and constraints associated with a Goldstone boson.

There are several ways to avoid the decay $N_1^m \to \nu^m \chi$ for a complex ϕ. First, if ϕ is charged under a discrete symmetry and terms of the form $\phi^n + \phi^{\dagger n}$ are allowed, these terms give χ a mass and can kinematically forbid the decay $N_1^m \to \nu^m \chi$. If the analogous decays $N_2^m, N_3^m \to \nu^m \chi$ are still allowed, they can relax the constraint (2.5) to $M \gtrsim$ few MeV [118]. Alternatively, if χ remains light enough to allow $N_1^m \to \nu^m \chi$ then the mixing of N_1 with other neutrino species can be suppressed or forbidden by a symmetry, thereby suppressing the decay. This case is particularly interesting since χ can contribute to the effective number of neutrino species and give a value of N_{eff} above the SM or νMSM prediction, as recent measurements prefer (see [141] and references therein).[11] The contribution of χ to N_{eff} depends on the freeze-out temperature T_f: it can be as large as $\Delta N_{\text{eff}} \sim 1$ for a thermal distribution of χ or much smaller if χ decouples early. The Planck experiment and other future CMB experiments will therefore be able to constrain these models with a complex ϕ [143].

[10] If these interactions bring N_2^m and N_3^m into thermal equilibrium below T_L, the asymmetry in the sterile neutrinos will be wiped out but the asymmetry in the active neutrinos will remain.

[11] The real component of ϕ can also contribute to N_{eff} during BBN if $m_\phi \lesssim 10$ MeV [142]. For the models of the scalar sector considered in section 2.3, however, $m_\phi \gg 10$ MeV.

2.3 Symmetries and the νNMSM

The νNMSM, like the νMSM, requires parameters that are constrained to be hierarchically small. An important question is whether it is possible for such structure to come from an underlying symmetry. In the context of the νMSM, flavour symmetries [118–120], the split seesaw mechanism [121, 122], and the Froggatt-Nielsen mechanism [123–125] have been explored for producing the required pattern of Majorana masses and Yukawa couplings. Following this approach, we would like to demonstrate explicitly how the flavour sector parameters of the νNMSM can arise from symmetries broken at or near the Planck scale. Since the values of some parameters (e.g. λ_{11} in (2.18)) depend on an unspecified scalar sector, we first keep the discussion general and then consider two specific models of the scalar sector: one in which ϕ helps stabilize the EW vacuum [113] and one in which ϕ is the inflaton [103–105]. These models of the scalar sector, though motivated as minimal solutions to other possible problems with the νMSM, are meant only to provide definite examples for the symmetries used in the flavour sector; other realizations of the scalar sector may certainly be considered.

Note that we do not provide an explanation for the values of parameters in the scalar sector or the associated hierarchy problems in this chapter. A separate symmetry or mechanism, such as the scale symmetry discussed in chapter 4, may be responsible for producing hierarchically small scalar sector parameters that are technically natural and hence avoid a hierarchy problem.

2.3.1 Symmetries in the flavour sector

First consider how the structure of the νNMSM Lagrangian,

$$\Delta\mathcal{L} = -F_{\alpha I}\bar{L}_\alpha N_I H - \frac{\lambda_{IJ}}{2}\phi\bar{N}_I^c N_J + \text{h.c.}, \tag{2.22}$$

can arise from an underlying symmetry without regard to the size of the couplings $F_{\alpha I}$ and λ_{IJ}. There are several ways this structure can arise:

- *Conformal symmetry/scale invariance*: The structure (2.22), which has only terms with dimensionless couplings, can arise from models with a classical conformal symmetry [144–146] or hidden scale invariance [147, 148]. These models have been motivated

	N_1	N_2	N_3	L_α	E_α	Q_i	U_i	D_i	H	ϕ
U(1)	-1	-1	-1	-1	-1	1/3	1/3	1/3	0	2
Z_3	1	1	1	1	1	0	0	0	0	1

Table 2.1: Examples of an anomaly-free global U(1) and Z_3 symmetry that can give the Lagrangian structure (2.22). Note: E_α are the right-handed charged leptons, Q_i $(i = 1, 2, 3)$ are the left-handed quark doublets, and U_i, D_i are the right-handed quarks.

as a solution to the hierarchy problem: the conformal symmetry forbids tree-level scalar mass terms while radiative breaking of this symmetry by the conformal anomaly is responsible for EW symmetry breaking and, in [147, 148], a hierarchy between the EW and Planck scales from a choice of large scale f.

- *(Approximate) Global U(1) symmetry*: For a complex ϕ, the structure (2.22) can arise from a global U(1) symmetry under which ϕ is charged. We use a global symmetry to avoid introducing a new low-energy gauge sector. Since it has been argued that the only symmetries allowed in an effective low-energy theory are those that derive from gauge symmetries [149], note that approximate global symmetries (approximate because they are broken by non-perturbative effects) can arise from string theory as the remnant of a non-linearly realized U(1) gauge symmetry in which the gauge boson acquires a string scale mass through its coupling to a Stueckelberg field [150]. For a consistent model, the underlying U(1) gauge symmetry must be anomaly-free or Green-Schwarz anomalous [151, 152]. An anomaly-free example in which matter fields have $\mathrm{U}(1)_{B-L}$ charges is given in table 2.1.

- *Discrete Z_N symmetry*: A discrete Z_N symmetry can also give the structure (2.22). Such symmetries can arise from the spontaneous breaking of a gauge symmetry at a high scale [153] or from coupling selection rules on heterotic orbifolds (see [154] and references therein). Note that it is often easier to satisfy the anomaly cancellation conditions for Z_N symmetries [154, 155] than those for U(1) symmetries: an anomaly-free Z_3 example is given in table 2.1.[12] However, the spontaneous breaking of discrete symmetries can produce domain walls [158] and care must be taken to avoid these, such as by having the symmetry breaking phase transition occur below 1 MeV [159].

[12]The mixed Z_N-$\mathrm{U}(1)_Y$-$\mathrm{U}(1)_Y$ anomaly does not pose a meaningful constraint since the hypercharge normalization is not fixed [156, 157].

Constructing a model with a classical scale invariance to give the desired Lagrangian structure (2.22) is intriguing but goes beyond the scope of this chapter; these ideas are considered further in chapter 4. For now, we use a global U(1) symmetry rather than a discrete Z_N symmetry to avoid introducing the problems associated with domain walls at this stage.

Now consider the hierarchy of Majorana masses and Yukawa couplings in the νNMSM. To explain the small Yukawa couplings $\tilde{F}_{\alpha 1} \lesssim 10^{-13}$ and, for a complex ϕ, to prevent the fast dark matter decay channel $N_1^m \to \nu^m \chi$, we introduce a Z_2 symmetry under which only N_1 is charged (see table 2.2).[13] This symmetry allows only the couplings

$$F_{\alpha I} = \begin{pmatrix} 0 & F_{e2} & F_{e3} \\ 0 & F_{\mu 2} & F_{\mu 3} \\ 0 & F_{\tau 2} & F_{\tau 3} \end{pmatrix}, \quad \lambda_{IJ} = \begin{pmatrix} \lambda_{11} & 0 & 0 \\ 0 & \lambda_{22} & \lambda_{23} \\ 0 & \lambda_{23} & \lambda_{33} \end{pmatrix}, \tag{2.23}$$

and hence forbids mixing of N_1 with the other neutrinos, making N_1^m completely stable ($\theta_1 = 0$) and one active neutrino exactly massless. The required pattern of Majorana masses and Yukawa couplings can then be produced if there are strong hierarchies in the remaining λ_{IJ} and $F_{\alpha I}$, specifically if

$$\begin{gathered} F_{\alpha 2} \sim F_2, \quad F_{\alpha 3} \sim F_3, \\ \lambda_{11} \sim \frac{M_1}{\langle\phi\rangle}, \quad \lambda_{23} \sim \frac{M}{\langle\phi\rangle}, \quad \max\{\lambda_{22}, \lambda_{33}\} \sim \frac{\Delta M}{\langle\phi\rangle}. \end{gathered} \tag{2.24}$$

We consider two possibilities for generating these hierarchies from an underlying symmetry, in which case the small couplings in (2.24) are preserved under the RG flow:

- *Froggatt-Nielsen mechanism*: The Froggatt-Nielsen mechanism [160] is a well-known method of generating hierarchical parameters. In brief, a new $\mathrm{U}(1)_{\mathrm{FN}}$ gauge symmetry that is spontaneously broken by a flavon field ϑ at a very high scale is introduced. Fields of the νNMSM are charged under this $\mathrm{U}(1)_{\mathrm{FN}}$ so that ϑ (or $\vartheta^\dagger$) must couple to the terms in (2.22) with various powers to form gauge singlets. After the $\mathrm{U}(1)_{\mathrm{FN}}$ is spontaneously broken, these non-renormalizable terms are suppressed by powers of $\eta \equiv \langle\vartheta\rangle / M_{\mathrm{Pl}}$, where η is a free parameter (though typically assumed to be on the order of the Cabibbo angle [123, 161]). Of course, multiple flavon fields ϑ_i with various $\eta_i \equiv \langle\vartheta_i\rangle / M_{\mathrm{Pl}}$ may be used, as well as a discrete Z_N symmetry in place of the $\mathrm{U}(1)_{\mathrm{FN}}$.

[13] The anomaly cancellation conditions for this Z_2 are trivially satisfied. Therefore this symmetry is exact at the quantum level.

- *Non-perturbative symmetry breaking*: Another possibility for generating hierarchical parameters comes from non-perturbative symmetry breaking in string theory. In [162], for example, it is shown that heterotic string compactifications on Calabi-Yau manifolds can give models with the SM gauge group and additional U(1) symmetries. These additional symmetries can play a role analogous to that of the $\mathrm{U}(1)_{\mathrm{FN}}$: if the νNMSM fields are charged under these symmetries, the terms in (2.22) may require couplings to various powers of $\vartheta_i \equiv e^{-T^i/M_{\mathrm{Pl}}}$ to form gauge singlets, where $T^i = t^i + 2i\chi^i$ are Kähler moduli with axionic components χ^i (not to be confused with the Goldstone boson χ) that transform non-linearly under the U(1). After these symmetries are spontaneously broken by $\langle t^i \rangle \gg M_{\mathrm{Pl}}$ [162, 163], the terms in (2.22) are suppressed by powers of $\eta_i \equiv e^{-\langle t^i \rangle/M_{\mathrm{Pl}}}$. Again, discrete Z_N symmetries may be used in place of the U(1) symmetries.

Although either mechanism may be used to generate the hierarchical parameters (2.24) for the same charge assignment, the non-perturbative symmetry breaking mechanism does not require additional symmetry breaking or scalar particles below the Planck scale and therefore adheres closer to the "minimal" philosophy of the νMSM.

To fix the absolute scale of the couplings λ_{IJ} and hence construct an explicit model of symmetries in the flavour sector, the values of m_ϕ and $\langle \phi \rangle$ must be fixed (see (2.18) and (2.24)) by some model of the scalar sector. We now consider two models of the scalar sector that are motivated as solutions to other possible problems with the νMSM.

2.3.2 Stabilization of the electroweak vacuum

For a Higgs mass $m_h \simeq 125$–126 GeV, the SM (and hence νMSM) potential develops an instability below the Planck scale unless the top mass is about 2σ below its central value [110]. While it is possible that more precise measurements of the top mass will lower its central value and relieve this tension, we first consider a model of the scalar sector in which the Higgs singlet can, for the central value of the top mass, stabilize the EW vacuum through a scalar threshold effect.

This model, described in [113], considers a complex ϕ and scalar potential of the form

$$V = \lambda_h \left(H^\dagger H - \frac{v^2}{2} \right)^2 + \lambda_\phi \left(\phi^\dagger \phi - \frac{w^2}{2} \right)^2 + 2\lambda_{h\phi} \left(H^\dagger H - \frac{v^2}{2} \right) \left(\phi^\dagger \phi - \frac{w^2}{2} \right), \qquad (2.25)$$

which is the most general renormalizable potential that respects a global Abelian symmetry under which only ϕ is charged. Values of $\lambda_h, \lambda_\phi > 0$ and $\lambda_{h\phi}^2 < \lambda_h \lambda_\phi$ are assumed so that the minimum of this potential is given by

$$\left\langle H^\dagger H \right\rangle = \frac{v^2}{2}, \quad \left\langle \phi^\dagger \phi \right\rangle = \frac{w^2}{2}, \tag{2.26}$$

where $v = 246$ GeV. The mass matrix for the real components of H and ϕ is then

$$\mathcal{M}^2 = 2 \begin{pmatrix} \lambda_h v^2 & \lambda_{h\phi} v w \\ \lambda_{h\phi} v w & \lambda_\phi w^2 \end{pmatrix}, \tag{2.27}$$

while the imaginary component of ϕ (i.e. χ) remains massless. In contrast to other models that use a Higgs singlet to stabilize the EW vacuum (e.g. [111, 112]), this model assumes $w \gg v$. The two eigenstates of (2.27) then have masses

$$m_h^2 = 2v^2 \left[\lambda_h - \frac{\lambda_{h\phi}^2}{\lambda_\phi} + \mathcal{O}\left(\frac{v^2}{w^2}\right) \right], \tag{2.28}$$

$$m_\phi^2 = 2w^2 \left[\lambda_\phi + \frac{\lambda_{h\phi}^2}{\lambda_\phi} \left(\frac{v^2}{w^2}\right) + \mathcal{O}\left(\frac{v^4}{w^4}\right) \right], \tag{2.29}$$

with a mixing angle $\theta_{h\phi} \sim v/w$. Integrating out the heavier state for scales below m_ϕ gives the effective potential

$$V_{\text{eff}} = \lambda \left(H^\dagger H - \frac{v^2}{2} \right)^2, \quad \lambda \equiv \lambda_h - \frac{\lambda_{h\phi}^2}{\lambda_\phi}, \tag{2.30}$$

where the matching condition for the Higgs quartic coupling gives a tree-level shift $\delta\lambda \equiv \lambda_{h\phi}^2/\lambda_\phi$ from λ just below m_ϕ to λ_h just above m_ϕ. Provided m_ϕ is below the instability scale $\Lambda \simeq 10^{11}$ GeV [110], a value of $\delta\lambda \simeq 0.01$ can push the instability beyond the Planck scale.

Due to the massless Goldstone boson χ, the value of $\lambda_{h\phi}$ is constrained by limits on the invisible branching ratio of the Higgs. For $m_h \simeq 125$ GeV, the total SM decay width of the Higgs is [164]

$$\Gamma_{\text{SM}} = 4.07 \text{ MeV}, \tag{2.31}$$

while the invisible decay width for $h^m \to \chi\chi$ is [165]

$$\Gamma_{\text{inv}} = \frac{\lambda_{h\phi}^2 v^2}{8\pi m_h}. \tag{2.32}$$

Allowing an invisible branching ratio of up to 30% [140] gives the constraint

$$\lambda_{h\phi}(m_h) \lesssim 0.01. \tag{2.33}$$

	N_1	N_2	N_3	L_α	E_α	Q_i	U_i	D_i	H	ϕ	ϑ_1	ϑ_2
U(1)	-1	-1	-1	-1	-1	1/3	1/3	1/3	0	-1	3	0
Z_3	0	1	-1	0	0	0	0	0	0	0	0	1
Z_2	1	0	0	0	0	0	0	0	0	0	0	0

Table 2.2: Charge assignments for the stabilization of the EW vacuum scenario. The global U(1) symmetry gives the structure (2.22) while the discrete Z_3 and Z_2 symmetries, together with the fields ϑ_1 and ϑ_2, give the required hierarchies in $F_{\alpha I}$ and λ_{IJ}.

A value of $\delta\lambda$ that stabilizes the EW vacuum and is consistent (2.33) can then be obtained for $\lambda_\phi \lesssim 0.01$ (the running of $\lambda_{h\phi}$ and λ_ϕ is small for these values). We illustrate this by constructing a model with $\lambda_{h\phi}, \lambda_\phi \sim 0.01$ and hence an invisible branching ratio of the Higgs of about 30%.[14] For these values, one can show that χ remains in thermal equilibrium down to temperatures just below m_μ. The model therefore has a $\Delta N_{\rm eff} \simeq 4/7$ contribution to the effective number of neutrino species from χ and hence a total value of $N_{\rm eff} \simeq 3.6$. This value can be tested by the Planck experiment and other future CMB experiments [143].

Now consider the flavour sector of the νNMSM for this model of the scalar sector. For $\lambda_{h\phi} \sim 0.01$, the interactions $H^\dagger H \leftrightarrow \phi^m \phi^m$ keep ϕ^m (the real component of ϕ) in thermal equilibrium down to temperatures $T \ll m_\phi$ for any mass $m_\phi \lesssim \Lambda$. We are therefore in the dark matter production case $r_f \gg 1$. For $\lambda_\phi \sim 0.01$, the ratio $m_\phi / \langle\phi\rangle$ is fixed by (2.29) and (2.18) gives a value of

$$\lambda_{11} \sim 1 \times 10^{-8} \tag{2.34}$$

to produce the correct dark matter abundance.[15] The Lyman-α forest bound (2.20) is therefore satisfied for a choice $\langle\phi\rangle \gtrsim 500$ GeV. Taking $\langle\phi\rangle \simeq 10^8$ GeV, a pattern of masses M_{IJ} and couplings $F_{\alpha I}$ that gives the correct dark matter abundance and baryon asymmetry can be achieved with two fields ϑ_1, ϑ_2, the values $\eta_1 \simeq 10^{-8}$, $\eta_2 \simeq 10^{-7}$, and the charge assignments given in table 2.2. We stress that this is the simplest anomaly-free model we could find, though other charge assignments are possible.[16]

For the sake of definiteness, suppose that the non-perturbative symmetry breaking mechanism is used for generating the hierarchies in $F_{\alpha I}$ and λ_{IJ}; that is, $\vartheta_i = e^{-T^i/M_{\rm Pl}}$ and

[14] It is, however, quite simple to construct models with a smaller invisible branching ratio by taking smaller $\lambda_{h\phi}$ and λ_ϕ while keeping $\delta\lambda$ fixed.

[15] Here we have used $S \simeq 1$ (anticipating $M \sim 1$ GeV) and taken $m_\phi \gtrsim T_{\rm EW}$ for $f(m_\phi)$. Also, λ_{11} must be a factor of $\sqrt{2}$ larger than in (2.18) for a complex ϕ since only the real component of ϕ can decay to N_1^m.

[16] The Z_3 and Z_2 symmetries could be combined in a single Z_6, if desired.

$\eta_i = e^{-\langle t^i \rangle / M_{\rm Pl}}$ for $i = \{1, 2\}$. From table 2.2, the Lagrangian for the flavour sector is then

$$\begin{aligned}\Delta\mathcal{L} = &-f_{\alpha 2}\vartheta_2^\dagger \bar{L}_\alpha N_2 H - f_{\alpha 3}\vartheta_2 \bar{L}_\alpha N_3 H - \frac{h_{11}}{2}\vartheta_1 \phi \bar{N}_1^c N_1 - \frac{h_{22}}{2}\vartheta_1\vartheta_2 \phi \bar{N}_2^c N_2 \\ &- \frac{h_{23}}{2}\vartheta_1 \phi \bar{N}_2^c N_3 - \frac{h_{32}}{2}\vartheta_1 \phi \bar{N}_3^c N_2 - \frac{h_{33}}{2}\vartheta_1\vartheta_2^\dagger \phi \bar{N}_3^c N_3 + \text{h.c.},\end{aligned} \tag{2.35}$$

where $f_{\alpha I}$ and h_{IJ} are $\mathcal{O}(1)$ couplings. Meanwhile, the scalar potential is given by (2.25) plus the additional terms $\vartheta_i^\dagger \vartheta_i H^\dagger H$, $\vartheta_i^\dagger \vartheta_i \phi^\dagger \phi$, and $\vartheta_1 \phi^3 + \vartheta_1^\dagger \phi^{\dagger 3}$ involving ϑ_1 and ϑ_2. Note that we must assume these additional terms, which are allowed by the symmetries, have sufficiently small coefficients to preserve (2.25). For the former two terms, this assumption corresponds to a hierarchy problem in the scalar sector unless the small coefficients of these terms can arise in a technically natural way. Demonstrating that such a scenario is possible, if indeed it is, goes beyond the scope of this chapter. It is interesting to see, however, that in order to produce hierarchical parameters in the flavour sector of the νNMSM with symmetries the hierarchy problem in the scalar sector may be made worse.[17] For the latter terms $\vartheta_1 \phi^3 + \vartheta_1^\dagger \phi^{\dagger 3}$, we similarly accept a small parameter in the scalar sector without explanation,[18] but note that these terms could also be forbidden by an additional U(1) symmetry under which ϕ and ϑ_1 have opposite charges.

After the spontaneous symmetry breaking associated with ϑ_1 and ϑ_2, (2.35) reduces to (2.22) with the textures

$$F_{\alpha I} \sim \begin{pmatrix} 0 & \eta_2 & \eta_2 \\ 0 & \eta_2 & \eta_2 \\ 0 & \eta_2 & \eta_2 \end{pmatrix}, \quad \lambda_{IJ} \sim \begin{pmatrix} \eta_1 & 0 & 0 \\ 0 & \eta_1\eta_2 & \eta_1 \\ 0 & \eta_1 & \eta_1\eta_2 \end{pmatrix}. \tag{2.36}$$

The parameters of the νNMSM are then

$$\begin{gathered} F_{\alpha 2} \sim 1 \times 10^{-7}, \quad F_{\alpha 3} \sim 1 \times 10^{-7}, \\ M_1 \sim 1 \text{ GeV}, \quad M \sim 1 \text{ GeV}, \quad \Delta M \sim 100 \text{ eV}, \end{gathered} \tag{2.37}$$

up to $\mathcal{O}(1)$ constants. This example shows that, in contrast to the νMSM, dark matter in the νNMSM can be much heavier than the keV scale. Active neutrino mixing in this model

[17] This point is particularly relevant to the recent work [166], which has suggested that the Higgs mass in the SM does not have the quadratic divergence that is usually identified with the hierarchy problem. In this case, trying to explain the hierarchical parameters of any model with additional heavy scalars may reintroduce the hierarchy problem.

[18] The $\vartheta_1 \phi^3 + \vartheta_1^\dagger (\phi^\dagger)^3$ terms give χ a small mass and lead to the formation of a discrete Z_3 symmetry in ϕ after the spontaneous symmetry breaking associated with ϑ_1, which can introduce potentially dangerous domain walls when this Z_3 is later broken by the vev of ϕ. The domain wall problem can be avoided for sufficiently small coefficients that bias the different vacua, which leads to a subsequent collapse of the domain wall structure [159].

is anarchical (up to charged lepton corrections) while the charged lepton and quark Yukawa couplings remain unsuppressed. Therefore additional flavour symmetries using the Green-Schwarz anomaly cancellation mechanism, such as in [123, 167], must be used to produce hierarchies in the charged lepton and quark sectors.

As a consistency check on this model, we must verify that N_2^m and N_3^m are out of thermal equilibrium at the characteristic temperature of leptogenesis $T_L \sim 3\times10^3$ GeV. Since $m_\phi \simeq 2 \times 10^7$ GeV $\gg T_L$, ϕ^m has decayed away by leptogenesis[19] and only the scattering processes $H^\dagger H \leftrightarrow N_2^m N_2^m$ and $H^\dagger H \leftrightarrow N_3^m N_3^m$ mediated by ϕ^m and χ need to be considered. For $\lambda_{h\phi} \sim 0.01$, these processes are out of equilibrium at T_L for $\lambda_2, \lambda_3 \simeq \lambda_{23} \lesssim 10^{-5}$, which is satisfied by (2.36).

This model demonstrates that it is possible to use symmetries broken at or near the Planck scale to obtain the hierarchical pattern of Majorana masses and Yukawa couplings required for successful baryogenesis and dark matter production in the νNMSM. The model obeys all phenomenological constraints and allows for the possibility of Higgs inflation by ensuring that the Higgs potential does not develop a second minimum before the Planck scale. Of course, the symmetries used do not address the hierarchy problem associated with radiative corrections to the scalar sector. To do so would involve implementing a supersymmetric version of the theory, which departs from the underlying philosophy of the νMSM, or implementing a conformal symmetry solution, which requires an understanding of how to include gravity in such a theory. This is something we cannot do at present.

2.3.3 ϕ Inflation

Although the Higgs inflation of the νMSM has not been ruled out, it relies on the questionable assumption that new strong dynamics appearing at the scale of perturbative unitarity breakdown, $M_{\rm Pl}/\xi$, preserve the intact shape of the Higgs potential even above $M_{\rm Pl}/\xi$ [82]. We now consider another model of the scalar sector for the νNMSM, given in [103] and developed further in [104, 105], in which the Higgs singlet ϕ can be a light inflaton ($m_\phi < m_h$) and thus provide an alternative to Higgs inflation. The scalar potential of this model is

$$V = \lambda\left(H^\dagger H - \frac{\alpha}{\lambda}\phi^\dagger\phi\right)^2 + \frac{\beta}{4}\left(\phi^\dagger\phi\right)^2 - \frac{1}{2}m^2\phi^\dagger\phi, \tag{2.38}$$

[19] Note that a relic CP-even distribution of N_2^m and N_3^m from the decays of ϕ^m does not affect leptogenesis.

where it is assumed that $m \ll \sqrt{\beta} M_{\rm Pl}$ so that chaotic inflation proceeds via the quartic term and, in contrast to [103–105], we require ϕ to be complex to explain the hierarchical parameters of the νNMSM with an underlying symmetry. The potential (2.38) is then the most general renormalizable potential that respects a global U(1) symmetry under which only ϕ is charged, assuming the bare mass term for the Higgs is negligible.[20] Successful chaotic inflation requires $\beta \simeq 1.5 \times 10^{-13}$ to give the correct amplitude of adiabatic scalar perturbations and $\alpha \lesssim 10^{-7}$, $\lambda_{IJ} \lesssim 1.5 \times 10^{-3}$ to ensure that the flatness of the potential is not spoiled by radiative corrections from the loops of SM particles and sterile neutrinos [105].[21] Achieving a sufficiently high reheating temperature $T_r > T_L$ for baryogenesis requires $\alpha \gtrsim 7 \times 10^{-10}$ [104]. Moreover, a value of $\lambda \simeq 0.13$ is required for $m_h \simeq 125$ GeV. For these parameters, expanding the potential (2.38) about its minimum gives the relations

$$\begin{gathered} \langle H \rangle = \frac{v}{\sqrt{2}}, \quad \langle \phi \rangle = \sqrt{\frac{\lambda}{2\alpha}} v, \quad m_h \simeq \sqrt{2\lambda} v, \\ m_\phi \simeq m \simeq \sqrt{\frac{\beta\lambda}{2\alpha}} v, \quad \theta_{h\phi} \simeq \sqrt{\frac{\alpha}{\lambda}}, \end{gathered} \tag{2.39}$$

where $v = 246$ GeV. The upper bound on α can be further strengthened by limits on axion searches in the CHARM experiment [105]. The mass range allowed by this experiment, 270 MeV $\lesssim m_\phi \lesssim$ 1.8 GeV, corresponds to $2 \times 10^{-10} \lesssim \alpha \lesssim 8 \times 10^{-9}$ for $m_h \simeq 125$ GeV. Note that we do not provide an explanation for the small values of α and β in the scalar potential; we simply take their values to be within the range allowed by successful inflation. Also note that, for $\alpha \lesssim 8 \times 10^{-9}$, the invisible branching ratio of the Higgs is negligible.

Now consider the flavour sector of the νNMSM for this model of the scalar sector. As in [103], we assume an inflaton mass $m_\phi \gtrsim 300$ MeV so that the mixing angle $\theta_{h\phi}$ is large enough to keep ϕ^m in thermal equilibrium down to temperatures $T \ll m_\phi$ via the interactions $\phi^m \leftrightarrow e^- e^+, \phi^m \leftrightarrow \mu^- \mu^+$, etc. We are therefore in the dark matter production case $r_f \gg 1$. The ratio $m_\phi / \langle \phi \rangle = \sqrt{\beta}$ is fixed by (2.39) and (2.18) gives a value of

$$\lambda_{11} \sim 3 \times 10^{-11} \tag{2.40}$$

[20] For a real ϕ, (2.38) was originally presented as the most general scale invariant potential in which the scale invariance is explicitly broken by a mass term for ϕ [103].

[21] As mentioned in [103], chaotic inflation with a quartic potential is disfavoured by WMAP data [168]. However, only a very small non-minimal coupling to gravity of $\xi \gtrsim 0.0027$ can help bring this model in line with the data [169].

	N_1	N_2	N_3	L_α	E_α	Q_i	U_i	D_i	H	ϕ	ϑ_1	ϑ_2
U(1)	5	-4	-4	-1	-1	1/3	1/3	1/3	0	2	3	0
Z_4	0	1	-1	0	0	0	0	0	0	0	0	1
Z_2	1	0	0	0	0	0	0	0	0	0	0	0

Table 2.3: Charge assignments for the ϕ inflation scenario. The global U(1) symmetry gives the structure (2.22) while the discrete Z_4 and Z_2 symmetries, together with the fields ϑ_1 and ϑ_2, give the required hierarchies in $F_{\alpha I}$ and λ_{IJ}.

to produce correct dark matter abundance.[22] The absolute scale of $\langle\phi\rangle$, however, is not fixed. There is a relatively narrow window 7×10^5 GeV $\lesssim\langle\phi\rangle\lesssim 2\times10^6$ GeV that is consistent with the constraints on α, the assumption $m_\phi\gtrsim 300$ MeV, and the Lyman-α forest bound. Taking $\langle\phi\rangle\simeq 10^6$ GeV, a pattern of masses M_{IJ} and couplings $F_{\alpha I}$ that gives the correct dark matter abundance and baryon asymmetry can be achieved with two fields ϑ_1, ϑ_2, the values $\eta_1\simeq 2\times10^{-3}$, $\eta_2\simeq 5\times10^{-5}$, and the charge assignments given in table 2.3. Again, this is the simplest anomaly-free model we could find, though other charge assignments are possible.

Suppose this time that the Froggatt-Nielsen mechanism is used for generating the hierarchies in $F_{\alpha I}$ and λ_{IJ}, and hence $\eta_1=\langle\vartheta_1\rangle/M_{\rm Pl}$ and $\eta_2=\langle\vartheta_2\rangle/M_{\rm Pl}$.[23] From table 2.3, the Lagrangian for the flavour sector is then

$$\begin{aligned}\Delta\mathcal{L}=&-f_{\alpha2}\left(\frac{\vartheta_1\vartheta_2^\dagger}{M_{\rm Pl}^2}\right)\bar L_\alpha N_2 H-f_{\alpha3}\left(\frac{\vartheta_1\vartheta_2}{M_{\rm Pl}^2}\right)\bar L_\alpha N_3 H-\frac{h_{11}}{2}\left(\frac{\vartheta_1^{\dagger4}}{M_{\rm Pl}^4}\right)\phi\bar N_1^c N_1\\&-\frac{h_{22}}{2}\left(\frac{\vartheta_1^2\vartheta_2^{\dagger2}}{M_{\rm Pl}^4}\right)\phi\bar N_2^c N_2-\frac{h_{23}}{2}\left(\frac{\vartheta_1^2}{M_{\rm Pl}^2}\right)\phi\bar N_2^c N_3\\&-\frac{h_{32}}{2}\left(\frac{\vartheta_1^2}{M_{\rm Pl}^2}\right)\phi\bar N_3^c N_2-\frac{h_{33}}{2}\left(\frac{\vartheta_1^2\vartheta_2^2}{M_{\rm Pl}^4}\right)\phi\bar N_3^c N_3+\text{h.c.},\end{aligned}\tag{2.41}$$

where $f_{\alpha I}$ and h_{IJ} are $\mathcal{O}(1)$ couplings. Meanwhile, the scalar potential is given by (2.38) plus the additional terms $\vartheta_i^\dagger\vartheta_i H^\dagger H$, $\vartheta_i^\dagger\vartheta_i\phi^\dagger\phi$, and $\vartheta_1^{\dagger2}\phi^3+\vartheta_1^2\phi^{\dagger3}$ involving ϑ_1 and ϑ_2. Again, we must assume that these additional terms in the scalar sector, which are allowed by the symmetries, have sufficiently small coefficients to preserve (2.38). Once ϑ_1 and ϑ_2 acquire vevs, (2.41) reduces to (2.22) with the textures

$$F_{\alpha I}\sim\begin{pmatrix}0&\eta_1\eta_2&\eta_1\eta_2\\0&\eta_1\eta_2&\eta_1\eta_2\\0&\eta_1\eta_2&\eta_1\eta_2\end{pmatrix},\quad \lambda_{IJ}\sim\begin{pmatrix}\eta_1^4&0&0\\0&\eta_1^2\eta_2^2&\eta_1^2\\0&\eta_1^2&\eta_1^2\eta_2^2\end{pmatrix}.\tag{2.42}$$

[22] We have anticipated $S\simeq 1$ and $m_\phi\simeq 400$ MeV in obtaining (2.40), though these parameters only have an $\mathcal{O}(1)$ effect on λ_{11}.

[23] Here we assume that the messenger states that are integrated out to give the higher dimensional operators have Planck-scale masses.

The parameters of the νNMSN are then

$$\begin{gathered} F_{\alpha 2} \sim 1 \times 10^{-7}, \quad F_{\alpha 3} \sim 1 \times 10^{-7}, \\ M_1 \sim 20 \text{ keV}, \quad M \sim 4 \text{ GeV}, \quad \Delta M \sim 10 \text{ eV}, \end{gathered} \tag{2.43}$$

up to $\mathcal{O}(1)$ constants. As before, active neutrino mixing is anarchical (up to charged lepton corrections) and additional flavour symmetries must be used to produce hierarchies in the charged lepton and quark sectors. We also have the parameters

$$\alpha \simeq 4 \times 10^{-9}, \quad m_\phi \simeq 400 \text{ MeV}, \quad \theta_{h\phi} \simeq 2 \times 10^{-4}. \tag{2.44}$$

For these values, it can be shown that χ remains in thermal equilibrium roughly while ϕ^m does (to temperatures below m_μ) via the interactions $\phi^m \leftrightarrow \chi\chi$. The near massless χ therefore contributes $\Delta N_{\text{eff}} \simeq 4/7$ to the effective number of neutrino species.

As a consistency check on this model, we must verify that N_2^m and N_3^m are out of thermal equilibrium at the characteristic temperature of leptogenesis $T_L \sim 2 \times 10^3$ GeV. Since $m_\phi < 2M$, the processes $\phi^m \to N_2^m N_2^m$ and $\phi^m \to N_3^m N_3^m$ are kinematically forbidden and the dominant processes are $H^\dagger H \leftrightarrow N_2^m N_2^m$ and $H^\dagger H \leftrightarrow N_3^m N_3^m$. These are out of equilibrium at T_L for $\lambda_{23} \lesssim 0.01$, which is satisfied by (2.42). One can also verify that the reheating temperature for $\alpha \simeq 4 \times 10^{-9}$ can be as large as $T_r \simeq 5 \times 10^3$ GeV [104], which is above the leptogenesis temperature.

This model demonstrates that, for a scenario in which ϕ is a light inflaton, it is again possible to use symmetries broken at or near the Planck scale to obtain the pattern of Majorana masses and Yukawa couplings required for successful baryogenesis and dark matter production in the νNMSM. This model obeys all phenomenological constraints and provides an alternative to the Higgs inflation of the νMSM, but it requires small parameters in the scalar potential without explanation (a problem that plagues virtually all inflationary models) and does not improve the stability of the EW vacuum.

2.4 Conclusion

The νMSM is an extension of the SM that attempts to explain neutrino oscillations, dark matter, the baryon asymmetry of the universe, and inflation using only three sterile neutrinos with masses below the EW scale. Despite the phenomenological successes of the νMSM, a

further extension may be necessary to accommodate the Lyman-α forest bound, stabilize the EW vacuum, and allow for inflation. In this chapter, we have studied extensions of the νMSM by a Higgs singlet ϕ that can address these issues and have demonstrated how the required pattern of masses and couplings in the flavour sector of such models can arise from an underlying symmetry.

Our starting point has been an extension of the νMSM in which the decays of ϕ give a primordial production of dark matter that is readily consistent with the Lyman-α forest bound and in which the vev of ϕ produces the Majorana masses of the sterile neutrinos. For this next-to-minimal model, or νNMSM, we have considered two specific models of the scalar sector: one in which ϕ helps stabilize the EW vacuum through a scalar threshold effect and one in which ϕ is a light inflaton. For these definite examples, we have demonstrated that symmetries broken at or near the Planck scale can produce the required hierarchical pattern of Majorana masses and Yukawa couplings. The former model uses a $\mathrm{U}(1) \times Z_3 \times Z_2$ symmetry while the latter uses a $\mathrm{U}(1) \times Z_4 \times Z_2$ symmetry; both require a complex ϕ rather than, as typically assumed, a real ϕ. The domain wall problem associated with the breaking of the discrete Z_N symmetries can be avoided for an appropriate choice of scalar sector parameters. We have not, however, provided an explanation for scalar sector parameters or addressed the hierarchy problem associated with radiative corrections to the scalar sector.

The models presented in this chapter satisfy all phenomenological constraints and make several experimental predictions that are distinct from the νMSM. These predictions include completely stable N_1^m dark matter (hence no visible X/γ-ray signals from its decays) as well as anarchical active neutrino mixing angles (up to charged lepton corrections) with one active neutrino exactly massless. Moreover, due to the complex ϕ, both models have $N_{\mathrm{eff}} \simeq 3.6$ for the effective number of neutrino species while the former model has an invisible branching ratio of the Higgs of about 30%. It will therefore be possible to test these models with the Planck experiment and the LHC in the near future.

2.5 Recent developments

Since the publication of this work, two independent collaborations have claimed the detection of a 3.55 keV photon line using data from the XMM and Chandra satellites [170, 171]. One

possible interpretation of the signal, if confirmed, is a sterile neutrino with a mass of 7.1 keV and a mixing angle of $\sin^2(2\theta) \simeq 7 \times 10^{-11}$. In the context of this work, such a state is naturally identified with N_1 and is just within the range where the Lyman-α bounds might be satisfied for a RP of dark matter scenario in the νMSM (see discussion around (2.12)). Alternatively, in the νNMSM it is within the Lyman-α bound (2.20) for $g_{*s}(T_{\rm prod}) \gtrsim 30$ and is compatible with dark matter production from the decay of the Higgs singlet. It should be mentioned, however, that similar X-ray signals have been reported in the past [172] and subsequently disappeared [173], and the strength of the current signal shows a significant dependence on the modelling of nearby potassium and chlorine lines [174–176].

Updated limits from the LHC have also put a stronger bound on the invisible branching ratio of the Higgs, which now must be less than about 18% [177]. The example of the νNMSM presented here with the stabilization of the EW vacuum, which has $\lambda_{h\phi}, \lambda_\phi \sim 0.01$ and an invisible Higgs branching ratio of approximately 30%, is therefore in some tension with the new bound. As mentioned above, though, it is straightforward to take $\lambda_{h\phi}$ and λ_ϕ slightly smaller while maintaining the ratio $\delta\lambda = \lambda_{h\phi}^2/\lambda_\phi$ so that the EW vacuum is stabilized and the Higgs invisible branching ratio bound is also satisfied. Interestingly, the pattern of couplings $\lambda_\phi \sim \lambda_{h\phi}^2 \ll 1$, which is what is needed to stabilize the EW vacuum through a scalar threshold effect, is technically natural (see chapter 4) and can avoid the hierarchy problem associated with large corrections to the Higgs mass from the singlet scalar ϕ for $\lambda_\phi \sim v/w$. The hierarchy problem from the additional scalar fields ϑ_i, however, remains unless the couplings for the terms $\vartheta_i^\dagger \vartheta_i H^\dagger H$ and $\vartheta_i^\dagger \vartheta_i \phi^\dagger \phi$ are also sufficiently small and arise in a technically natural way.

Chapter 3

Higgs ξ-inflation for the 125–126 GeV Higgs: a two-loop analysis

The second topic of the thesis also studies the phenomenology of the νMSM, but the focus is on issues related to the model of Higgs inflation used in the νMSM. Specifically, the work is concerned with the technical details of Higgs ξ-inflation and its numerical predictions in the region for which the Higgs self-coupling λ runs to small values near the Planck scale, as suggested by the Higgs mass measurement of $M_h \simeq 125$–126 GeV. This small λ scenario is relevant to the picture of the SM up to the Planck scale if there is some underlying symmetry enforcing the boundary condition $\lambda(M_{\rm Pl}) \sim 0$.

Disclaimer: This chapter contains a nearly identical copy of my work in ref. [178] plus a discussion of recent developments that have occurred since publication.

3.1 Introduction

A period of exponential expansion of the early universe driven by the potential energy of a scalar field — the inflaton — is an elegant explanation for the flatness, isotropy and homogeneity of the universe today [45–49]. Furthermore, it provides a very plausible mechanism for generating the nearly scale invariant spectrum of primordial density fluctuations that have been imprinted on the CMB [11, 50] and have grown into the large scale structure of galaxies [179]. The nature of the inflaton is, however, still unknown. While a large number of inflationary models that extend the scalar degrees of freedom of the SM have been proposed (see e.g. [52, 53]), the possibility that the SM Higgs boson is the inflaton — a scenario attractive for its minimality — still remains for the model of Higgs inflation from a

non-minimal coupling to gravity [54].[1]

This model of Higgs inflation, based on the work of [180–183], makes use of a large non-minimal gravitational coupling $\xi H^\dagger H \mathcal{R}$ between the Higgs doublet H and the Ricci scalar $\mathcal{R}$.[2] The effect of this coupling is to flatten the SM potential above the scale $M_{\rm Pl}/\sqrt{\xi}$, thereby allowing a sufficiently flat region for slow roll inflation. An analysis of the tree-level potential finds $\xi \simeq 5 \times 10^4 \sqrt{\lambda}$ is required to produce the correct amplitude of primordial density fluctuations [54], which for $M_h \simeq 125$–126 GeV [184] gives $\xi \sim 2 \times 10^4$. The predictions for the spectral index and the tensor-to-scalar ratio are also well within the current 1σ allowed regions from WMAP9 [11] and *Planck* 2013 [50].

It has been pointed out, however, that Higgs ξ-inflation with the large value $\xi \sim 10^4$ suffers from a serious problem. Perturbative unitarity is violated at the scale $M_{\rm Pl}/\xi$, and new physics entering at $M_{\rm Pl}/\xi$ to restore unitarity is naively expected to contain new particles and interactions that affect the potential in an uncontrollable way [185–188].[3] The self-consistency of the model in the inflationary region $h \gtrsim M_{\rm Pl}/\sqrt{\xi}$ is therefore questionable. To address the issue of unitarity violation while preserving the minimality of Higgs inflation, one must make a rather strong assumption that either additional non-renormalizable Higgs interactions accompany the non-minimal coupling and restore unitarity [116] or that new strong dynamics entering at $M_{\rm Pl}/\xi$ restores unitarity in a non-perturbative way [114, 189, 191, 192]. It is unknown whether the former approach can be made consistent with quantum corrections or the effect of additional potential and Yukawa interactions [117], while it is unclear whether strong coupling in graviton exchange processes for the latter scenario can unitarize scattering cross sections without requiring new physics [117]. If the latter scenario is possible, however, an approximate shift symmetry of the potential in the inflationary

[1] Other proposed models of Higgs inflation make use of special features of the SM potential that develop if the Higgs quartic coupling λ runs to very small values. The quasiflat SM potential considered in [55], however, predicts too large an amplitude of density fluctuations while false vacuum inflation [56–58] requires an additional scalar particle to achieve a graceful exit from inflation. Further possibilities, not discussed here, make use of derivative couplings of the Higgs to gravity or other non-renormalizable Higgs couplings [59–63].

[2] This is the only local, gauge-invariant interaction with mass dimension four or less that can be added to the SM once gravity is included.

[3] It has been argued that the scale of perturbative unitarity violation for a large background Higgs field is higher than the small background field estimate $M_{\rm Pl}/\xi$ and, in particular, does not spoil the perturbative analysis of inflation [114, 189, 190]. In this case, one must make a non-trivial assumption about the new physics sector that the scale of new physics is background dependent [117]. In this chapter, we make the more conservative assumption that the scale of new physics is independent of the background Higgs field and therefore must be taken to be the lowest scale of perturbative unitarity violation, $M_{\rm Pl}/\xi$.

region $h \gtrsim M_{\rm Pl}/\sqrt{\xi}$ may keep quantum corrections to the potential under control [114].

The problem of perturbative unitarity violation in Higgs ξ-inflation, at least with regard to new physics entering at $M_{\rm Pl}/\xi$ below the inflationary scale, is perhaps not as severe as the tree-level estimate of ξ suggests. A Higgs mass $M_h \simeq 125$–126 GeV is in the region that, for a top quark mass only about 2σ below its central value, the effective Higgs quartic coupling $\lambda_{\rm eff}(\mu)$ can run to very small (positive) values near the Planck scale [64, 82, 193]. The effect of small $\lambda_{\rm eff}(\mu)$ near the Planck scale is to reduce the value of ξ necessary for successful inflation [189, 191, 194] and hence push the scale of perturbative unitarity violation toward the inflationary scale. If inflation with $\xi \sim 1$ is possible for sufficiently small $\lambda_{\rm eff}(\mu)$ — a scenario that is not yet explored — the problem of perturbative unitarity violation occurring below the inflationary scale can be avoided.[4] Of course, an investigation of this possibility requires a proper treatment of the RG evolution and effective potential within the framework of Higgs ξ-inflation.

Extending the analysis of Higgs ξ-inflation to higher loop order is not entirely straightforward. While the RG equations of the SM are perfectly adequate for describing the RG evolution below $M_{\rm Pl}/\xi$, there are two ambiguities in the RG evolution above $M_{\rm Pl}/\xi$ due to the non-minimal coupling of the Higgs. First, quantum loops involving the physical Higgs field (and not the Nambu-Goldstone bosons present in the Landau gauge) are heavily suppressed in this region [189, 191]. To deal with this, one can either use the chiral EW theory (SM with frozen radial Higgs mode) to derive the RG equations above $M_{\rm Pl}/\xi$ [189] or one can simply use the RG equations of the SM with a suppression factor for each Higgs running in a loop [191, 195–197]. Second, radiative corrections to the SM potential (in particular the choice of the renormalization scale $\mu(h)$) depend on whether they are computed in the Einstein or Jordan frame [194], and it is unclear which frame should be used without knowledge of physics at the Planck scale.

In this chapter, we extend the two-loop analysis of Higgs ξ-inflation [189, 191] to include the three-loop SM beta functions for the gauge couplings [198] as well as the leading three-loop terms for the RG evolution of λ, the top Yukawa coupling y_t, and the Higgs anomalous dimension γ [199]. For the first time, a complete two-loop insertion of suppression factors

[4] In this case, note that although the potential during inflation $V^{1/4} \lesssim 2 \times 10^{16}$ GeV is constrained to be sub-Planckian [11, 50], the non-minimal coupling $\xi H^\dagger H \mathcal{R}$ with $\xi \sim 1$ is still relevant to inflation since the Higgs field $h \sim M_{\rm Pl}/\sqrt{\xi}$ is then assumed to be near the Planck scale.

for the *physical* Higgs loops, which was missing in [191], is carried out. The use of these RG equations provides a modest update to the previous analyses of Higgs ξ-inflation. The main focus of this chapter, however, is to investigate the region of parameter space with $\lambda_{\rm eff}(\mu) \ll 1$ near the Planck scale that exists for the recently measured Higgs mass $M_h \simeq 125$–126 GeV and a top quark mass $M_t \sim 171$ GeV, about 2σ below its central value.[5]

The chapter is organized as follows. In section 3.2, we give a brief review of Higgs ξ-inflation and the tree-level analysis. In section 3.3, the RG equations and the effective potential relevant for a two-loop analysis of Higgs ξ-inflation are presented. The numerical results and inflationary predictions for both the Einstein and Jordan frame renormalization prescriptions, with a particular focus on the small $\lambda_{\rm eff}^{\rm min}$ region, are given in section 3.4. A summary of the results and the conclusions are given in section 3.5.

3.2 Tree-level analysis

Let us first briefly review Higgs ξ-inflation and the tree-level computation of the inflationary predictions. Although the tree-level results will differ from those in the two-loop analysis, many qualitative features of the computation will remain the same.

As an example of inflation from a non-minimally coupled scalar, Higgs ξ-inflation is characterized by a non-minimal gravitational coupling $\xi H^\dagger H \mathcal{R}$ between the Higgs doublet H and the Ricci scalar $\mathcal{R}$. The Lagrangian of the model is given by [54]

$$\mathcal{L} = \mathcal{L}_{\rm SM} - \frac{M^2}{2}\mathcal{R} - \xi H^\dagger H \mathcal{R}, \tag{3.1}$$

where $\mathcal{L}_{\rm SM}$ is the SM Lagrangian and M is a mass parameter (the bare Planck mass) that can safely be identified with the present Planck mass value $M_{\rm Pl} = (8\pi G_N)^{-1/2} \simeq 2.4 \times 10^{18}$ GeV for $\sqrt{\xi} \ll 10^{17}$. The part of (3.1) that is relevant to inflation gives the action

$$S_J = \int d^4x\sqrt{-g}\left[-\frac{M_{\rm Pl}^2}{2}\left(1 + \frac{2\xi H^\dagger H}{M_{\rm Pl}^2}\right)\mathcal{R} + (\partial_\mu H)^\dagger(\partial^\mu H) - V\right], \tag{3.2}$$

where $V = \lambda\left(H^\dagger H - v^2/2\right)^2$ is the SM potential and the subscript J denotes the Jordan frame. This is the frame in which the inflationary model is defined.

[5] For the top quark mass central value, the SM potential develops an instability at around 10^{11} GeV [82, 193]. Since Higgs ξ-inflation requires the stability of the potential up to the inflationary scale $M_{\rm Pl}/\sqrt{\xi}$, one could interpret this result as disfavouring Higgs ξ-inflation at 2σ. The position advocated here is that a special region of Higgs ξ-inflation with $\lambda_{\rm eff}(\mu) \ll 1$ exists within only 2σ of experimental measurements.

To compute the inflationary observables, it is convenient to first remove the non-minimal coupling to gravity in (3.2) by performing the conformal transformation

$$g_{\mu\nu} \to \tilde{g}_{\mu\nu} = \Omega^2 g_{\mu\nu}, \qquad \Omega^2 = 1 + \frac{2\xi H^\dagger H}{M_{\rm Pl}^2}. \tag{3.3}$$

The resulting Einstein frame action is given by [200]

$$S_E = \int d^4x\sqrt{-\tilde{g}}\left[-\frac{M_{\rm Pl}^2}{2}\tilde{\mathcal{R}} + \frac{1}{\Omega^2}\left(\partial_\mu H\right)^\dagger\left(\partial^\mu H\right) + \frac{3\xi^2}{\Omega^4 M_{\rm Pl}^2}\partial_\mu(H^\dagger H)\partial^\mu(H^\dagger H) - \frac{V}{\Omega^4}\right], \tag{3.4}$$

where $\tilde{\mathcal{R}}$ is calculated with the metric $\tilde{g}$. The action (3.4) simplifies greatly in the unitary gauge $H = \frac{1}{\sqrt{2}}\binom{0}{h}$, which may be used for the tree-level computation, giving

$$S_E = \int d^4x\sqrt{-\tilde{g}}\left[-\frac{M_{\rm Pl}^2}{2}\tilde{\mathcal{R}} + \frac{1}{2}\left(\frac{\Omega^2 + 6\xi^2 h^2/M_{\rm Pl}^2}{\Omega^4}\right)\partial_\mu h\partial^\mu h - \frac{V}{\Omega^4}\right], \tag{3.5}$$

where $V = \frac{\lambda}{4}\left(h^2 - v^2\right)^2$ and $\Omega^2 = 1 + \xi h^2/M_{\rm Pl}^2$. It is also convenient to remove the non-canonical kinetic term for the Higgs field in (3.5) by changing to a new scalar field χ, defined by

$$\frac{d\chi}{dh} = \sqrt{\frac{\Omega^2 + 6\xi^2 h^2/M_{\rm Pl}^2}{\Omega^4}}. \tag{3.6}$$

The Einstein frame action then takes the form

$$S_E = \int d^4x\sqrt{-\tilde{g}}\left[-\frac{M_{\rm Pl}^2}{2}\tilde{\mathcal{R}} + \frac{1}{2}\partial_\mu\chi\partial^\mu\chi - U(\chi)\right], \tag{3.7}$$

where the potential is given by

$$U(\chi) = \frac{V}{\Omega^4} = \frac{\lambda(h^2 - v^2)^2}{4(1 + \xi h^2/M_{\rm Pl}^2)^2} \tag{3.8}$$

with $h = h(\chi)$. It is the flattening of the potential $U(\chi)$ to a constant value $U_0 \equiv \lambda M_{\rm Pl}^4/4\xi^2$ in the region $h \gtrsim M_{\rm Pl}/\sqrt{\xi}$ that allows slow roll inflation to occur.

The standard analysis of inflation in the slow roll approximation can be carried out for the field χ and potential $U(\chi)$. In the inflationary region $h^2 \gtrsim M_{\rm Pl}^2/\xi \gg v^2$, the slow roll parameters for $\xi \gg 1$ can be approximated by [191, 201] (see [182] for exact expressions)

$$\epsilon = \frac{M_{\rm Pl}^2}{2}\left(\frac{dU/d\chi}{U}\right)^2 \simeq \frac{4M_{\rm Pl}^4}{3\xi^2 h^4}, \tag{3.9}$$

$$\eta = M_{\rm Pl}^2\frac{d^2U/d\chi^2}{U} \simeq \frac{4M_{\rm Pl}^4}{3\xi^2 h^4}\left(1 - \frac{\xi h^2}{M_{\rm Pl}^2}\right), \tag{3.10}$$

$$\zeta^2 = M_{\rm Pl}^4\frac{\left(d^3U/d\chi^3\right)dU/d\chi}{U^2} \simeq \frac{16M_{\rm Pl}^6}{9\xi^3 h^6}\left(\frac{\xi h^2}{M_{\rm Pl}^2} - 3\right). \tag{3.11}$$

Slow roll ends when either $\epsilon \simeq 1$ or $|\eta| \simeq 1$. For (3.9) and (3.10), this occurs when $\epsilon \simeq 1$ at a field value $h_{\rm end} \simeq (4/3)^{1/4}\, M_{\rm Pl}/\sqrt{\xi} \simeq 1.07 M_{\rm Pl}/\sqrt{\xi}$. The number of e-folds of inflation as h changes from h_0 to $h_{\rm end}$ is given by [202]

$$N = \int_{h_{\rm end}}^{h_0} \frac{1}{M_{\rm Pl}^2} \frac{U}{dU/dh} \left(\frac{d\chi}{dh}\right)^2 dh \simeq \frac{3}{4}\left[\frac{h_0^2 - h_{\rm end}^2}{M_{\rm Pl}^2/\xi} + \ln\left(\frac{1+\xi h_{\rm end}^2/M_{\rm Pl}^2}{1+\xi h_0^2/M_{\rm Pl}^2}\right)\right]. \tag{3.12}$$

The values of the parameters (3.9)–(3.11) at a particular field value h_0, corresponding to the time at which the pivot scale $k_* \simeq 0.002{\rm Mpc}^{-1}$ left the horizon during inflation, can be used to compare with the CMB data. This value of h_0 (or equivalently N) is a model-dependent quantity that is sensitive to the details of reheating. For Higgs ξ-inflation, an analysis of reheating finds that $N \simeq 59$, or equivalently $h_0 \simeq 9.14 M_{\rm Pl}/\sqrt{\xi}$, is the value at which k_* left the horizon during inflation [202, 203]. Using (3.9) in the WMAP9 normalization $U/\epsilon \simeq (0.0274 M_{\rm Pl})^4$ [11], the required value of ξ is[6]

$$\xi \simeq 48000\sqrt{\lambda} = 48000 \frac{M_h}{\sqrt{2}v} \simeq 17000. \tag{3.13}$$

The predictions for the spectral index n_s, the tensor-to-scalar ratio r, and the running of the spectral index $dn_s/d\ln k$ are given by

$$n_s = 1 - 6\epsilon + 2\eta \simeq 0.967, \tag{3.14}$$

$$r = 16\epsilon \simeq 0.0031, \tag{3.15}$$

$$\frac{dn_s}{d\ln k} = 24\epsilon^2 - 16\epsilon\eta + 2\zeta^2 \simeq 5.4 \times 10^{-4}. \tag{3.16}$$

These predictions for n_s and r are well within the current 1σ allowed regions from [11, 50], while the prediction of $dn_s/d\ln k$ is consistent with observations at the 1–2σ level.

3.3 Two-loop analysis

An analysis of Higgs ξ-inflation beyond the tree level must include both the running of the couplings and loop corrections to the (effective) potential [189, 191, 194]. The most significant effect of these higher order corrections comes from the running of the Higgs quartic coupling $\lambda = \lambda(\mu)$. For $M_h \simeq 125$–126 GeV, it is well known that the running of $\lambda(\mu)$ — or more specifically $\lambda_{\rm eff}(\mu)$ — causes the SM potential to develop an instability below

[6] The *Planck* 2013 normalization $U/\epsilon \simeq (0.0269 M_{\rm Pl})^4$ [50] gives $\xi \simeq 18000$.

the Planck scale unless the top quark mass is about 2σ below its central value [82, 193]. Since Higgs ξ-inflation requires the stability of the potential up to the inflationary scale $M_{\rm Pl}/\sqrt{\xi}$, in order to realize this model of inflation one must make the moderate assumption of a top quark mass $M_t \lesssim 171$ GeV. In this case, it has been shown that the small values of $\lambda_{\rm eff}(\mu)$ near the Planck scale can significantly reduce the non-minimal coupling ξ required for successful inflation [189, 191, 194].[7] The reason for this is relatively simple: the tree-level estimate (3.13) shows that it is the combination λ/ξ^2 that must be small ($\sim 4 \times 10^{-10}$) to give the proper normalization of the CMB power spectrum. If $\lambda_{\rm eff}(\mu)$ is much smaller in the inflationary region than its tree-level value $\lambda \simeq 0.13$, then ξ must also be smaller than the tree-level estimate $\xi \simeq 18000$.

The smaller value of ξ required for successful inflation is particularly important since it is closely related to one of the most significant drawbacks of Higgs ξ-inflation: the violation of perturbative unitarity at the scale $M_{\rm Pl}/\xi$. For $\xi \to 1$, this scale is pushed toward the inflationary scale $M_{\rm Pl}/\sqrt{\xi}$ and the questionable assumptions of non-renormalizable operators [116] or new strong dynamics [114, 189, 191, 192] entering to restore unitarity are no longer required.[8] Since the lower limit of ξ in the case of small $\lambda_{\rm eff}(\mu)$ during inflation has not been explored, an important question is whether it is possible to realize Higgs ξ-inflation with $\xi \sim 1$ and hence avoid the perturbative unitarity issues with the model. Such a region is, by its nature, highly sensitive to the running of $\lambda_{\rm eff}(\mu)$ and requires a proper loop analysis within the Higgs ξ-inflation framework.

To investigate the lower limit of ξ with $\lambda_{\rm eff}(\mu) \ll 1$ during inflation, we first describe the RG equations and the two-loop effective potential that are appropriate for Higgs ξ-inflation in sections 3.3.1 and 3.3.2, respectively. The analysis of inflation, including the lower limits on ξ and the inflationary predictions, are presented in section 3.4.

[7] Actually, the one-loop [194] and two-loop [189, 191] analyses predate the Higgs mass measurement and were carried out to determine the range of M_h allowed for Higgs ξ-inflation. In retrospect, however, a Higgs mass near the lower end of the allowed region suggests a value of $\xi \lesssim 10^3$ is required for successful inflation, with the lower limit of ξ unknown.

[8] Of course, the Higgs field h during inflation becomes trans-Planckian in this case and one must worry about the effects of higher dimensional operators suppressed by the Planck scale, which may spoil the flatness of the potential or the inflationary predictions [202]. As remarked in [191], however, the same worry applies to many minimal models of inflation, such as $m^2\phi^2$ chaotic inflation.

3.3.1 Renormalization group equations

The modification of the well-known RG equations of the SM for the Higgs ξ-inflation scenario has been discussed in [189, 191, 194–197]. Essentially, the scalar propagator of the physical Higgs field, which enters into loop diagram calculations for the RG equations, must be multiplied by the field-dependent factor [191, 196][9]

$$s(h) = \frac{1 + \xi h^2/M_{\rm Pl}^2}{1 + (1+6\xi)\xi h^2/M_{\rm Pl}^2}. \tag{3.17}$$

For small field values $h \ll M_{\rm Pl}/\xi$, $s \simeq 1$ and the RG equations for the SM are perfectly adequate for describing the RG evolution. For large field values $h \gg M_{\rm Pl}/\xi$, however, the physical Higgs propagator is suppressed by a factor $s \simeq 1/(1+6\xi)$ and hence the RG equations differ from those of the SM. Two methods of dealing with this effect have been considered in the literature [189, 191], leading to somewhat different results.

The first method of treating the suppressed Higgs loops, which is described in [191], is to insert one suppression factor s into the RG equations of the SM for each off-shell Higgs propagator. Originally this was done by extracting out all Higgs doublet propagators at one-loop order and inserting the appropriate factors of s, repeating the process only for obvious terms at two-loop order [191]. It was later pointed out, however, that only the propagator of the physical Higgs field and not the Nambu-Goldstone bosons that are present in the Landau gauge should come with such a factor [189]. The corrected RG equations with systematic insertions of s for all two-loop terms, except for β_λ, are given in [197]. By using these RG equations in the full two-loop SM effective potential from [82] (with $m^2 \to 0$ and $M_h^2 \to 3s\lambda h^2$) and demanding that the potential be independent of μ, we have been able to extract the two-loop part for β_λ.[10] A similar procedure can then be used to obtain the two-loop RG equation for the Higgs mass parameter m^2 (in the notation of [82]) with appropriate suppression factors. Although β_{m^2} is not actually required for an analysis of Higgs ξ-inflation, it can be used to derive the RG equation for ξ through the relation $\beta_\xi = (\xi + 1/6)\,\gamma_m$, where $\gamma_m = \beta_{m^2}/m^2$ [196]. The complete set of two-loop RG equations

[9] The reason for this suppression is that the canonical momentum of h (which is evaluated in the Einstein frame with a canonical gravity sector) gives a non-standard commutator $[h(\vec{x}), \dot{h}(\vec{y})] = i\hbar s(h)\delta^3(\vec{x}-\vec{y})$ in the Jordan frame after imposing the standard commutation relations $[h(\vec{x}), \pi(\vec{y})] = i\hbar\delta^3(\vec{x}-\vec{y})$.

[10] In the process, we believe that two typos in the complete expression for the two-loop SM effective potential have been discovered. In [82], the final term of (A.3) should read $-\chi I_{ttg}$ instead of $-\chi I_{ttz}$ and the second last term on the third line of (A.5) should read $-3I_{w00}$ instead of $+I_{w00}$.

with suppressed physical Higgs loops is given in appendix A.

The second method of treating the suppressed Higgs loops is to instead view the effect as a suppression of the effective Higgs coupling to other SM fields and, for large ξ, neglect the physical Higgs field altogether in the region $h \gtrsim M_{\rm Pl}/\xi$ [189]. The resulting theory (SM with frozen radial Higgs mode) is known as the chiral EW theory and has been studied previously in the literature. It is therefore possible to extract one-loop RG equations, which are valid for $\xi \gg 1$, from earlier works such as [204]. In [189], however, the RG equations for λ, y_t, and ξ derived in this way differ from (A.1), (A.2), and (A.6) with $s = 0$. A closer look reveals two sources (though not necessarily errors) for this discrepancy. First, the equation for the running of v^2 used in [189], which was first given in [204], differs from the running of the SM Higgs field h^2 in the Landau gauge,

$$16\pi^2 \mu \frac{\partial}{\partial \mu} h^2 = \left(\frac{3}{2} g'^2 + \frac{9}{2} g^2 - 6 y_t^2 \right) h^2 . \tag{3.18}$$

In the usual SM case, the running of the Higgs vacuum expectation value v^2 and the Higgs field h^2 are both gauge-dependent quantities [205] and have the same running [206]. Although it has been argued that v^2 in the chiral EW theory is a gauge-invariant parameter and therefore its running should also be gauge invariant, we have found it difficult to reproduce the chiral EW theory result using Feynman diagrams and understand why its running differs from the running of h^2 in the SM. In any case, if eq. (5.6) of [189] is replaced by the similar expression (3.18), the resulting one-loop equation for β_{y_t} agrees with (A.2) for $s = 0$. Second, β_λ is derived in [189] by demanding that the one-loop effective potential be independent of μ, where the one-loop potential does not include the usual contribution from the Nambu-Goldstone bosons [82]

$$\Delta U_1 = \frac{3 M_G^4}{64\pi^2} \left(\ln \frac{M_G^2}{\mu^2} - \frac{3}{2} \right) , \tag{3.19}$$

where $M_G^2 = \lambda h^2$. Although the Goldstone boson contribution to the effective potential is strongly suppressed for prescription I (see section 3.3.2), the result of excluding this term in deriving β_λ is equivalent to suppressing some Feynman diagrams with off-shell Goldstone boson propagators; that is, the $(6 + 18 s^2)\, \lambda^2$ term in (A.1) disappears entirely. While this difference is small in the region $h \gtrsim M_{\rm Pl}/\xi$ (numerically it is smaller than the two-loop correction to β_λ), if the contribution (3.19) is included in eq. (4.1) of [189] the resulting one-loop equation for β_λ agrees with (A.1) for $s = 0$. Note that the one-loop equation for β_ξ

in [189] still differs from (A.6) even after accounting for these changes. Specifically, the latter has a factor of $\xi+1/6$ instead of ξ and an additional term $(6+6s)\,\lambda$ compared to the former. Again, these differences in β_ξ are small (typically below the size of the two-loop correction to β_ξ) since we always have $\xi \gg 1/6$ and since λ is small in the region $M_{\rm Pl}/\xi \lesssim h \lesssim M_{\rm Pl}/\sqrt{\xi}$ over which ξ runs.

It is also worth mentioning that the second method includes the effects of additional counterterms taken from the chiral EW theory [204] that arise to cancel divergences in the non-renormalizable SM sector without a Higgs field. These effects appear through the additional couplings α_0 and α_1 that modify the renormalization of the Z boson mass [189] and contribute to the effective potential at the two-loop level. Numerically, however, the Z boson mass contribution at the two-loop level, and hence this effect, is subleading [82].

The two methods of treating the suppressed Higgs loops for $h \gtrsim M_{\rm Pl}/\xi$ are therefore quite similar, at least for large ξ. The first method uses s factors to smoothly interpolate between the SM-like RG evolution at low energies and the RG evolution with suppressed physical Higgs propagators at high energies, while the second method models this transition as an abrupt change at $M_{\rm Pl}/\xi$.[11] Since the s-factor treatment also handles the case $\xi \sim 1$, though, we adopt the first method [191, 195–197] and use a suppression factor s for each off-shell Higgs propagator in the SM RG equations for our analysis of Higgs ξ-inflation. Despite the different treatments of the RG equations described above, the numerical differences are small enough that a two-loop analysis in the region $h \gtrsim M_{\rm Pl}/\xi$ should be justified.

With the recent SM calculation of the three-loop beta functions for the gauge couplings [198] and the leading three-loop terms for β_λ, β_{y_t}, and γ [199], it is relatively simple to include these contributions in the RG equations (A.1)–(A.7) so that the Higgs ξ-inflation analysis matches the NNLO analysis of [82] for $h \lesssim M_{\rm Pl}/\xi$ (see appendix A). Note that we do not attempt to insert the appropriate factors of s into these expressions since the corrections would be smaller than the uncertainty in the RG equations for $h \gtrsim M_{\rm Pl}/\xi$.

For a complete description of the RG evolution in Higgs ξ-inflation, the equations (A.1)–(A.7) with the three-loop corrections (A.8)–(A.13) must be supplemented by values of the SM couplings at the EW scale and the value of ξ at some high scale, say $M_{\rm Pl}/\xi$. Appropriate

[11] A smooth interpolation is preferred, but for $\xi \gg 1$ the function $s(h)$ changes rapidly in the region $h \sim M_{\rm Pl}/\xi$ and so the modification of the numerics is negligible [189].

initial values for the SM couplings can be found in [82]. For the central values of $\alpha_Y^{-1}(M_Z)$ and $\alpha_2^{-1}(M_Z)$, the initial values of the gauge couplings g' and g are

$$g'(M_Z) = \sqrt{\frac{4\pi}{98.35}} \simeq 0.3575, \tag{3.20}$$

$$g(M_Z) = \sqrt{\frac{4\pi}{29.587}} \simeq 0.65171, \tag{3.21}$$

where $M_Z = 91.1876$ GeV. For the strong gauge coupling g_s, the initial value depends more sensitively on the uncertainty in $\alpha_s(M_Z) = 0.1184 \pm 0.0007$. It is given by

$$g_s(M_t) = 1.1645 + 0.0031 \left(\frac{\alpha_s(M_Z) - 0.1184}{0.0007} \right) - 0.00046 \left(\frac{M_t}{\text{GeV}} - 173.15 \right), \tag{3.22}$$

where M_t is the top quark pole mass determined from experiment. The initial value of the top quark Yukawa coupling y_t is

$$\begin{aligned} y_t(M_t) = 0.93587 &+ 0.00557 \left(\frac{M_t}{\text{GeV}} - 173.15 \right) - 0.00003 \left(\frac{M_h}{\text{GeV}} - 125 \right) \\ &- 0.00041 \left(\frac{\alpha_s(M_Z) - 0.1184}{0.0007} \right) \pm 0.00200_{\text{th}}, \end{aligned} \tag{3.23}$$

where M_h is the Higgs pole mass, while the initial value of the Higgs quartic coupling λ is

$$\lambda(M_t) = 0.12577 + 0.00205 \left(\frac{M_h}{\text{GeV}} - 125 \right) - 0.00004 \left(\frac{M_t}{\text{GeV}} - 173.15 \right) \pm 0.00140_{\text{th}}. \tag{3.24}$$

Note that the theoretical uncertainty for $\lambda(M_t)$ in (3.24) is equivalent to an uncertainty in the Higgs pole mass of ± 0.7 GeV [82]. This means, in particular, that for the measured Higgs mass $M_h = 125.7 \pm 0.4$ [207] it is quite reasonable to use values of $M_h \simeq 124$–127 GeV in (3.23) and (3.24). For the non-minimal coupling ξ, we are (a priori) free to choose its initial value ξ_0 at some high scale. We take the scale to be M_{Pl}/ξ_0 so that, by definition,

$$\xi(M_{\text{Pl}}/\xi_0) = \xi_0. \tag{3.25}$$

The RG equations (A.1)–(A.13) with the initial values (3.20)–(3.25) are therefore the ones we use to describe the RG evolution of the couplings for Higgs ξ-inflation.

3.3.2 Two-loop effective potential

The effective potential for Higgs ξ-inflation, like the RG equations, differs from the well-known SM result [82, 208] due to the suppression of the physical Higgs propagators. As

described in [194], however, the effective potential cannot be fixed unambiguously; there are two inequivalent renormalization prescriptions depending on whether quantum corrections to the potential are computed in the Einstein frame (prescription I) [54] or the Jordan frame (prescription II) [209]. Without knowing the behaviour of the quantum theory at the Planck scale, it is unclear which prescription should be used; the two choices lead to different theories with different predictions. The former prescription has been connected to ideas of a possible quantum scale invariance [210–212] while [209] has argued that the latter prescription is correct because the Jordan frame is the one in which physical distances are measured.

For sufficiently large $\lambda_{\text{eff}}(\mu)$, the running of $\lambda_{\text{eff}}(\mu)$ during inflation is small and the choice of renormalization prescription is irrelevant from a practical point of view [82, 189, 194]. For the small $\lambda_{\text{eff}}(\mu)$ allowed by the recent Higgs mass measurement, however, the choice of renormalization prescription can significantly affect the behaviour of $\lambda_{\text{eff}}(\mu)$ and hence the potential during inflation. Both renormalization prescriptions must therefore be considered.

For prescription I, the tree-level SM potential

$$V_0(h) = \frac{\lambda}{4}\left(h^2 - v^2\right)^2 \simeq \frac{\lambda}{4}h^2 \tag{3.26}$$

is first rewritten in the Einstein frame ($h = h(\chi)$) using (3.8), giving

$$U_0(\chi) = \frac{\lambda h^4}{4\Omega^4}. \tag{3.27}$$

Note that the v^2 term in (3.26) has been safely neglected in the inflationary region $h^2 \gtrsim M_{\text{Pl}}^2/\xi \gg v^2$. The one-loop radiative corrections induced by the fields of the SM then take the CW form [82][12]

$$\begin{aligned} U_1(\chi) = \frac{1}{16\pi^2}\Bigg[&\frac{3M_W^4}{2}\left(\ln\frac{M_W^2}{\mu^2} - \frac{5}{6}\right) + \frac{3M_Z^4}{4}\left(\ln\frac{M_Z^2}{\mu^2} - \frac{5}{6}\right) - 3M_t^4\left(\ln\frac{M_t^2}{\mu^2} - \frac{3}{2}\right) \\ &+ \frac{M_h^4}{4}\left(\ln\frac{M_h^2}{\mu^2} - \frac{3}{2}\right) + \frac{3M_G^4}{4}\left(\ln\frac{M_G^2}{\mu^2} - \frac{3}{2}\right)\Bigg], \end{aligned} \tag{3.28}$$

where the particle masses M_W, M_Z, M_t, M_h, and M_G are computed from the tree-level

[12] Up to corrections from the time-dependence of the background Higgs field as it rolls down its potential. Such corrections have been considered in [213, 214] for the simpler Abelian Higgs model but have not yet been studied for the Higgs ξ-inflation model. Analyzing these corrections goes beyond the scope of this chapter.

potential (3.27), giving [54, 194, 215][13]

$$M_W^2 = \frac{g^2 h^2}{4\Omega^2}, \qquad M_Z^2 = \frac{(g^2+g'^2)\,h^2}{4\Omega^2}, \qquad M_t^2 = \frac{y_t^2 h^2}{2\Omega^2},$$
$$M_h^2 = \frac{3s\lambda h^2}{\Omega^4}\left(\frac{1-\xi h^2/M_{\rm Pl}^2}{1+\xi h^2/M_{\rm Pl}^2}\right), \qquad M_G^2 = \frac{\lambda h^2}{\Omega^4}. \tag{3.29}$$

Note that the particle masses M_W^2, M_Z^2, and M_t^2 in (3.29) differ from the flat space results by the conformal factor $\Omega^2 = 1+\xi h^2/M_{\rm Pl}^2$ that appears in the denominator, while the physical Higgs mass M_h^2 and Goldstone boson mass M_G^2 contain additional factors. With the exception of the suppression factor $s = s(h)$ in the physical Higgs mass, the appearance of these additional factors in M_h^2 and M_G^2 is due to using the asymptotically flat tree-level potential (3.27) to determine particle masses rather than the Jordan frame potential (3.26). These additional factors lead to a suppression of the physical Higgs and Goldstone boson contributions to the effective potential (relative to those from W, Z, and t) during inflation for prescription I, as found in [54, 194, 215].

The two-loop radiative corrections $U_2(\chi)$ can easily be found by using the modified particle masses (3.29) in the two-loop SM result of [82], but due to the rather long and unenlightening form of this expression we do not reproduce it here. The RG-improved effective potential is then determined from $U_{\rm eff}(\chi) = U_0 + U_1 + U_2$ in the usual way by using the RG equations from appendix A to run the couplings and making the replacement $h \to e^{\Gamma(\mu)}h$, where

$$\Gamma(\mu) = -\int_{M_t}^{\mu} \gamma(\mu')\, d\ln\mu' \tag{3.30}$$

and $\gamma = -d\ln h/d\ln\mu$ is the anomalous dimension of the Higgs field [216].[14] The effective Higgs quartic coupling $\lambda_{\rm eff}(\mu)$ is then defined through

$$U_{\rm eff}(\chi) \equiv \frac{\lambda_{\rm eff}(\mu) h^4}{4\Omega^4}, \tag{3.31}$$

where all couplings in (3.31) are evaluated at some renormalization scale μ. The dependence of the effective potential on the scale μ is spurious, but to minimize the logarithms from higher loop corrections it is appropriate to take $\mu = \kappa h/\Omega$ proportional to the back-

[13] We obtain this result by expanding $H = \frac{1}{\sqrt{2}}\binom{0}{h} + \binom{\hat{G}^+}{(\hat{h}+i\hat{G}^0)/\sqrt{2}}$ in the full expression for the tree-level potential $U_0 = \lambda(H^\dagger H)^2/\Omega^4 = \lambda(H^\dagger H)^2/(1+2\xi H^\dagger H/M_{\rm Pl}^2)^2$ to quadratic order in the fields $\hat{h}$, $\hat{G}^+$, $\hat{G}^0$, where h is the classical background value of the Higgs field $\hat{h}$ [215].

[14] Note the difference in sign between the definition of γ here and the definition of γ in [82].

ground mass of a vector boson or top quark [189]. For simplicity, we choose the constant of proportionality to be $\kappa = 1$.

For prescription II, quantum corrections to the potential (3.26) are computed in the Jordan frame before transforming to the Einstein frame. In this case, the one-loop radiative corrections to the effective potential take the form [196]

$$U_1(\chi) = \frac{1}{16\pi^2\Omega^4}\left[\frac{3M_W^4}{2}\left(\ln\frac{M_W^2}{\mu^2} - \frac{5}{6}\right) + \frac{3M_Z^4}{4}\left(\ln\frac{M_Z^2}{\mu^2} - \frac{5}{6}\right) - 3M_t^4\left(\ln\frac{M_t^2}{\mu^2} - \frac{3}{2}\right) + \frac{M_h^4}{4}\left(\ln\frac{M_h^2}{\mu^2} - \frac{3}{2}\right) + \frac{3M_G^4}{4}\left(\ln\frac{M_G^2}{\mu^2} - \frac{3}{2}\right)\right], \tag{3.32}$$

where the particle masses M_W^2, M_Z^2, M_t^2, M_h^2, and M_G^2 appear without the conformal factor Ω^2 or additional factors in their denominators,

$$M_W^2 = \frac{g^2h^2}{4}, \qquad M_Z^2 = \frac{(g^2+g'^2)\,h^2}{4}, \qquad M_t^2 = \frac{y_t^2h^2}{2},$$
$$M_h^2 = 3s\lambda h^2, \qquad M_G^2 = \lambda h^2. \tag{3.33}$$

The two-loop radiative corrections $U_2(\chi)$ can be found by using the particle masses (3.33) in the two-loop SM result [82] and dividing the expression by the conformal factor Ω^4. The effective Higgs quartic coupling $\lambda_{\text{eff}}(\mu)$ is again defined through (3.31), but in this case taking the renormalization scale to be proportional to the background mass of a vector boson or top quark requires $\mu = \kappa h$. For simplicity, we again choose $\kappa = 1$.

In practice, the most significant difference between the effective potentials for the two renormalization prescriptions is the functional dependence $\mu = \mu(h)$.[15] For prescription I, $\mu = h/\Omega$ approaches a constant value in the inflationary region $h \gtrsim M_{\text{Pl}}/\sqrt{\xi}$ (and hence so do the couplings $g(\mu)$, $g'(\mu)$, etc. in (3.29)) while for prescription II the renormalization scale $\mu = h$ does not. As a result, the effective potential for prescription I approaches a constant value in the inflationary region (even after including radiative corrections) while the effective potential for prescription II, due to the continued running of the couplings, does not. This difference, as we will see, can have a large impact on Higgs ξ-inflation and its predictions for small $\lambda_{\text{eff}}(\mu)$.

[15] The additional suppression of the physical Higgs and Goldstone boson masses for prescription I is relatively minor since these masses, and hence their contributions to the effective potential, are small compared to M_W, M_Z, and M_t for the small λ in the inflationary region.

3.4 Numerical results

For a fixed Higgs mass M_h, top quark mass M_t, strong coupling $\alpha_s(M_Z)$, and non-minimal coupling ξ_0, it is straightforward to solve the RG equations (A.1)–(A.13) numerically with the initial conditions (3.20)–(3.25) and use the effective potential $U(\chi)$ (for either prescription I or II) to compute the inflationary parameters. However, since the focus of this chapter is on the region of parameter space with $\lambda_{\text{eff}}(\mu) \ll 1$, we instead replace the parameter M_t in favour of $\lambda_{\text{eff}}^{\text{min}} \equiv \min\{\lambda_{\text{eff}}(\mu)\}$. Intuitively, this can be understood as adjusting the top quark mass M_t to yield the desired $\lambda_{\text{eff}}^{\text{min}}$ for a fixed choice of M_h, $\alpha_s(M_Z)$, and ξ_0. Figure 3.1 shows that the special region $\lambda_{\text{eff}}^{\text{min}} \simeq 0$ exists for a top quark mass $M_t \sim 171$ GeV about 2–3σ below its central value. Since values of $\lambda_{\text{eff}}^{\text{min}} \sim 0.01$ are typical within the experimental and theoretical uncertainty of the various parameters, a fine-tuning of some combination of parameters is necessary to achieve $0 < \lambda_{\text{eff}}^{\text{min}} \lesssim 0.01$.[16] Note that negative values of $\lambda_{\text{eff}}^{\text{min}}$, as well as sufficiently small positive values, cause the effective potential to develop a second minimum below the inflationary scale and hence spoil Higgs ξ-inflation. We therefore restrict ourselves to the region $0 < \lambda_{\text{eff}}^{\text{min}} \lesssim 0.01$ in which the effective potential is stable.

The non-minimal coupling ξ_0 is not actually a free parameter, of course, but must be chosen to give the correct normalization of the CMB power spectrum (see section 3.2). For a fixed M_h and $\alpha_s(M_Z)$, the procedure for determining the inflationary predictions for a particular choice of $\lambda_{\text{eff}}^{\text{min}}$ and renormalization prescription is as follows:

1. Choose a value of ξ_0. Adjust the top quark mass M_t to give the desired value of $\lambda_{\text{eff}}^{\text{min}}$ when solving the RG equations. For $\lambda_{\text{eff}}^{\text{min}} \lesssim 0.01$, this may involve fine-tuning M_t.

2. Use the effective potential $U(\chi)$ (for prescription I or II) to compute the inflationary parameters and determine $U(h_0)/\epsilon(h_0)$ at a field value h_0 corresponding to $N = 59$ e-folds before the end of inflation.

3. Repeat the steps above for different values of ξ_0 until the correct normalization $U/\epsilon \simeq (0.0274 M_{\text{Pl}})^4$ is achieved.[17]

[16] In [64] it is argued that a IR fixed point in an asymptotically safe theory of gravity may ensure very small values of $\lambda(\mu)$ near the Planck scale. In this case, fine-tuning may only be necessary for values of $\lambda_{\text{eff}}^{\text{min}}$ smaller than the typical size of the shift in $\lambda_{\text{eff}}(\mu)$ due to radiative corrections to the effective potential, $\delta\lambda_{\text{eff}}(\mu \sim M_{\text{Pl}}) \sim 4 \times 10^{-4}$.

[17] Note that prescription II with sufficiently small $\lambda_{\text{eff}}^{\text{min}}$ can have two solutions for ξ_0. The large ξ_0 solution, however, predicts $n_s > 1.02$ and is therefore inconsistent with observations [11, 50].

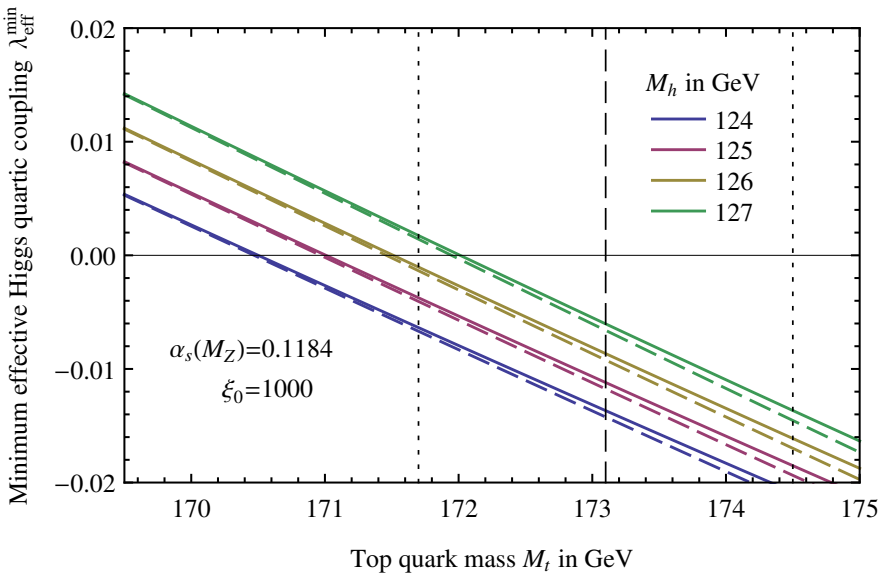

Figure 3.1: Values of $\lambda_{\text{eff}}^{\text{min}}$ as a function of M_t for fixed $\alpha_s(M_Z) = 0.1184$ and $\xi_0 = 1000$. The four solid (dashed) curves correspond to a Higgs mass M_h of 124, 125, 126, and 127 GeV from bottom to top for renormalization prescription I (II). The vertical dashed and dotted lines give the central value and $\pm 2\sigma$ range for M_t [82]. A shift in $\alpha_s(M_Z)$ of $\pm 1\sigma$ (± 0.0007) roughly corresponds to a shift in M_h of ± 0.5 GeV while changing ξ_0 by an order of magnitude has little effect.

4. Compute the inflationary predictions for the spectral index n_s, the tensor-to-scalar ratio r, and the running of the spectral index $dn_s/d\ln k$.

We discuss the numerical results for prescriptions I and II separately.

3.4.1 Inflationary predictions for prescription I

For prescription I, the results for ξ_0 and the inflationary predictions for n_s and r (as a function of $\lambda_{\text{eff}}^{\text{min}}$) are presented in figure 3.2. The running of the spectral index $dn_s/d\ln k$ always remains small, within the range (5.0–5.6) $\times 10^{-4}$.

Let us first discuss the non-minimal coupling ξ_0. Figure 3.2 shows that the value of ξ_0 required for the CMB normalization deviates from the tree-level estimate $\xi_0 \simeq 48000\sqrt{\lambda_{\text{eff}}^{\text{min}}}$ as $\lambda_{\text{eff}}^{\text{min}}$ decreases below about 10^{-4}. In particular, ξ_0 reaches a minimum value of $\xi_0 \sim 400$ at $\lambda_{\text{eff}}^{\text{min}} \sim 10^{-4.4}$ and then begins to increase. This behaviour can be traced to the rapid decrease in ϵ (and hence the tensor-to-scalar ratio $r = 16\epsilon$) over this range, which causes U/ϵ to increase despite smaller values of $\lambda_{\text{eff}}^{\text{min}}$. A larger non-minimal coupling ξ_0 is therefore required to give the correct CMB normalization. This result demonstrates that the sharp decrease in ξ_0 seen in [194] and figure 4 of [189] for prescription I does not continue indefinitely

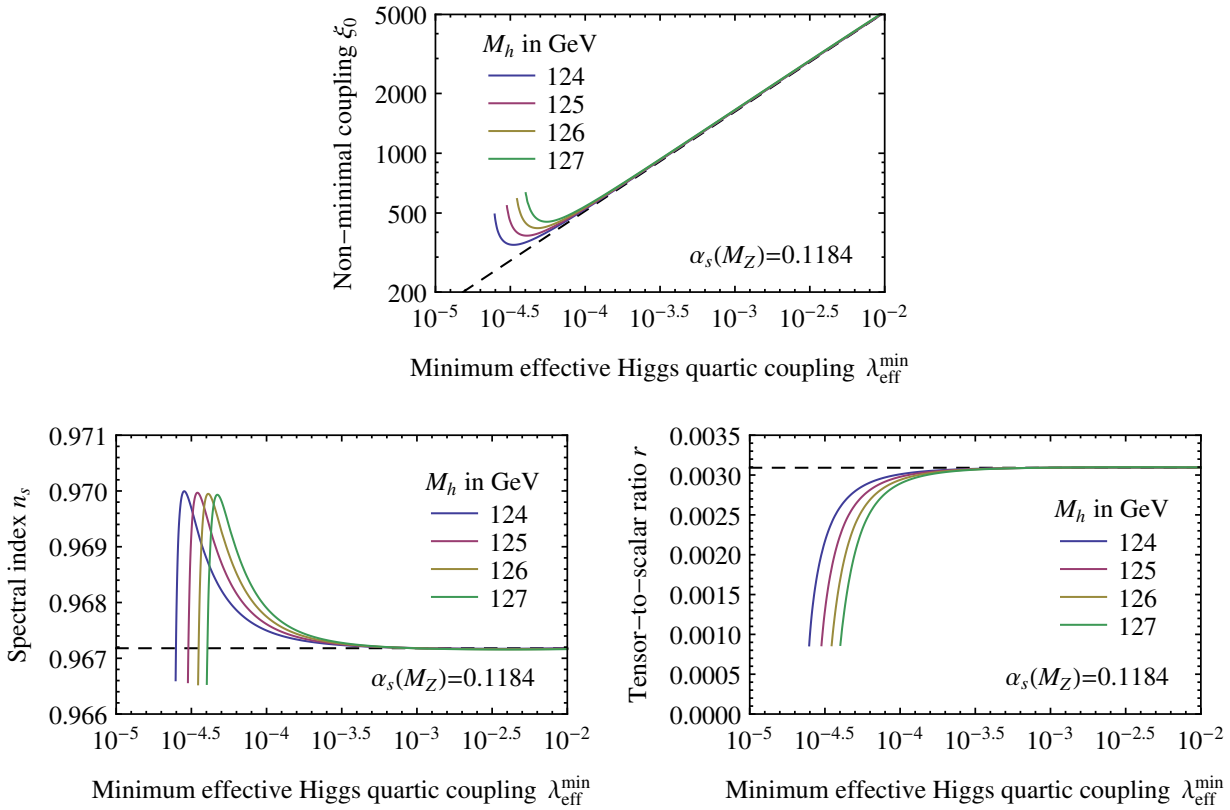

Figure 3.2: Numerical results for the non-minimal coupling ξ_0 and inflationary predictions for the spectral index n_s and the tensor-to-scalar ratio r as a function of $\lambda_{\rm eff}^{\rm min}$ for prescription I. The four solid curves correspond to a Higgs mass M_h of 124, 125, 126, and 127 GeV from left to right while the dashed lines give the tree-level predictions. A shift in $\alpha_s(M_Z)$ of $\pm 2\sigma$ (± 0.0014) roughly corresponds to a shift in M_h of ∓ 0.5 GeV. Changing the number of e-folds from $N = 59$ to 62 shifts the tree-level predictions by a small (calculable) amount but does not change the qualitative behaviour of the curves about the tree-level predictions.

but only allows ξ_0 as small as about 400. The violation of perturbative unitarity at the scale $M_{\rm Pl}/\xi_0 \ll M_{\rm Pl}/\sqrt{\xi_0}$ therefore remains a problem for Higgs ξ-inflation in the small $\lambda_{\rm eff}^{\rm min}$ region. For sufficiently small $\lambda_{\rm eff}^{\rm min}$ (e.g. $\lesssim 10^{-4.6}$), no solutions for ξ_0 are possible since the effective potential develops a second minimum and hence spoils the Higgs ξ-inflation scenario.[18]

Figure 3.2 also shows small deviations in the inflationary predictions for the spectral index n_s and the tensor-to-scalar ratio r. As $\lambda_{\rm eff}^{\rm min}$ decreases below about $10^{-3.5}$, the spectral index rises to about 0.970 from its tree-level prediction of 0.967 before decreasing rapidly, while the tensor-to-scalar ratio drops quickly below its tree-level prediction of 0.0031. Although a similarly rapid change in n_s and r can be seen in [189, 194] as the Higgs mass approaches values corresponding to $\lambda_{\rm eff}^{\rm min} \simeq 0$, the results presented here (as a function of $\lambda_{\rm eff}^{\rm min}$) provide a much clearer picture of Higgs ξ-inflation in this now experimentally favoured region. From a practical point of view, we see that the deviations of n_s and r from the tree-level predictions are sufficiently small that they would be difficult to distinguish from the tree-level results observationally. Consequently, for all allowed values $10^{-4.6} \lesssim \lambda_{\rm eff}^{\rm min} \lesssim 10^{-2}$, the predictions for n_s and r are well within the current 1σ limits [11, 50]. The small prediction for $dn_s/d\ln k \sim 5 \times 10^{-4}$ is also consistent with observations at the 1–2σ level [11, 50].

3.4.2 Inflationary predictions for prescription II

For prescription II, there are two disjoint regions of $\lambda_{\rm eff}^{\rm min}$ that can lead to acceptable inflation: one with larger values $\lambda_{\rm eff}^{\rm min} \gtrsim 10^{-3.3}$–$10^{-2.3}$ (depending on M_h) and one with smaller values $\lambda_{\rm eff}^{\rm min} \sim 10^{-4}$. The results for ξ_0 and the inflationary predictions for n_s and r are quite different for these two regions and are presented in figures 3.3 and 3.4, respectively.

Let us first consider the region of larger values of $\lambda_{\rm eff}^{\rm min}$, which is the only one that has been considered previously in the literature [189, 191, 194]. Figure 3.3 shows that the required value of ξ_0 in this region behaves similarly to that of prescription I except that the minimum value of ξ_0 — if it can be reached without the potential developing a second minimum — occurs at larger $\lambda_{\rm eff}^{\rm min}$ (i.e. $\lambda_{\rm eff}^{\rm min} \gtrsim 10^{-3}$). This difference is due to the stronger effect of the running of $\lambda_{\rm eff}(\mu)$ for prescription II. Specifically, the running of $\lambda_{\rm eff}(\mu)$ to its minimum

[18] In this case, the effective potential rises to a local maximum and then decreases slowly to a constant value as $h \to \infty$. The shape of the potential may be suitable for a sort of false vacuum inflation in which the Higgs field can start with any value $h \gtrsim M_{\rm Pl}/\sqrt{\xi}$, but an analysis of this case goes beyond the scope of this chapter.

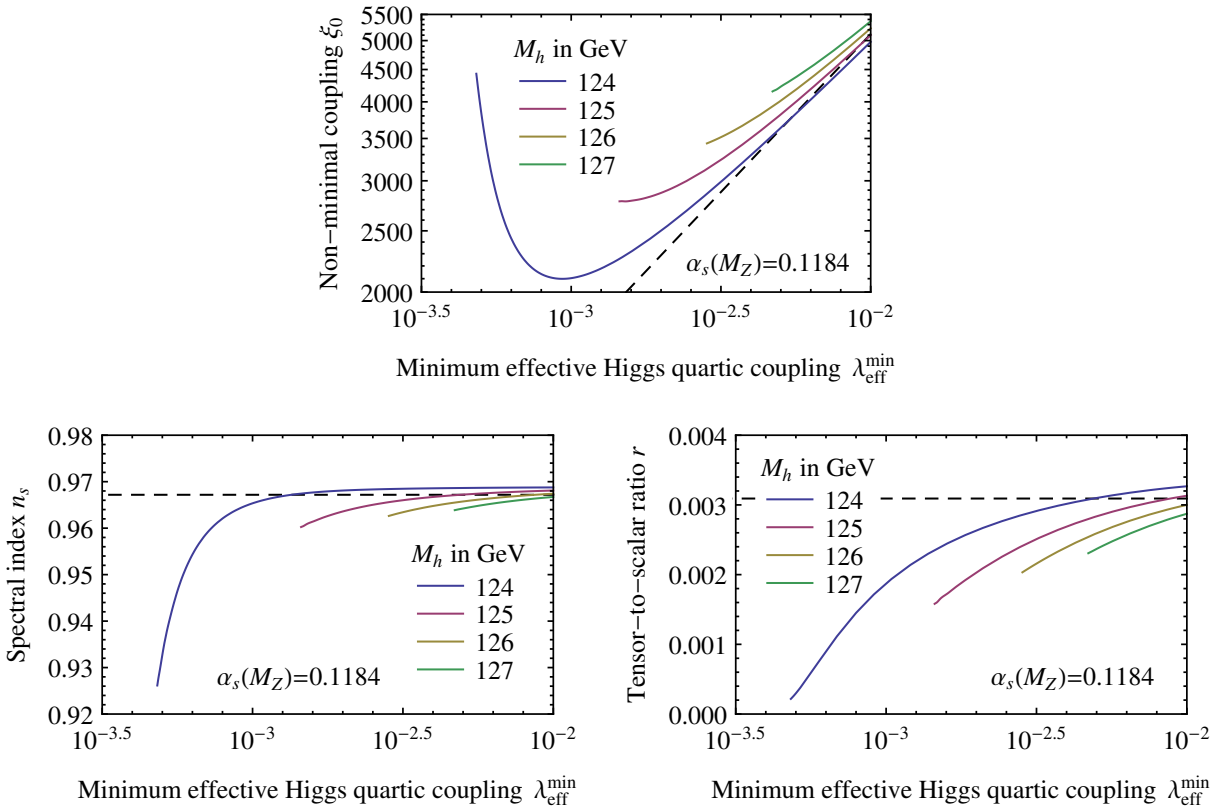

Figure 3.3: Numerical results for the non-minimal coupling ξ_0 and inflationary predictions for the spectral index n_s and the tensor-to-scalar ratio r in the larger $\lambda_{\rm eff}^{\rm min}$ region for prescription II. The four solid curves correspond to a Higgs mass M_h of 124, 125, 126, and 127 GeV from left to right while the dashed lines give the tree-level predictions. A shift in $\alpha_s(M_Z)$ of $\pm 2\sigma$ (± 0.0014) roughly corresponds to a shift in M_h of ∓ 0.5 GeV. Changing the number of e-folds from $N = 59$ to 62 shifts the tree-level predictions by a small (calculable) amount but does not change the qualitative behaviour of the curves about the tree-level predictions.

value overcomes the flattening of the potential in the inflationary region more quickly than for prescription I, and hence causes the effective potential to develop a second minimum for more moderate values of $\lambda_{\text{eff}}^{\min}$. As a result, a non-minimal coupling only as small as $\xi_0 \sim 2000$–4000 (depending on M_h) is allowed for this region of $\lambda_{\text{eff}}^{\min}$. Similar lower limits for ξ_0, as well as the qualitative rise in ξ_0 as $\lambda_{\text{eff}}^{\min}$ decreases, have been found in [189, 194] for prescription II. Again, these values of ξ_0 are not small enough to prevent the perturbative unitarity violation at M_{Pl}/ξ_0 from occurring well below the inflationary scale.

Figure 3.3 also shows that the predictions for the spectral index n_s and the tensor-to-scalar ratio r *decrease* from their tree-level values as $\lambda_{\text{eff}}^{\min} \to 0$. The decrease observed here (similar to prescription I) is consistent with the results of [189, 194] rather than with the increase observed in [191]. Also note that the variation in n_s over the allowed range of $\lambda_{\text{eff}}^{\min}$ is larger for prescription II than for prescription I. Since a deviation from the tree-level prediction of $\Delta n_s \gtrsim 0.01$ should be visible by *Planck* [217], it may therefore be possible to connect a measurement of the spectral index with the RG evolution of $\lambda_{\text{eff}}(\mu)$ near the Planck scale for prescription II. The running of the spectral index $dn_s/d\ln k$ always remains quite small, within the range $(4.5\text{–}6.4) \times 10^{-4}$.

While the results of the larger $\lambda_{\text{eff}}^{\min}$ region for prescription II are qualitatively similar to those for prescription I, prescription II also allows a region of smaller $\lambda_{\text{eff}}^{\min}$ and ξ_0 with distinct inflationary predictions. The existence of this region, which has not been considered in the literature before, can be understood as follows. For typical Higgs ξ-inflation with large $\lambda_{\text{eff}}^{\min}$, the slow roll parameter ϵ decreases rapidly in the inflationary region (see eq. (3.9)) and the required $N = 59$ e-folds of inflation are produced quickly (see eq. (3.12)). For smaller $\lambda_{\text{eff}}^{\min}$ and ξ_0, however, there is a region of parameter space in which the running of $\lambda_{\text{eff}}(\mu)$ causes ϵ to increase before the $N = 59$ e-folds are reached. The inflationary observables are then computed at a field value h_0 in a qualitatively different region of parameter space with larger ϵ, leading to distinct predictions.

Figure 3.4 gives the numerical results for ξ_0 and the inflationary predictions for the spectral index n_s and the tensor-to-scalar ratio r in this region. The results are shown together with the most recent constraints from *Planck* [50]. Since many well-motivated models with Higgs ξ-inflation contain additional degrees of freedom that can contribute to the effective number of neutrino species N_{eff} (e.g. the νMSM [87, 88] with 3 light sterile

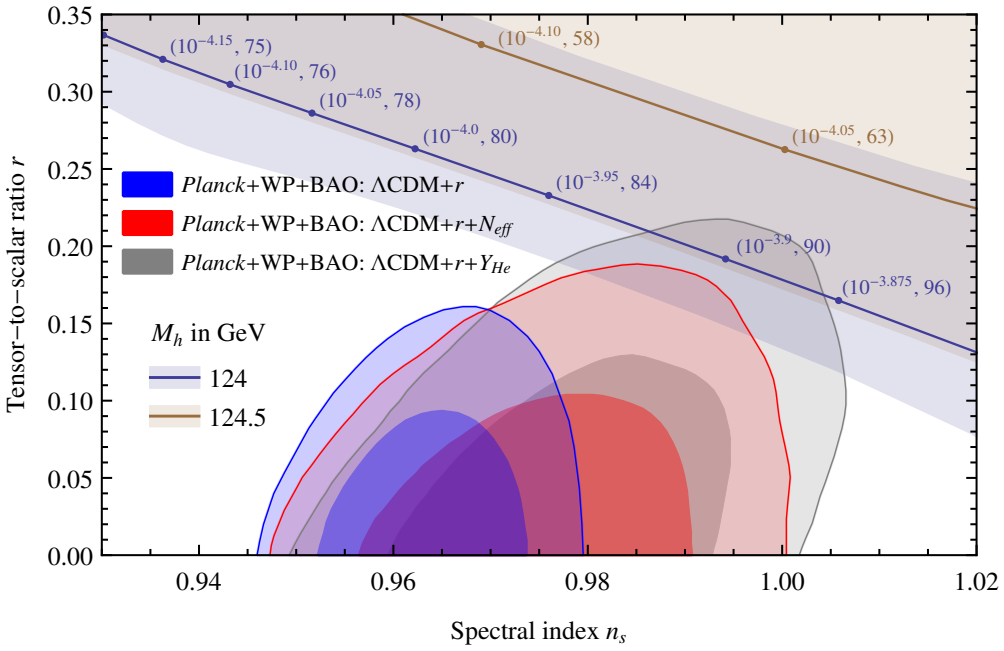

Figure 3.4: Predictions for the spectral index n_s and the tensor-to-scalar ratio r for Higgs ξ-inflation with prescription II and $\lambda_{\rm eff}^{\rm min} \sim 10^{-4}$. The solid blue (brown) curve gives the results for a Higgs mass $M_h = 124$ GeV (124.5 GeV) while the lower and upper shaded regions correspond to a shift in $\alpha_s(M_Z) = 0.1184$ of up to $\pm 2\sigma$ (± 0.0014), respectively. The marked points along the solid curves indicate values of $(\lambda_{\rm eff}^{\rm min}, \xi_0)$. Results are shown with the marginalized joint 68% and 95% confidence level regions from *Planck* 2013 [50].

neutrinos), it is most appropriate to compare the results with the ΛCDM+r+$N_{\rm eff}$ data. It can be seen that, for $\lambda_{\rm eff}^{\rm min} \sim 10^{-3.9}$ and $M_h \simeq 124$ GeV, there is a region of Higgs ξ-inflation that is consistent with *Planck* at the 2–3σ level.[19] This region, though marginally disfavoured, is important for two reasons. First, unlike for the larger $\lambda_{\rm eff}^{\rm min}$ region, the tensor-to-scalar ratio $r \gtrsim 0.15$ in this region is quite large and would be visible by *Planck* [217]. It is therefore possible that the tensor modes from Higgs ξ-inflation could be detected in the *Planck* polarization data.[20] Second, the non-minimal coupling $\xi_0 \sim 90$ required in this region is about an order of magnitude smaller than previously considered in the literature. Although still not small enough to address the problem of perturbative unitarity violation occurring below the inflationary scale, it provides the lower limit on ξ_0 that is acceptable for Higgs ξ-inflation. Smaller non-minimal couplings, including $\xi_0 \sim 1$, seem generally unattainable because they require $\lambda_{\rm eff}^{\rm min} \lesssim 10^{-6}$ to give the correct CMB normalization, which ultimately causes the effective potential to develop a second minimum before the inflationary scale.

3.5 Conclusion

Higgs ξ-inflation is an attractive model of inflation since it does not require scalar degrees of freedom in addition to those of the SM. For a large non-minimal coupling ξ, however, the violation of perturbative unitarity at the scale $M_{\rm Pl}/\xi \ll M_{\rm Pl}/\sqrt{\xi}$ threatens the self-consistency of the model in the inflationary region. In this chapter we have investigated the possibility that a Higgs mass $M_h \simeq 125$–126 GeV — a mass for which the effective Higgs quartic coupling $\lambda_{\rm eff}(\mu)$ runs to very small values near the Planck scale — may significantly reduce the size of ξ required for inflation and address the perturbative unitarity violation problem. This possibility, like the Higgs ξ-inflation scenario in general, requires a top quark mass $M_t \sim 171$ GeV, about 2σ below its central value.

To investigate this possibility we have updated the two-loop analysis of Higgs ξ-inflation to include the three-loop SM beta functions for the gauge couplings as well as the leading

[19] Recall that even with the Higgs mass measurement of $M_h = 125.7 \pm 0.4$ [207], using $M_h \simeq 124$ GeV in the RG evolution is still quite reasonable due to the theoretical uncertainty in determining λ at the EW scale.

[20] The running of the spectral index in this region is also much larger (and negative) than typically found in Higgs ξ-inflation: $dn_s/d\ln k \sim -0.002$ and -0.008 for $M_h = 124$ and 124.5 GeV, respectively. A large running of the spectral index relaxes the constraints on r from *Planck* [50] and could open up even more of the small $\lambda_{\rm eff}^{\rm min}$ region for detection.

three-loop terms for the RG evolution of λ, the top Yukawa coupling y_t, and the Higgs anomalous dimension γ. We have also included, for the first time, a complete two-loop insertion of suppression factors for the physical Higgs loops in the RG equations. The two-loop SM effective potential with particle masses modified appropriately for Higgs ξ-inflation has been used to match the level of the RG equations.

We have found that successful inflation in the region $\lambda_{\rm eff}(\mu) \ll 1$ requires smaller ξ than previously considered in the literature, but even with a fine-tuning of parameters to give arbitrarily small $\lambda_{\rm eff}^{\rm min}$ it is not possible to achieve $\xi \sim 1$ and prevent the violation of perturbative unitarity below the inflationary scale. Specifically, we have found that the Einstein frame renormalization prescription (prescription I) allows a non-minimal coupling as small as $\xi \sim 400$ for $\lambda_{\rm eff}^{\rm min} \sim 10^{-4.4}$ without the potential developing a second minimum and hence spoiling inflation. The predictions for the spectral index n_s and the tensor-to-scalar ratio r remain close to their tree-level values in this case and are within the 1σ allowed region from CMB measurements. For the Jordan frame renormalization prescription (prescription II), there are two distinct regions of $\lambda_{\rm eff}^{\rm min}$ that can lead to successful inflation. The larger $\lambda_{\rm eff}^{\rm min}$ region behaves similarly to prescription I and allows a non-minimal coupling as small as $\xi \sim 2000$ without the potential developing a second minimum. The smaller $\lambda_{\rm eff}^{\rm min}$ region, which has not been considered in the literature before, requires $\xi \sim 90$ and predicts an observable tensor-to-scalar ratio $r \gtrsim 0.15$ for $\lambda_{\rm eff}^{\rm min} \sim 10^{-3.9}$. Smaller non-minimal couplings, including $\xi \sim 1$, seem generally unattainable since they require $\lambda_{\rm eff}^{\rm min} \lesssim 10^{-6}$ to give the correct CMB normalization, which ultimately causes the effective potential to develop a second minimum before the inflationary scale.

3.6 Recent developments

Since the publication of this work, the BICEP2 collaboration has released data indicating the detection of B-modes in the polarization of the CMB at greater than 5σ [218]. Interpreted as a primordial signal from inflation (at a lesser significance, of course), the result suggests a tensor-to-scalar ratio $r \simeq 0.2^{+0.07}_{-0.05}$ that is incompatible with the tree-level estimate of $r \simeq 0.003$ for Higgs ξ-inflation. Consequently, after the BICEP2 announcement several studies of Higgs ξ-inflation in the region with small λ near the Planck scale were carried out

to determine if Higgs ξ-inflation is compatible with a large tensor-to-scalar ratio [219–221]. Qualitatively, these studies arrive at the same conclusion as this work in that larger r can be consistent with the BICEP2 result near the critical point $\lambda_{\text{eff}}^{\text{min}} \simeq 0$. However, smaller values of $\xi \sim 10$ are quoted in these studies, which this work has found is incompatible with the overall stability of the SM effective potential. The discrepancy is likely due to the approximate one-loop expansion of the potential used in the works [220, 221] rather than the two-loop effective potential used here.

The question of whether Higgs ξ-inflation is compatible with the BICEP2 result may be moot; there is now a general consensus that the analysis from BICEP2 underestimates the polarized emissions from foreground and that modelling uncertainties can account for most of the primordial B-mode signal being claimed [222]. The upcoming data release from *Planck* and other experiments in the near future should clarify the existence of a primordial signal in the BICEP2 range.

Chapter 4

Classical scale invariance and the strong CP problem

We now turn our attention to a fine-tuning problem in the SM (or the νMSM) that persists even if the model is valid up to the Planck scale: the strong CP problem. This problem, unlike the cosmological constant problem, can be formulated within the framework of the SM alone and hence its solution may not be related to the correct theory of quantum gravity. Moreover, there does not appear to be an anthropic reason for having a small CP-violating angle $\bar{\theta}$. In this chapter, we consider how new physics that is introduced to solve the strong CP problem in a classically scale invariant theory can preserve the technical naturalness of the SM, even though it will be necessary to relax the assumption of no intermediate scales of new physics.

Disclaimer: The work contained in this chapter has been carried out jointly with Graham Ross and Christopher Hill. Though I have written the chapter myself, some of the more technical results (most notably the derivation of the interaction rate of the dilaton with the thermal background at finite temperature) and the overall progression of ideas has developed from collaborative efforts rather than mine alone. The original works can be found in refs. [223, 224].

4.1 Introduction

Since the discovery that a classically scale invariant theory can lead to spontaneous symmetry breaking through the conformal anomaly [90], an attractive scenario for spontaneous EW symmetry breaking has been to set the Higgs mass parameter m^2 to zero and induce the EW scale radiatively. In this scenario, the EW scale does not have to be introduced by hand into

the SM with a bare mass term but can be generated from a theory with only dimensionless parameters.

The SM with a classical scale invariance and radiative EW symmetry breaking can also be motivated by the hierarchy problem and the principle of technical naturalness. From a field theoretical point of view, the quadratically divergent corrections to the bare Higgs mass parameter are not physically meaningful; they are absorbed into the definition of the physically measurable parameter m^2 in the renormalization procedure. Without heavy intermediate states such as GUT states that couple significantly to the Higgs, logarithmic corrections to the Higgs mass parameter are under control and small m^2 is technically natural [89]. Even in the presence of gravity, small m^2 might emerge from the RG evolution of mass parameters in UV physics down to the Planck scale. It is therefore interesting to consider the possibility that $m^2 = 0$, which corresponds to a classical scale invariance in the SM, and that EW symmetry breaking arises as a purely quantum mechanical effect.

Unfortunately, EW symmetry breaking through the CW mechanism is not possible in the SM alone for the measured values of the top quark and Higgs mass. The original CW scenario applied to the SM, which predates the large top quark mass measurement, requires $\lambda \sim g^4$ and a Higgs mass of approximately 10 GeV [225]. Similarly, including the effects of a large top quark Yukawa coupling requires a Higgs mass of about 218 GeV [225, 226]. Some extension of the SM is therefore required to realize EW symmetry breaking through the CW mechanism.

A large number of recent papers [226–252] have therefore explored classical scale invariance and radiative EW symmetry breaking in minimal extensions of the SM. Although these papers typically address the hierarchy problem, they do not address the strong CP problem. This is an important omission since it is unclear whether a solution to the strong CP problem can be consistent with the classical scale invariance approach.

One of the most attractive solutions to the strong CP problem is that of the invisible axion. This solution introduces a new SM singlet scalar field S that is charged under a $\mathrm{U}(1)_{\mathrm{PQ}}$ symmetry [71, 72] and develops a large vev [68]. There have been two main proposals for the implementation of the PQ symmetry. The DFSZ axion model [253, 254] extends the SM Higgs sector to include a second Higgs doublet in addition to the complex PQ scalar S. Both Higgs doublets are charged under the PQ symmetry and couple to S through

terms in the potential. Alternatively, the Kim-Shifman-Vainshtein-Zakharov (KSVZ) axion model [255, 256] takes all the SM fields to be singlets under the PQ symmetry and adds a new heavy quark that carries non-zero PQ charge and couples to S. In both models, the axion is identified with the phase (angular component) of S while the modulus (radial component) is identified with a new real scalar field. The spontaneous breaking of the PQ symmetry through the vev of S is typically generated with a large negative mass term for the PQ scalar, in which case the modulus obtains a large mass and can be integrated out of the low-energy theory.

In this chapter, we study classically scale invariant versions of the invisible axion models — those in which the negative mass term for S is forbidden — and determine whether they are consistent with spontaneous symmetry breaking through the CW mechanism. In particular, we show that a classically scale invariant version of the DFSZ model solves the strong CP problem and can give rise to successful radiative breaking of the PQ symmetry followed by a spontaneous breaking of the EW symmetry. The result relies on an ultra-weak coupling of the scalar S to the SM sector, which is technically natural due to an underlying approximate shift symmetry of the model. The model therefore does not contain a hierarchy problem from the large vev of S. Due to the classical scale invariance, the modulus of S obtains only a small loop-induced mass and can be identified as a light pseudo-dilaton. We discuss the cosmological consequences of this unusually light state in detail.

4.2 Electroweak symmetry breaking via the Coleman-Weinberg mechanism

The invisible axion models with EW symmetry breaking via the CW mechanism are developed in two steps. First, in section 4.2.1 we discuss radiative EW symmetry breaking in a classically scale invariant extension of the SM with a real singlet scalar. This model provides, in a simplified context, some intuition for the ultra-weak sector in the invisible axion models that follow. It is also relevant to schemes in which the Planck scale is spontaneously generated from the vev of a real singlet scalar. The full DFSZ and KSVZ invisible axion models with a complex PQ scalar, as well as the other model-specific states, are then discussed in sections 4.2.2 and 4.2.3.

4.2.1 The real singlet scalar model

Consider an extension of the SM in which the Higgs sector includes an additional real scalar field σ that is a singlet under the SM gauge group. Moreover, suppose that the model has a classical scale invariance so that only dimension four terms in the Lagrangian are allowed; that is, the bare mass terms for the Higgs and σ are forbidden. The most general Lagrangian for the scalar sector of the model is then

$$\mathcal{L} = \frac{1}{2}\partial_\mu\sigma\partial^\mu\sigma + (D_\mu H)^\dagger D^\mu H - V(H,\sigma), \tag{4.1}$$

where D_μ is the usual covariant derivative, $H = \begin{pmatrix} \phi^+ \\ \frac{1}{\sqrt{2}}(v + h + i\phi^0) \end{pmatrix}$ is the SU(2) Higgs doublet, $v \simeq 246$ GeV is the Higgs vev, and the potential $V(H,\sigma)$ is given by

$$V(H,\sigma) = \lambda\left(H^\dagger H\right)^2 + \frac{\zeta_1}{2}\left(H^\dagger H\right)\sigma^2 + \frac{\zeta_2}{4}\sigma^4. \tag{4.2}$$

The basic idea of this model is that once σ obtains a vev through the CW mechanism, EW symmetry breaking is driven by the negative Higgs mass term $m^2 \simeq \zeta_1 w^2/2$ that is induced through the Higgs portal coupling $\zeta_1\left(H^\dagger H\right)\sigma^2/2$ with $\zeta_1 < 0$. Since the invisible axion models discussed later must have a large vev for the PQ scalar, we consider the case $\langle\sigma\rangle \gg v$ for this real singlet scalar model. The coupling $\zeta_1 \sim m_h^2/\langle\sigma\rangle^2 \ll 1$ must then be ultra-weak.

The CW mechanism uses loop-level effects to break the classical scale invariance and generate a vev for σ. These effects can be captured through the one-loop RG equations of λ, ζ_1, and ζ_2, which are given by

$$\beta_\lambda = \frac{1}{16\pi^2}\left[24\lambda^2 - 3\lambda\left(3g^2 + g'^2\right) + \frac{3}{8}\left(g^2 + g'^2\right)^2 + \frac{3}{4}g^4 + 12\lambda y_t^2 - 6y_t^4 + \frac{1}{2}\zeta_1^2\right], \tag{4.3}$$

$$\beta_{\zeta_1} = \frac{1}{16\pi^2}\left[6\zeta_1\zeta_2 + 12\zeta_1\lambda + 4\zeta_1^2 - \frac{3}{2}\zeta_1\left(3g^2 + g'^2\right) + 6\zeta_1 y_t^2\right], \tag{4.4}$$

$$\beta_{\zeta_2} = \frac{1}{16\pi^2}\left[2\zeta_1^2 + 18\zeta_2^2\right], \tag{4.5}$$

where $\beta_\lambda \equiv d\lambda(\mu)/d\ln\mu$ and $\beta_{\zeta_i} \equiv d\zeta_i(\mu)/d\ln\mu$. An immediately obvious feature of the RG equations (4.3)–(4.5) is that the set of couplings ζ_i is multiplicatively renormalized. Therefore if all the couplings ζ_i are small, they remain small over a large range of scales in the RG running and are technically natural. This result is due to the approximate shift symmetry of the Lagrangian under the transformation $\sigma \to \sigma + f$, which is broken only by the couplings ζ_i. According to the 't Hooft naturalness condition [257], the enhanced shift

symmetry of the Lagrangian in the limit $\zeta_i \to 0$ protects the ultra-weak couplings ζ_i from large radiative corrections, and hence small ζ_i are technically natural. The Higgs doublet, in contrast, does not have an approximate shift symmetry due to its gauge couplings and so λ receives large corrections from the gauge sector.

Despite the ultra-weak couplings ζ_i, the σ field can have a one-loop CW potential with a non-trivial minimum at some high energy scale. To see this, let us momentarily neglect all terms in the potential that involve the Higgs. Then only the quartic term for σ remains and ζ_2 must change from negative to positive values under the RG running to give a non-trivial minimum. Integrating (4.5), the solution for ζ_2 is, to a good approximation,

$$\zeta_2(\mu) \simeq \beta_{\zeta_2} \ln\left(\frac{\mu}{M}\right), \tag{4.6}$$

where $\beta_{\zeta_2} > 0$ is treated as a constant and M is the scale at which $\zeta_2(M) = 0$. Substituting this result back into (4.2) and taking the renormalization scale $\mu = \sigma$, the effective CW potential for the σ field is given by

$$V_{\rm CW} \simeq \frac{\beta_{\zeta_2}}{4}\sigma^4 \ln\left(\frac{\sigma}{M}\right), \tag{4.7}$$

which has a minimum at $w \equiv \langle\sigma\rangle = e^{-1/4}M$. Note that at this minimum the coupling ζ_2 satisfies

$$\zeta_2(w) \simeq -\frac{1}{4}\beta_{\zeta_2} = -\frac{1}{64\pi^2}\left(2\zeta_1^2 + 18\zeta_2^2\right). \tag{4.8}$$

This relation shows that the minimum of the CW potential occurs when the one-loop expression β_{ζ_2} is comparable to the tree-level coupling ζ_2. It also shows how the CW mechanism generates a dimensionful scale w from a dimensionless theory.

To satisfy (4.8) for a perturbative coupling $\zeta_2 \lesssim 4\pi$, the dominant term in β_{ζ_2} must be ζ_1^2. Thus

$$\beta_{\zeta_2} \simeq \frac{\zeta_1^2}{8\pi^2} \quad \Longrightarrow \quad \zeta_2 \simeq -\frac{1}{4}\beta_{\zeta_2} \simeq -\frac{\zeta_1^2}{32\pi^2}, \tag{4.9}$$

and so there is a large hierarchy $\zeta_2 \sim \zeta_1^2 \ll |\zeta_1| \ll 1$ amongst the ultra-weak couplings. Although the origin of this hierarchy is not the focus of this chapter, we note that it might arise from an underlying symmetry for which every power of σ^2 that appears in the terms of a Lagrangian is associated with a small symmetry breaking parameter $\epsilon \sim |\zeta_1|$.

To describe EW symmetry breaking in the real singlet scalar model, though, we must also include the terms in the potential that involve the Higgs field. Reintroducing these terms gives the mixed Higgs-σ potential

$$V(H,\sigma) \simeq \lambda \left(H^\dagger H\right)^2 + \frac{\zeta_1}{2}\left(H^\dagger H\right)\sigma^2 + \frac{\zeta_2}{4}\sigma^4. \tag{4.10}$$

The minimum of this more complicated potential can be found by writing (4.10) as the sum of two terms

$$V(H,\sigma) \simeq \lambda \left(H^\dagger H - \epsilon\sigma^2\right)^2 + \frac{\zeta_2'}{4}\sigma^4, \tag{4.11}$$

where

$$\epsilon = -\frac{\zeta_1}{4\lambda}, \qquad \zeta_2' = \zeta_2 - \frac{\zeta_1^2}{4\lambda}, \tag{4.12}$$

and ζ_1 is negative. In analogy to (4.7), the second term in (4.11) leads *a priori* to a CW potential for σ with a minimum at $w \equiv \langle\sigma\rangle = e^{-1/4}M$, where M now corresponds to the scale at which $\zeta_2'(M) = 0$. However, the running of ζ_2' is dominated by the top quark Yukawa coupling,

$$\beta_{\zeta_2'} = \beta_{\zeta_2} - \frac{\zeta_1}{2\lambda}\beta_{\zeta_1} + \frac{\zeta_1^2}{4\lambda^2}\beta_\lambda \simeq \frac{1}{16\pi^2}\left[-\frac{3y_t^4}{2\lambda}\zeta_1^2\right], \tag{4.13}$$

and hence $\beta_{\zeta_2'} < 0$. This gives a CW potential that is unbounded from below and hence does not lead to successful EW symmetry breaking — at least for a phenomenologically viable version of this model.[1] One of the invisible axion models that follows, however, has a potential similar to (4.11) with the corresponding beta function positive. We therefore continue the discussion of this simpler model assuming $\beta_{\zeta_2'} > 0$ and a minimum $w = e^{-1/4}M$ to further develop our intuition for the invisible axion model.

For $\langle\sigma\rangle = w$, the minimum of the first term in (4.11) occurs at

$$\langle H\rangle \equiv \frac{v}{\sqrt{2}} = \sqrt{\epsilon}w, \tag{4.14}$$

where $v \simeq 246$ GeV is fixed by EW symmetry breaking in the SM. Equations (4.12) and (4.14) also give the useful relations

$$\epsilon = \frac{v^2}{2w^2} = -\frac{\zeta_1}{4\lambda}, \tag{4.15}$$

which show that $\epsilon \sim v^2/w^2$ can be used as an expansion parameter in the limit $v \ll w$.

[1] If the top quark was lighter, $\beta_{\zeta_2'}$ would be dominated by the gauge boson contribution in β_λ and have the correct sign to give successful EW symmetry breaking.

Now consider the phenomenology of this model. The scalar mass eigenstates can be found in the unitary gauge ($H^\dagger H \to h^2/2$) by diagonalizing the mass matrix

$$\mathcal{M} = \left\langle \frac{d^2V}{d\phi_i d\phi_j} \right\rangle = \begin{pmatrix} 2\lambda v^2 & -\dfrac{2\lambda v^3}{w} \\ -\dfrac{2\lambda v^3}{w} & \dfrac{2\lambda v^4}{w^2} + \beta_{\zeta_2'} w^2 \end{pmatrix}, \tag{4.16}$$

where $\phi_i = \{h, \sigma\}$. To obtain the simplified form (4.16), the approximate solution $\zeta_2' \simeq \beta_{\zeta_2'} \ln(\sigma/M)$ has been used in (4.11) together with the minimization conditions

$$\left\langle \frac{dV}{dh} \right\rangle = \lambda v^3 + \frac{\zeta_1}{2} v w^2 = 0, \tag{4.17}$$

$$\left\langle \frac{dV}{d\sigma} \right\rangle = \frac{\zeta_1}{2} v^2 w + \frac{\beta_{\zeta_2'}}{4} w^3 + \beta_{\zeta_2'} w^3 \ln\left(\frac{w}{M}\right) = 0 \tag{4.18}$$

for $v, w \neq 0$. Denoting the physical mass eigenstates by $\hat{h}$ and $\hat{\sigma}$, in the limit $v \ll w$ we find

$$\hat{h} \simeq h - \frac{v}{w}\sigma, \qquad \hat{\sigma} \simeq \sigma + \frac{v}{w} h. \tag{4.19}$$

The corresponding masses of the physical eigenstates are

$$m_h^2 \simeq 2\lambda v^2, \qquad m_\sigma^2 \simeq \beta_{\zeta_2'} w^2 \sim \frac{\zeta_1^2}{8\pi^2} w^2 \simeq \frac{\lambda^2 v^4}{2\pi^2 w^2} \simeq \frac{m_h^4}{8\pi^2 w^2}. \tag{4.20}$$

Note that $\hat{\sigma}$ is very light due to the classical scale invariance, which forbids a bare mass term for the state and forces $\hat{\sigma}$ to obtain only the much smaller loop-induced mass.

The real singlet scalar model is predictive for a specific choice of w. In particular, for $m_h \simeq 125.5$ GeV the model predicts a light scalar state $\hat{\sigma}$ with mass

$$m_\sigma \simeq 0.18 \left(\frac{10^{10}\ \text{GeV}}{w}\right)\ \text{keV}. \tag{4.21}$$

This state can be identified as a pseudo-dilaton that couples to everything the SM Higgs does, albeit with couplings that are suppressed over those of the Higgs by a factor of v/w due to the small h component in $\hat{\sigma}$. For instance, the dilaton can decay via the one-loop process $\hat{\sigma} \to \gamma\gamma$ through the dimension five operator $\hat{\sigma} F_{\mu\nu} F^{\mu\nu}$. The decay width of this process can be found by rescaling eq. (1) of [258], giving

$$\Gamma_{\hat{\sigma}\to\gamma\gamma} \simeq C_\sigma^2 \frac{\alpha^2 m_\sigma^3}{256\pi^3 w^2}, \tag{4.22}$$

with the coefficient C_σ given by

$$C_\sigma = \sum_Q e_Q^2 N_c A_f(0) + A_W(0) = \frac{11}{3}, \tag{4.23}$$

where $A_f(0) = 4/3$, $A_W(0) = -7$, and the sum over Q extends over all charged fermions in the SM, yielding $\sum_Q e_Q^2 N_c = 8$.[2] Using (4.21), the lifetime of $\hat{\sigma}$ is then

$$\tau_\sigma \simeq 1.3 \times 10^{23} \left(\frac{w}{10^{10}\ \text{GeV}}\right)^5 \ \text{sec.} \tag{4.24}$$

The dilaton is therefore a viable dark matter candidate for certain choices of w, provided there is a production mechanism for $\hat{\sigma}$ that can give the necessary abundance. A more complete analysis of the dilaton as a dark matter candidate, however, is left for the discussion of the invisible axion models.

4.2.2 The DFSZ model

To consider a realistic invisible axion model with classical scale invariance, replace the real singlet scalar field σ from the previous section with the complex singlet scalar field S — the PQ scalar. The strong CP problem is solved in the usual way by giving S a charge under a new global chiral $\mathrm{U}(1)_{\mathrm{PQ}}$ symmetry.[3] The spontaneous breaking of the $\mathrm{U}(1)_{\mathrm{PQ}}$ gives a light pseudo-Nambu-Goldstone boson, the axion a, whose vev promotes $\bar{\theta}$ in (1.8) to a dynamical variable that depends on $\langle a \rangle$.[4] The axion then adjusts its vev spontaneously to reach the CP-conserving minimum $\bar{\theta} = 0$ of its QCD potential [259].

There is some freedom in the implementation of the $\mathrm{U}(1)_{\mathrm{PQ}}$ for invisible axion models. The DFSZ invisible axion model [253, 254] contains two Higgs doublets H_1 and H_2 that couple to the up-type and down-type fermions, respectively, in addition to the PQ scalar S. The vev of H_1 gives masses to the up-type fermions while the vev of H_2 gives masses to the down-type fermions. In this model, the PQ transformation can be taken to be a chiral rotation of the right-handed quark and lepton fields [260]

$$\begin{aligned} &u_{\mathrm{R}} \to e^{-i\alpha X_1} u_{\mathrm{R}}, \qquad && d_{\mathrm{R}} \to e^{i\alpha X_2} d_{\mathrm{R}}, \qquad && e_{\mathrm{R}} \to e^{i\alpha X_2} e_{\mathrm{R}}, \\ &H_1 \to e^{+i\alpha X_1} H_1, \qquad && H_2 \to e^{-i\alpha X_2} H_2, \qquad && S \to e^{+i\alpha (X_1 + X_2)/2} S, \end{aligned} \tag{4.25}$$

where $X_1 \neq -X_2$ to ensure that the transformation is chiral. The most general classically scale invariant potential for H_1, H_2, and S that is consistent with the PQ symmetry (4.25)

[2] This is in contrast to the Higgs case for which the sum only includes the top quark and W loops and the functions $A_f(\tau_f)$ and $A_W(\tau_W)$ in eq. (2) of [258] are evaluated at non-zero τ_i since $m_h \sim m_i$.

[3] The original PQ model [71, 72] did not have the SM singlet field S but instead had the SM Higgs doublet, as well a second Higgs doublet necessary for absorbing the independent chiral transformations of the quarks, charged under the PQ symmetry. The resulting EW scale axions were quickly ruled out by experiment, hence the need for invisible axion models [67].

[4] The axion would be massless if the $\mathrm{U}(1)_{\mathrm{PQ}}$ was exact, but the symmetry is broken by the QCD anomaly.

is

$$V(H_1, H_2, S) = \lambda_1(H_1^\dagger H_1)^2 + \lambda_2(H_2^\dagger H_2)^2 + \lambda_3(H_1^\dagger H_1)(H_2^\dagger H_2) + \lambda_4(H_1^\dagger H_2)^2 + \zeta_1(H_1^\dagger H_1)(S^* S) + \zeta_2(H_2^\dagger H_2)(S^* S) + \Big(\zeta_3(H_1^\dagger H_2)(S^* S) + \text{h.c.}\Big) + \zeta_4(S^* S)^2, \tag{4.26}$$

where the Higgs doublets and the PQ scalar are parametrized as

$$H_1 = \begin{pmatrix} \phi_1^+ \\ \frac{\phi_1}{\sqrt{2}} e^{i a_1/v_1} \end{pmatrix}, \qquad H_2 = \begin{pmatrix} \phi_2^+ \\ \frac{\phi_2}{\sqrt{2}} e^{i a_2/v_2} \end{pmatrix}, \qquad S = \frac{\phi_s}{\sqrt{2}} e^{i a_s/v_s}, \tag{4.27}$$

with $\langle \phi_1 \rangle \equiv v_1$, $\langle \phi_2 \rangle \equiv v_2$, and $\langle \phi_s \rangle \equiv v_s$. For an invisible axion model, we also have the relation $v_1, v_2 \ll v_s$ since the axion decay constant $f_a \equiv v_s / N_{\text{DW}}$ must be very large to escape the experimental and astrophysical limits [261].[5] For the DFSZ model, $N_{\text{DW}} = 6$ and so v_s must fall within the range

$$2 \times 10^9 \text{ GeV} \lesssim v_s \lesssim 10^{12} \text{ GeV}, \tag{4.28}$$

where the lower limit is given by constraints from SN 1987A [261] and the upper limit is given by constraints on the energy density contained in axions (see section 4.4 for details).

At this point, we simplify the model by taking $\lambda_4 = 0$; λ_4 is generated by gauge interactions, but in this case it remains negligibly small compared to other terms in the potential [252] (see appendix B). We also consider the parameter range for which $v_2 \ll v_1$, thereby allowing for an analytic diagonalization of the mass matrix.[6] A more complete study of the model's parameter space requires a numerical analysis, which goes beyond the scope of this discussion.

Scalar mass spectrum

The scalar mass spectrum of the DFSZ model can be found by diagonalizing the mass matrix $\mathcal{M}^2_{ij} = \langle \partial^2 V / (\partial \phi_i \partial \phi_j) \rangle$. For (4.26) with $\lambda_4 = 0$, the mass matrix is a $3 \times 3 \times 2$ block-diagonal matrix where the blocks are formed by the CP-even neutral fields $\{\phi_1, \phi_2, \phi_s\}$, the CP-odd neutral fields $\{a_1, a_2, a_s\}$, and the charged fields $\{\phi^+, \phi^-\}$, which separately mix to form the

[5] Here N_{DW} is the model-dependent domain wall number or colour anomaly factor.

[6] Because only the down-type fermions obtain their masses from v_2, the bottom quark Yukawa coupling remains perturbative for values of v_2 as small as about a GeV.

physical mass eigenstates.[7] At the tree level, we have

$$V_{\rm mass} = \frac{1}{2}\left(\phi_1,\phi_2,\phi_s\right)\mathcal{M}^{(1)}_{ij}\begin{pmatrix}\phi_1\\ \phi_2\\ \phi_s\end{pmatrix} + \frac{1}{2}\left(a_1,a_2,a_s\right)\mathcal{M}^{(2)}_{ij}\begin{pmatrix}a_1\\ a_2\\ a_s\end{pmatrix} + \left(\phi_1^+,\phi_2^+\right)\mathcal{M}^{(3)}_{ij}\begin{pmatrix}\phi_1^-\\ \phi_2^-\end{pmatrix}, \quad (4.29)$$

where

$$\mathcal{M}^{(1)}_{ij} = \begin{pmatrix} 3\lambda_1 v_1^2 + \frac{\lambda_3}{2}v_2^2 + \frac{\zeta_1}{2}v_s^2 & \lambda_3 v_1 v_2 + \frac{\zeta_3}{4}v_s^2 & \zeta_1 v_1 v_s + \frac{\zeta_3}{2}v_2 v_s \\ \lambda_3 v_1 v_2 + \frac{\zeta_3}{4}v_s^2 & 3\lambda_2 v_2^2 + \frac{\lambda_3}{2}v_1^2 + \frac{\zeta_2}{2}v_s^2 & \zeta_2 v_2 v_s + \frac{\zeta_3}{2}v_1 v_s \\ \zeta_1 v_1 v_s + \frac{\zeta_3}{2}v_2 v_s & \zeta_2 v_2 v_s + \frac{\zeta_3}{2}v_1 v_s & \frac{\zeta_1}{2}v_1^2 + \frac{\zeta_2}{2}v_2^2 + \frac{\zeta_3}{2}v_1 v_2 + 3\zeta_4 v_s^2 \end{pmatrix}, \quad (4.30)$$

$$\mathcal{M}^{(2)}_{ij} = \begin{pmatrix} -\frac{\zeta_3}{4}\frac{v_2}{v_1}v_s^2 & \frac{\zeta_3}{4}v_s^2 & \frac{\zeta_3}{2}v_2 v_s \\ \frac{\zeta_3}{4}v_s^2 & -\frac{\zeta_3}{4}\frac{v_1}{v_2}v_s^2 & -\frac{\zeta_3}{2}v_1 v_s \\ \frac{\zeta_3}{2}v_2 v_s & -\frac{\zeta_3}{2}v_1 v_s & -\zeta_3 v_1 v_2 \end{pmatrix}, \quad (4.31)$$

$$\mathcal{M}^{(3)}_{ij} = \begin{pmatrix} 2\lambda_1 v_1^2 + 2\lambda_3 v_2^2 + \zeta_1 v_s^2 & \lambda_4 v_1 v_2 + \frac{\zeta_3}{2}v_s^2 \\ \lambda_4 v_1 v_2 + \frac{\zeta_3}{2}v_s^2 & 2\lambda_2 v_2^2 + \lambda_3 v_1^2 + \zeta_2 v_s^2 \end{pmatrix}. \quad (4.32)$$

The tree-level tadpole conditions that can be used to simplify (4.30)–(4.32) before diagonalization are

$$\left\langle \frac{\partial V}{\partial \phi_1} \right\rangle = \lambda_1 v_1^3 + \frac{\lambda_3}{2}v_1 v_2^2 + \frac{\zeta_1}{2}v_1 v_s^2 + \frac{\zeta_3}{4}v_2 v_s^2 = 0, \quad (4.33)$$

$$\left\langle \frac{\partial V}{\partial \phi_2} \right\rangle = \lambda_2 v_2^3 + \frac{\lambda_3}{2}v_1^2 v_2 + \frac{\zeta_2}{2}v_2 v_s^2 + \frac{\zeta_3}{4}v_1 v_s^2 = 0, \quad (4.34)$$

$$\left\langle \frac{\partial V}{\partial \phi_s} \right\rangle = \frac{\zeta_1}{2}v_1^2 v_s + \frac{\zeta_2}{2}v_2^2 v_s + \frac{\zeta_3}{2}v_1 v_2 v_s + \zeta_4 v_s^3 = 0. \quad (4.35)$$

For the region of parameter space with $v_2 \ll v_1$, it is best to use (4.33)–(4.35) to eliminate the parameters λ_1, ζ_3, and ζ_4 from the mass matrices. Eliminating these parameters and diagonalizing the mass matrices gives

$$V^0_{\rm mass} = \frac{1}{2}\left(h,H,s\right)\begin{pmatrix} m_h^2 & 0 & 0 \\ 0 & m_H^2 & 0 \\ 0 & 0 & 0 \end{pmatrix}\begin{pmatrix} h \\ H \\ s \end{pmatrix} + \frac{1}{2}\left(G^0,A,a\right)\begin{pmatrix} 0 & 0 & 0 \\ 0 & m_A^2 & 0 \\ 0 & 0 & 0 \end{pmatrix}\begin{pmatrix} G^0 \\ A \\ a \end{pmatrix} + \left(G^+,H^+\right)\begin{pmatrix} 0 & 0 \\ 0 & m_{H^\pm}^2 \end{pmatrix}\begin{pmatrix} G^- \\ H^- \end{pmatrix}, \quad (4.36)$$

[7] By writing $\langle H_1\rangle = \frac{1}{\sqrt{2}}\begin{pmatrix}0\\ v_1\end{pmatrix}$, $\langle H_2\rangle = \frac{1}{\sqrt{2}}\begin{pmatrix}0\\ v_2\end{pmatrix}$, and $\langle S\rangle = \frac{1}{\sqrt{2}}v_s$, we have assumed that the form of the potential is such that the Higgs vacuum structure is automatically both CP and charge conserving [262]. In this case, one can distinguish between the CP-even and CP-odd scalar fields since they do not mix.

where h is the observed Higgs boson, H is a heavier CP-even neutral Higgs, s is the dilaton, G^0 and $G^\pm$ are the Nambu-Goldstone bosons eaten by the Z and W bosons respectively, A is a massive CP-odd neutral scalar, and a is the axion.[8] The masses of the fields are given by the approximate expressions

$$m_h^2 \simeq -\zeta_1 v_s^2, \tag{4.37}$$

$$m_H^2 \simeq m_A^2 \simeq m_{H^\pm}^2 \simeq \frac{\zeta_2}{2} v_s^2 + \frac{\lambda_3}{2} v_1^2, \tag{4.38}$$

where the dilaton and axion are massless.

It is important to note that (4.37) and (4.38) are only the tree-level results; the breaking of the classical scale invariance through the CW mechanism gives rise to a non-zero mass for the dilaton s [228], thereby turning it into a pseudo-dilaton, and the axion a obtains its usual zero temperature mass from the QCD anomaly of [263]

$$m_a \simeq 6.0 \times 10^{-6} \left(\frac{v_s / N_{\rm DW}}{10^{12}\ \text{GeV}} \right)^{-1} \text{eV}. \tag{4.39}$$

CW symmetry breaking

There are two ways in which the CW mechanism can break EW symmetry in this model. In the first, the dominant one-loop CW term is proportional to λ_3^2 and the interaction between the two Higgs doublets drives λ_1 negative at some scale. This case is equivalent to that studied in [252] and requires such a large λ_3 that there is a Landau pole in the 3–10 TeV range.

To avoid the appearance of a Landau pole below the Planck scale, we therefore turn to the second possibility in which λ_3 is negligible and EW symmetry breaking is triggered by a negative Higgs mass squared $\zeta_1 v_s^2$ (where ζ_1 is negative) from the vev of the PQ scalar. This case is analogous to EW symmetry breaking mechanism used in the real singlet scalar model. Since 2×10^9 GeV $\lesssim v_s \lesssim 10^{12}$ GeV, the singlet couplings $\zeta_{1,2,3}$ must be very small; $\zeta_{1,2,3} \lesssim m_h^2 / v_s^2$, where m_h is the observed Higgs mass. Moreover, for CW symmetry breaking to proceed through v_s it is necessary for ζ_4 to be even smaller; $\zeta_4 \lesssim \zeta_{1,2,3}^2$. Again, the ultra-weak couplings ζ_i are technically natural due to the underlying approximate shift symmetry $S \to S + f$, which is broken only by ζ_i and ensures that these couplings are multiplicatively

[8] The axion is composed primarily of the phase of S and, up to normalization, is given by $a \simeq a_s + \frac{2v_1}{v_s} a_1$.

renormalized as a whole (see appendix B). The smaller value of ζ_4 is also stable under radiative corrections due to the partial scale symmetry $S \to \lambda S$, where $\zeta_{1,2,3}$ scale as λ and ζ_4 scales as λ^2. It is interesting to note that if this symmetry is broken by a term scaling as λ, perhaps by gravity, the hierarchy $\zeta_4 \ll |\zeta_{1,2,3}| \ll 1$ results automatically.

Even though the couplings ζ_i are ultra-weak, CW symmetry breaking in the ϕ_s-ϕ_1 sector is possible. To see this, consider the limit in which the term proportional to ζ_2 provides the dominant one-loop CW term in the potential; that is, neglect the $\lambda_3 v_1^2/2$ term in (4.38). In this case, the additional Higgs states H, A, and $H^\pm$ coming from the second Higgs doublet can be heavy enough to have escaped detection to date [264–267]. The potential, including the dominant one-loop correction, can be written as

$$V(\phi_1, \phi_s) \simeq \frac{\lambda_1}{4}\left(\phi_1^2 - \alpha\phi_s^2\right)^2 + \frac{\zeta_4'}{4}\phi_s^4 + \frac{1}{64\pi^2}\left(\zeta_2\phi_s^2\right)^2\left[\ln\left(\frac{\zeta_2\phi_s^2}{2M^2}\right) - \frac{3}{2}\right], \tag{4.40}$$

where

$$\alpha \equiv -\frac{\zeta_1}{2\lambda_1}, \qquad \zeta_4' \equiv \zeta_4 - \frac{\zeta_1^2}{4\lambda_1}, \tag{4.41}$$

and M is the scale at which the couplings are defined. Note that, in contrast to the real singlet scalar model, $\beta_{\zeta_4'} \simeq \zeta_2^2/(8\pi^2)$ is dominated by the positive contribution from the heavy Higgs states in β_{ζ_4} rather than the negative contribution from the top quark in β_{λ_1}. This ensures $\beta_{\zeta_4'} > 0$ and that a proper minimum for ϕ_s is generated, thus leading to successful EW symmetry breaking. In particular, the minimum of (4.40) occurs at

$$v_s^2 \simeq \frac{2M^2}{\zeta_2}\exp\left(1 - \frac{16\pi^2\zeta_4'}{\zeta_2^2}\right), \qquad v_1^2 \simeq \alpha v_s^2. \tag{4.42}$$

The vev v_2 is, in turn, driven by the term proportional to ζ_3 in (4.34), giving

$$v_2 \simeq -\frac{\zeta_3}{2\zeta_2}v_1. \tag{4.43}$$

Now let us find an expression for the mass of the pseudo-dilaton s, which is induced by the breaking of the classical scale invariance through the CW mechanism. The minimum (4.42) allows the potential (4.40) to be written in the form

$$V(\phi_1, \phi_s) \simeq \frac{\lambda_1}{4}\left(\phi_1^2 - \alpha\phi_s^2\right)^2 + \frac{\zeta_2^2\phi_s^4}{64\pi^2}\left[\ln\left(\frac{\phi_s^2}{v_s^2}\right) - \frac{1}{2}\right]. \tag{4.44}$$

Since the mixing between the states $\phi_{1,2}$ and ϕ_s is small, $\phi_s \simeq s$ and hence the latter term of (4.44), denoted by $V_{\rm CW}(\phi_s)$, induces a mass for the pseudo-dilaton of

$$m_s^2 \simeq \left\langle \frac{d^2 V_{\rm CW}}{d\phi_s^2} \right\rangle \simeq \frac{\zeta_2^2}{8\pi^2}v_s^2. \tag{4.45}$$

The model therefore predicts a very light scalar field in the mass spectrum. Its origin is ultimately due to the classical scale invariance of the model, which forbids a large mass term for this field and hence requires a small coupling ζ_2 to achieve successful EW symmetry breaking through the CW mechanism.

To summarize, a classically scale invariant version of the DFSZ invisible axion model can give successful EW symmetry breaking through the CW mechanism with ultra-weak but technically natural couplings ζ_i. For a particular choice of v_s, we have

$$m_h^2 \simeq 2\lambda_1 v_1^2 \simeq -\zeta_1 v_s^2, \qquad m_H^2 \simeq m_A^2 \simeq m_{H^\pm}^2 \simeq \frac{\zeta_2}{2} v_s^2, \qquad m_s^2 \simeq \frac{\zeta_2^2}{8\pi^2} v_s^2, \tag{4.46}$$

as well as the axion with its usual zero temperature mass (4.39).

4.2.3 The KSVZ model

In the KSVZ invisible axion model [255, 256], the SM states are all singlets under the PQ symmetry. Instead of having the SM states feel the PQ symmetry directly, one introduces a new heavy quark $X_{\mathrm{L,R}}$ that carries a PQ charge and interacts directly with the PQ scalar S through the Yukawa interaction [260]

$$\Delta\mathcal{L}_{\mathrm{KSVZ}} = -f\bar{X}_{\mathrm{L}} S X_{\mathrm{R}} - f^* \bar{X}_{\mathrm{R}} S^\dagger X_{\mathrm{L}}. \tag{4.47}$$

After imposing a classical scale invariance on the model, the scalar potential has the relatively simple form

$$V(H,S) = \lambda (H^\dagger H)^2 + \eta_1 (H^\dagger H)(S^* S) + \eta_2 (S^* S)^2, \tag{4.48}$$

where H is the SM Higgs doublet. The vev of S, which is proportional to the axion decay constant f_a, must again be very large to satisfy experimental and astrophysical constraints. Using the same parametrization for S as in (4.27), the KSVZ model with $N_{\mathrm{DW}} = 1$ requires v_s to be within the range 4×10^8 GeV $\lesssim v_s \lesssim 10^{12}$ GeV [261].

Due to the non-observation of additional coloured states up to the TeV range ($m_X \sim f v_s \gtrsim$ TeV) and the need to keep the Higgs light ($\eta_1 v_s^2 \lesssim (100\text{ GeV})^2$), it can be seen from (4.47) and (4.48) that f must be the largest coupling to the S field. The dominant one-loop correction to the S potential therefore involves the new heavy quark, which gives a contribution to the potential with a sign opposite that of (4.40) in the DFSZ case. This does

not give rise to successful EW symmetry breaking because it gives a potential for S that is unbounded from below and drives the Higgs vev to an unacceptably large scale. Thus the KSVZ axion model with a classical scale invariance is not a viable model.

To produce a KSVZ-like model that leads to successful EW symmetry breaking, some additional CW term that dominates the potential with an opposite sign is required. Such a term could originate from additional SM singlet fields or it could be engineered at the two-loop level through fermion loops in a way similar to the model discussed in [252]. However, we do not explore these possibilities here and instead focus only on the DFSZ model by continuing with a discussion of its phenomenology.

4.3 Phenomenology of the DFSZ model

The DFSZ model requires the SM to be extended by a second Higgs doublet and a complex PQ scalar S, the latter of which contains the axion a and the pseudo-dilaton s. The fact that the couplings ζ_i are ultra-weak means that, for collider experiments, the phenomenology of the model is just that of the Type II two Higgs doublet model (2HDM) with the common mass scale of the additional Higgs states $\{H, A, H^{\pm}\}$ determined by the ratio

$$R \equiv \frac{m_H}{m_h} \simeq \sqrt{-\frac{\zeta_2}{2\zeta_1}}. \tag{4.49}$$

In most studies of the 2HDM, additional Higgs states with masses of roughly 350 GeV or more, corresponding to $R \gtrsim 3$, are allowed in significant regions of parameter space [264–267].[9] This lower bound on R comes from limits on the charged Higgs states $H^{\pm}$, so it is possible that a more detailed numerical study of this model that relaxes the assumptions $v_2 \ll v_1$ and $\lambda_4 = 0$ and produces different masses for $\{H, A, H^{\pm}\}$ will allow for smaller R. Meanwhile, an approximate upper bound $R \lesssim 5$ comes from the requirement that one does not introduce a little hierarchy problem from the coupling between the light and heavy Higgs sectors. This bound requires the masses of the heavy Higgs states to be smaller than roughly 600 GeV.

In the usual implementation of the DFSZ model, the pseudo-dilaton is very heavy with a mass of $\mathcal{O}(v_s)$. The novel feature of the model discussed here is that s is very light.

[9] Note that the convention in studying the Type II 2HDM is to have H_2 couple to the up-type quarks rather than H_1. Therefore when applying 2HDM limits to this model, one should use the definition $\tan\beta \equiv v_1/v_2$ rather than the usual $\tan\beta \equiv v_2/v_1$.

Specifically, from (4.46) we have

$$\zeta_1 \simeq -\frac{m_h^2}{v_s^2} \simeq -1.6 \times 10^{-20} \left(\frac{10^{12}\ \text{GeV}}{v_s}\right)^2 \tag{4.50}$$

and hence

$$\begin{aligned} m_s &\simeq \sqrt{-\frac{\zeta_1}{2\pi^2}} \left(\frac{m_H}{m_h}\right)^2 m_h \simeq \frac{R^2}{\sqrt{2}\pi} \frac{m_h^2}{v_s} \\ &\simeq 32 \left(\frac{10^{12}\ \text{GeV}}{v_s}\right) \left(\frac{R}{3}\right)^2\ \text{eV}, \end{aligned} \tag{4.51}$$

where $m_h \simeq 125.5$ GeV has been used. Since the pseudo-dilaton is light and couples to quarks through its mixing with the SM Higgs, one possible way to detect it is through fifth force experiments. However, using the estimate

$$\alpha_5 \sim \frac{1}{4\pi} \left[\sqrt{2} \left(\frac{2m_u + m_d}{v_s}\right)\right]^2 \tag{4.52}$$

for the coupling strength of the pseudo-dilaton to protons and $\lambda = 1/m_s$ for the effective range of the force, it can be seen that the pseudo-dilaton lies outside the region probed by Casimir-force and neutron scattering experiments [268]. It is possible that future terrestrial experiments can be devised to look for the pseudo-dilaton directly, but this remains unexplored. At present, the only way to constrain the pseudo-dilaton is through its cosmological influences, which we turn to a discussion of now.

4.4 Cosmology of the pseudo-dilaton

As an ultra-weakly interacting particle, the pseudo-dilaton influences cosmology primarily through its energy density. After the PQ scalar S acquires its vev and the PQ symmetry is broken, the energy stored in the dilaton potential is released as a coherent oscillation of the dilaton field. If this symmetry breaking occurs before inflation, the energy density contained in the dilaton is diluted away in the rapid expansion of the universe. This is the case if the dilaton mass is larger than the Hubble parameter during inflation, which requires a low scale of inflation

$$V_{\text{inf}}^{1/4} \lesssim 10^5 \left(\frac{10^{12}\ \text{GeV}}{v_s}\right)^{1/2} R\ \text{GeV}, \tag{4.53}$$

and if the reheat temperature is sufficiently low that the PQ symmetry is not restored after inflation. On the other hand, if the PQ symmetry breaking occurs after inflation, the energy

stored in the dilaton oscillation persists to late times (the Polonyi problem [269]) and can have a significant impact on the cosmological evolution. We consider both cases in turn, starting with the latter case.

4.4.1 High scale inflation

The energy stored in the dilaton potential depends on the initial value of the dilaton. For the case that the Hubble parameter during inflation is much larger than the dilaton mass, the dilaton performs a random walk of step length $H_{\rm inf}/2\pi$ in each Hubble time. The maximum dilaton energy corresponds to the largest initial value of ϕ_s, which in turn corresponds to the maximum Hubble parameter during inflation, $H_{\rm inf} \sim 10^{14}$ GeV, that is consistent with the BICEP2 result [218]. To be conservative, let us consider this extreme case since all others will have a smaller amount of energy initially stored in the dilaton and will be more weakly constrained. For 60 e-folds of inflation, one may expect the initial value of the dilaton field from the random walk to be given by $\phi_{s,\rm i} \sim 10^{14}$ GeV.[10]

After inflation and reheat, $s \simeq \phi_s$ begins to oscillate when its effective mass becomes larger than the Hubble parameter H. Even though s is not in thermal equilibrium, in the presence of a thermal plasma it obtains a large thermal mass [270]

$$m_{s,\rm th}^2 \simeq \frac{\zeta_2}{6} T^2, \tag{4.54}$$

where we have neglected all but the largest coupling of ϕ_s to thermalized particles, namely ζ_2. For a sufficiently high reheat temperature, the thermal mass (4.54) dominates the dilaton potential and the dilaton oscillates about a zero vev once it begins to roll, which occurs when $m_{s,\rm th} \sim H$ corresponding to the temperature

$$T_{\rm roll} \simeq 5 \times 10^7 R \left(\frac{10^{12}\ \text{GeV}}{v_s} \right) \text{GeV}. \tag{4.55}$$

The energy density in the dilaton at the beginning of its roll is given by

$$\rho_{s,\rm roll} \simeq \frac{1}{2} m_{s,\rm th}^2 \phi_{s,\rm i}^2 \simeq \frac{\zeta_2 T_{\rm roll}^2}{12} \phi_{s,\rm i}^2, \tag{4.56}$$

which is much less than the energy density of a relativistic degree of freedom at that time. Moreover, as the universe expands the energy density (4.56) redshifts as radiation, *i.e.*

[10] Some models of inflation have many more than 60 e-folds, in which case one might expect $\phi_{s,\rm i} \gg 10^{14}$ GeV from the longer random walk. The exact initial value of the dilaton field is not particularly important to the subsequent discussion so long as $\phi_{s,\rm i} \lesssim 10^{18}$ GeV.

$\rho_{s,\mathrm{roll}} \propto T^4$ [270]. This is faster than the matter redshift that one might expect because the temperature-dependent thermal mass also redshifts. Therefore the energy in the dilaton oscillations from the slow roll inflation era always remains negligible compared to the energy in the thermal plasma.[11]

When the temperature drops to $T \sim 20R$ GeV, the thermal mass term for the dilaton becomes comparable to the latter term of (4.44) and hence the minimum at $\phi_s = v_s$ appears. However, the amplitude of the dilaton oscillations $\bar{\phi}_s$ at this time is too small for the dilaton to make it over the potential barrier; $\bar{\phi}_s$ scales $\propto T$ from its initial value $\phi_{s,\mathrm{i}}$ at T_{roll}, so at $T \sim 20R$ GeV we have

$$\frac{\bar{\phi}_{s,\mathrm{CW}}}{v_s} \simeq 4 \times 10^{-5} \left(\frac{\phi_{s,\mathrm{i}}}{10^{14}\ \mathrm{GeV}} \right) \ll 1. \tag{4.57}$$

The tunnelling rate of the dilaton to the true vacuum is also very slow, therefore the dilaton continues to oscillate about a zero vev even after the minimum at v_s appears.

The dilaton oscillates about a zero vev until the EW symmetry is ultimately broken by non-perturbative effects in QCD, which occurs as follows. When the colour force becomes confining at $T \sim \Lambda_{\mathrm{QCD}} \sim 200$ MeV, it drives a quark condensate that gives masses to the W and Z bosons as well as the Higgs. Once the temperature drops below this Higgs boson mass, the stabilizing thermal mass term for the dilaton (4.54) rapidly vanishes due to the Boltzmann suppression of the Higgs [270] and the dilaton rolls to its minimum at v_s.

Until the EW symmetry is broken, though, the energy density of the universe is dominated by the potential energy in the Higgs and dilaton fields for temperatures below about $T \sim 10R$ GeV. This gives rise to a period of thermal inflation with approximately $\ln(10R\ \mathrm{GeV}/200\ \mathrm{MeV}) \sim 5$ e-folds of inflation. This period of inflation is sufficiently short that it does not affect the density perturbations coming from the initial stage of slow roll inflation and still allows for successful baryogenesis from an earlier epoch.

Once the EW symmetry is broken, the potential energy stored in the Higgs and dilaton fields (see (4.40))

$$\Delta V \simeq V(0,0) - V(v_1, v_s) \simeq \frac{\zeta_2^2 v_s^4}{128\pi^2} \simeq \frac{R^4 m_h^4}{32\pi^2} \tag{4.58}$$

[11] Note that the dilaton does not enter thermal equilibrium through processes such as $t\bar{t} \to h \to h + s$ since the $h^2 s$ coupling is proportional to the amplitude of the dilaton oscillations $\bar{\phi}_s$, which decreases with temperature as $\propto T$ [270].

is released as coherent oscillations of the fields. Due to the large decay width of the Higgs, which acts as a friction term in its equation of motion

$$\ddot{\phi}_1 + (3H + \Gamma_h)\,\dot{\phi}_1 + \lambda_1 \left(\phi_1^2 - \frac{v_1^2}{v_s^2}\phi_s^2\right)\phi_1 = 0, \tag{4.59}$$

the energy in the Higgs oscillations is quickly lost and goes into reheating the thermal plasma. Since the Higgs' couplings to the plasma are $\mathcal{O}(1)$, we approximate the reheating as instant. If roughly half of the energy (4.58) is released into the thermal plasma,[12] the resulting reheat temperature is

$$T_{\rm reh} \sim 30 \left(\frac{R}{3}\right)\left(\frac{90}{g_{*s}}\right)^{1/4} \text{GeV}. \tag{4.60}$$

The rest of the energy,

$$\rho_s \sim \frac{R^4 m_h^4}{64\pi^2}, \tag{4.61}$$

is released as coherent oscillations of the dilaton that redshift as matter, *i.e.* $\propto T^3$.

Dissipation of the dilaton oscillations

The energy density (4.61) is large enough that it will quickly dominate the energy density of the universe, thereby spoiling the predictions of BBN and other late-time cosmology, unless it is somehow dissipated. Following eqs. (3.27) and (3.28) of [271], the dissipation rate of the oscillating dilaton field through processes such as $s + c \to c \to$ SM states and $s + h \to h \to$ SM states is found by taking the imaginary part of the self energy

$$\tilde{\Pi}_J(m_{s,\rm eff}, \mathbf{0}) = \lambda_{s\bar{c}c}^2 \int \frac{d^4q}{(2\pi)^4}\left(f_F(q_0) - f_F(q_0 + m_{s,\rm eff})\right) \text{tr}\left[\rho_c^F(q_0,\mathbf{q})\rho_c^F(m_{s,\rm eff}+q_0,\mathbf{q})\right] \tag{4.62}$$

$$+ \Lambda_{shh}^2 \int \frac{d^4q}{(2\pi)^4}\left(f_B(q_0) - f_B(q_0 - m_{s,\rm eff})\right)\rho_h^B(q_0,\mathbf{q})\rho_h^B(m_{s,\rm eff}-q_0,\mathbf{q}). \tag{4.63}$$

In (4.62), $\lambda_{s\bar{c}c}$ is the coupling of s to the charm quark, which in analogy to (4.19) is given by

$$\lambda_{s\bar{c}c} \simeq \lambda_{h\bar{c}c}\left(\frac{v_1}{v_s}\right) = \frac{m_c}{v_1/\sqrt{2}}\frac{v_1}{v_s} = \frac{\sqrt{2}m_c}{v_s}. \tag{4.64}$$

[12] Writing the potential in the form $V \simeq \frac{\lambda_1}{4}v_1^4\left[\left(x^2-y^2\right)^2 + cy^4\left(-\frac{1}{2}+\ln y^2\right)\right]$, where $x \equiv \phi_1/v_1$, $y \equiv \phi_s/v_s$, and $c \equiv R^4 m_h^2/(2\pi^2 v_1^2) \sim 1$, one finds that the steepest descent of the potential is typically along the $x = y$ direction. Therefore if ϕ_s rolls some small distance dy to release energy dE in coherent oscillations of the dilaton, the much heavier Higgs field undergoes rapid oscillations with amplitude $dx = dy$ that are quickly damped and release the same energy dE into the thermal plasma.

The fermionic distribution function and spectral density in (4.62) are given by

$$f_F(q_0) = \frac{1}{e^{q_0/T}+1}, \qquad \rho_c^F(q_0,\mathbf{q}) \simeq \frac{1}{2}\frac{\Gamma_{c,\mathbf{q}}}{\left[q_0-\omega_{\mathbf{q}}\right]^2+\Gamma_{c,\mathbf{q}}^2/4}\left(\frac{\not{q}}{q_0}\right), \tag{4.65}$$

where $\omega_{\mathbf{q}} = \sqrt{m_c^2+|\mathbf{q}|^2}$ is the energy of the charm quark and $\Gamma_{c,\mathbf{q}}$ is its thermal width. Similarly, in (4.63), $\Lambda_{shh} = \zeta_1 v_s/2$ is the dimensionful coupling of the trilinear term shh and

$$f_B(q_0) = \frac{1}{e^{q_0/T}-1}, \qquad \rho_h^B(q_0,\mathbf{q}) = \frac{2q_0\Gamma_{h,\mathbf{q}}}{\left[q_0^2-\Omega_{\mathbf{q}}^2\right]^2+\left[q_0\Gamma_{h,\mathbf{q}}\right]^2}, \tag{4.66}$$

where $\Omega_{\mathbf{q}} = \sqrt{m_h^2+|\mathbf{q}|^2}$ is the energy of the Higgs h and $\Gamma_{h,\mathbf{q}}$ is its thermal width.[13] Consider the process $s+c\to c\to$ SM states for the moment since its rate turns out to be sufficiently large to dissipate the energy in the dilaton oscillations for all v_s of interest. For small $m_{s,\text{eff}}$, the dissipative rate corresponding to (4.62) can be approximated by [271]

$$\Gamma_s^{\text{diss}} \simeq \frac{\lambda_{s\bar{c}c}^2}{2T}\int\frac{d^4q}{(2\pi)^4} f_F(q_0)\left(1-f_F(q_0)\right)\text{tr}\left[\rho_c^F(q_0,\mathbf{q})\rho_c^F(q_0,\mathbf{q})\right]. \tag{4.67}$$

By replacing one of the spectral density functions in (4.67) by a delta function

$$\rho_c^F(q_0,\mathbf{q}) \simeq 2\pi\delta\left(2(q_0-\omega_{\mathbf{q}})\right)\frac{\not{q}}{q_0} = \pi\delta\left(q_0-\omega_{\mathbf{q}}\right)\frac{\not{q}}{q_0}, \tag{4.68}$$

which is applicable in the narrow width approximation, one obtains

$$\Gamma_s^{\text{diss}} \simeq \frac{\lambda_{s\bar{c}c}^2}{2T}\int\frac{d^3\mathbf{q}}{(2\pi)^3} f_F(q_0)\left(1-f_F(q_0)\right)\frac{4m_c^2}{q_0^2\Gamma_{c,\mathbf{q}}}, \tag{4.69}$$

where $q_0 = \sqrt{m_h^2+|\mathbf{q}|^2}$ is now a function of $\mathbf{q}$. The $1/\Gamma_{c,\mathbf{q}}$ behaviour of (4.69), which is critical to obtaining a large dissipation rate, can be understood physically from the fact that the coherent oscillation of a scalar field can be treated as a collection of zero momentum particles. Upon colliding with a charm quark from the thermal plasma, the dilaton produces a nearly on-shell quark $q_0 \simeq \omega_{\mathbf{q}}$ whose propagator is dominated by its decay width, thus leading to a resonant enhancement of the process.

The thermal width $\Gamma_{c,\mathbf{q}}$ can be found by computing the imaginary part of the one-loop self-energy diagram of the charm quark with the decay products running in the loop, as in [272]. Rather than perform this calculation, however, simply consider the region $T \lesssim m_c$ for which $\Gamma_{c,\mathbf{q}}$ can be approximated by the zero temperature decay width [273]

$$\Gamma_c \simeq \frac{G_F^2 m_c^5}{192\pi^3}. \tag{4.70}$$

[13] There are analogous formulas for the processes $s+b\to b\to$ SM states and $s+H\to H\to$ SM states, but as we will see it is not necessary to consider these.

Using $\Gamma_{c,\mathbf{q}} \simeq \Gamma_c$ in (4.69) and performing the integration over $\mathbf{q}$ in the non-relativistic limit gives

$$\Gamma_s^{\rm diss} \simeq \frac{\sqrt{2} m_c^4}{\pi^{3/2} v_s^2 \Gamma_c} \left(\frac{T}{m_c}\right)^{1/2} e^{-m_c/T}. \tag{4.71}$$

The exponential factor $e^{-m_c/T}$ arises from the Boltzmann suppression of the charm quark in the thermal plasma for $T \lesssim m_c$.

If $\Gamma_s^{\rm diss}$ is larger than the Hubble rate for some temperature $T \lesssim m_c$, all of the energy stored in the coherent oscillation of the dilaton is dissipated into the thermal plasma. Comparing (4.71) with the Hubble rate[14]

$$H \simeq \sqrt{\frac{8\pi}{3M_{\rm Pl}^2} \frac{R^4 m_h^4}{64\pi^2} \left[\left(\frac{T}{T_{\rm reh}}\right)^4 + \left(\frac{T}{T_{\rm reh}}\right)^3\right]}, \tag{4.72}$$

we find that values of $v_s \lesssim 5 \times 10^{14}$ GeV have $\Gamma_s^{\rm diss} \gtrsim H$ for some range of temperatures $T_* < T \lesssim m_c$. Thus for all values of v_s within the range of interest (4.28), the energy density in the dilaton oscillations is dissipated shortly after reheating at $T \sim m_c$, if not earlier.

Dark matter

Although the energy density in the zero momentum dilaton oscillations is quickly dissipated, a relativistic population of dilatons can still be produced at temperatures below $T_{\rm reh}$ through mixing with the Higgs states. The dominant production channel is the scattering process

$$g + q \to q \to q + s, \tag{4.73}$$

where g is a gluon and q is a thermalized quark. Note that these dilaton production processes do not have a resonant enhancement like the dissipation rate because none of the incoming particles are zero momentum coherent states. Due to the low reheat temperature (4.60), the number density of the top quark — and hence its associated interaction rate — is exponentially suppressed for $T < T_{\rm reh}$. Therefore it is the bottom quark in (4.73) that gives the largest rate of dilaton production. To estimate the dilaton abundance generated by this process, take the coupling of s to the bottom quark to be

$$y_{s\bar{b}b} \simeq y_{H\bar{b}b} \left(\frac{v_2}{v_s}\right) = \frac{m_b}{v_2/\sqrt{2}} \frac{v_2}{v_s} = \frac{\sqrt{2} m_b}{v_s} \tag{4.74}$$

[14]Starting from $T_{\rm reh}$, the energy density in the relativistic thermal plasma scales as T^4 while the energy density in the dilaton oscillations scales as T^3.

and the thermally averaged cross-section for $T \gtrsim m_q$, including the quark colour factor of 3, to be

$$\langle \sigma v \rangle \sim 3 \cdot \left(\frac{m_q}{v_s} \right)^2 \frac{\alpha_s}{T^2}. \tag{4.75}$$

Then the rate of dilaton production is given by

$$\begin{aligned} \Gamma_s^{\text{prod}} = n \langle \sigma v \rangle &\sim 4 \cdot \frac{3\zeta(3)}{4\pi^2} T^3 \times 3 \cdot \left(\frac{m_b}{v_s} \right)^2 \frac{\alpha_s}{T^2} \\ &\sim 6 \times 10^{-19} \left(\frac{2 \times 10^9 \text{ GeV}}{v_s} \right)^2 T, \end{aligned} \tag{4.76}$$

where n is the number density of the bottom quark with 4 degrees of freedom. As a rough estimate, the ratio of the dilaton abundance to that of a thermal distribution is given by the maximum of the ratio Γ_s^{prod}/H for $T \gtrsim m_b$. This estimate gives

$$\frac{n_s}{n_s^{\text{eq}}} \sim \max \left\{ \frac{\Gamma_s^{\text{prod}}}{H} \right\} = \left. \frac{\Gamma_s^{\text{prod}}}{H} \right|_{T=m_b} \sim 0.4 \left(\frac{2 \times 10^9 \text{ GeV}}{v_s} \right)^2, \tag{4.77}$$

where $g_{*s}(m_b) \simeq 90$ has been used.

After production, the energy density in the dilaton is given by the standard relic calculation. If the dilaton is sufficiently long lived, it is non-relativistic today with an energy density

$$\rho_{s,0} = \frac{n_s}{n_s^{\text{eq}}} \times m_s \frac{\zeta(3)}{\pi^2} \frac{g_{*s}(T_0)}{g_{*s}(m_b)} T_0^3 \tag{4.78}$$

and hence an abundance of

$$\Omega_s \sim 0.3 \left(\frac{R}{3} \right)^2 \left(\frac{7 \times 10^9 \text{ GeV}}{v_s} \right)^3, \tag{4.79}$$

where we have again taken $g_{*s}(m_b) \simeq 90$. For a region of parameter space with $R \sim 3$ and $v_s \sim 7 \times 10^9$ GeV, the dilaton would therefore have just the right relic abundance to be dark matter.[15] However, to constitute dark matter the dilaton must be stable on cosmological timescales. The dominant direct decay mode of the dilaton is to two axions with the decay rate

$$\Gamma_{s \to aa} = \frac{1}{32\pi} \frac{m_s^3}{v_s^2} \simeq \frac{R^6 m_h^6}{64\sqrt{2}\pi^4 v_s^5}, \tag{4.80}$$

[15] In this case, (4.51) shows that the dilaton is a warm dark matter (WDM) candidate with a mass in the keV range; specifically, $m_s \simeq 5 \left(\frac{R}{3}\right)^2$ keV. Since the observation of small scale structure through the Lyman-α forest excludes thermal relic dark matter candidates with masses $m_s \lesssim 3.3$ keV [274], the dilaton is sufficiently heavy that it should not wipe out small scale structure.

giving a lifetime

$$\tau_s \simeq 3.4 \times 10^{18} \left(\frac{3}{R}\right)^6 \left(\frac{v_s}{7 \times 10^{10}\ \text{GeV}}\right)^5 \text{sec.} \tag{4.81}$$

Constraints on decaying dark matter generally require the lifetime to be on the order of 100 Gyr (3×10^{18} sec) or longer, provided the particle makes up all of the dark matter [275–281].[16] For $v_s \sim 7 \times 10^9$ GeV, the dilaton is not stable on cosmological timescales and therefore cannot be dark matter. Moreover, the large conversion of energy density to relativistic axions at late times would likely pose problems for structure formation and rule out the parameter space with $v_s \lesssim 7 \times 10^9$ GeV. Conversely, for $v_s \gtrsim 7 \times 10^{10}$ GeV for which the dilaton is sufficiently long lived to be dark matter, (4.79) shows that the dilaton has a negligible dark matter abundance ($\Omega_s \lesssim 3 \times 10^{-4}$).

The axion, however, provides a very plausible cold dark matter candidate. The contribution to the energy density of the universe from the coherent oscillations (zero mode) of the axion through the vacuum realignment mechanism is [282]

$$\Omega_a h^2 \simeq 0.236 \theta_i^2 f(\theta_i) \left(\frac{v_s/N_{\text{DW}}}{10^{12}\ \text{GeV}}\right)^{7/6}, \tag{4.82}$$

where $N_{\text{DW}} = 6$ for this model, θ_i is the initial misalignment angle, and the function $f(\theta_i) = [\ln(e/(1-\theta_i^2/\pi^2))]^{7/6}$ encodes the anharmonic effect. Since the PQ symmetry is broken after inflation, the initial misalignment angle varies between horizons and so θ_i must be averaged over in (4.82); taking $\langle \theta_i^2 f(\theta_i) \rangle \sim 2.67 \times \pi^2/3$, for instance, is reasonable [282]. Meanwhile, the higher momentum axion modes and the axions produced in the decay of strings and domain walls contribute a comparable amount to the energy density as vacuum realignment (for details, see [283–285]). For $v_s \sim 10^{12}$ GeV, the axion can therefore provide all of the dark matter.

Domain walls

For invisible axion models with $N_{\text{DW}} = 1$, the network of domain walls that forms after the PQ symmetry breaking is unstable and decays away [284, 286]. For invisible axion models with $N_{\text{DW}} > 1$, which includes this DFSZ model, domain walls are stable and it is important to consider how the problem associated with their large energy density can be avoided [287].

[16] If the dilaton comprises only some of the dark matter, the bounds are relaxed accordingly.

In general, the energy density in stable domain walls is many orders of magnitude larger than the critical energy density for closing the universe. However, a small breaking of the PQ symmetry can cause the domains walls to decay and hence avoid their large energy density while preserving the axion solution to the strong CP problem [287]. A qualitative picture of how this can happen in our model is as follows. Note that the most general scale invariant potential $V(H_1, H_2, S)$ includes the terms

$$\Delta V(H_1, H_2, S) = \lambda_5 (H_1^\dagger H_2)^2 + \zeta_5 (H_2^\dagger H_1) S^2 + \zeta_6 S^4 + \text{h.c}, \tag{4.83}$$

which break the PQ symmetry and split the degeneracy of the discrete $Z(N_{\text{DW}})$ symmetry that leads to the domain wall problem. The couplings λ_5, ζ_5, and ζ_6 are multiplicatively renormalized and so they can be naturally small. With an explicit PQ symmetry breaking $\lambda_5 \sim \zeta_{1,2,3}$ of the same order as the breaking of the scale symmetry $S \to \lambda S$, the terms in (4.83) are in the range needed to solve the domain wall problem without disturbing the axion solution to the strong CP problem [287]. In this scheme, note that ζ_5 and ζ_6 are smaller than λ_5 by one and two powers of the scale symmetry breaking parameter, respectively, since they break both the PQ symmetry and the scale symmetry.

In summary, the large thermal mass of the dilaton produces a period of thermal inflation with approximately 5 e-folds after the usual slow roll inflation. At the end of this thermal inflation, the energy in the dilaton potential that is released as coherent oscillations of the field is large enough that it poses a potential problem for late-time cosmology. For all choices of v_s allowed in this model, though, the interactions of the dilaton with the thermal plasma are sufficiently fast to dissipate the energy density in the oscillations due to a resonant enhancement of the process. A significant relativistic population of dilatons is produced in the region of parameter space with $v_s \lesssim 7 \times 10^9$ GeV, but the decay of dilatons to two axions is too fast in this region to allow the dilaton to be dark matter. The dilaton can therefore only have a negligible contribution to dark matter. The coherent oscillations of the axion, on the other hand, can comprise all of the dark matter for $v_s \sim 10^{12}$ GeV. The axion domain wall problem can be solved with small but technically natural terms that explicitly break the PQ symmetry and hence the $Z(N_{\text{DW}})$ degeneracy between the vacua.

4.4.2 Low scale inflation

In the case that (4.53) is satisfied and the reheat temperature is sufficiently low ($T_{\rm reh} \lesssim$ 100 GeV) that the dilaton does not obtain a thermal mass that forces it to roll to $v_s = 0$, the PQ symmetry remains broken during and after slow roll inflation. As a result, the energy density in the dilaton oscillations are driven exponentially small and the axion field gets homogenized by the expansion of the universe during the inflationary phase, thereby preventing the formation of domain walls [284]. The usual result (4.82) for the axion contribution to the energy density from vacuum realignment still holds[17] and the axion can provide all of the dark matter for $v_s \sim 10^{12}$ GeV and $\theta_i \sim 1$.[18] The dilaton, however, never plays a significant role in cosmology.

4.5 Summary and conclusions

The discovery of a Higgs scalar with properties very close to that predicted by the SM, together with the lack of any strong indication of BSM physics at the LHC, has led some to rethink the need for such BSM physics to solve the hierarchy problem. An alternative approach, which is motivated by the technical naturalness of a small Higgs mass parameter in the absence of sufficiently strongly coupled new physics, takes $m^2 = 0$ corresponding to a classical scale invariance of the model. Simple extensions of the SM scalar sector then allow successful EW symmetry breaking through the CW mechanism.

These classically scale invariant extensions of the SM, however, do not address the strong CP problem or discuss whether the usual invisible axion solution is compatible with this approach. We therefore examined the DFSZ and KSVZ invisible axion models in the context of a classical scale invariance and CW symmetry breaking. We showed that while the KSVZ model with a classical scale invariance does not lead to successful radiative symmetry breaking, the DFSZ invisible axion model with a classical scale invariance and an ultra-weakly coupled PQ scalar can give rise to successful EW symmetry breaking through the CW mechanism. Moreover, the ultra-weak couplings ζ_i between the PQ scalar and the Higgs sector

[17] The contribution from the quantum fluctuations of the axion field during inflation, which are included by making the replacement $\theta_i^2 \to \theta_i^2 + \sigma_\theta^2$ in (4.82) where $\sigma_\theta^2 \simeq (H_I/2\pi f_a)^2$ [282], are negligible for H_I satisfying (4.53).

[18] As discussed in [263], with moderate fine-tuning to give $\theta_i \simeq \pi$, the axion can provide all of the dark matter for smaller values v_s due to the anharmonic effect.

are technically natural due to the underlying approximate shift symmetry of the model, and hence they do not introduce a hierarchy problem.

The DFSZ model requires two Higgs doublets and predicts a collection of new Higgs states that are observable at the LHC.[19] As a result of the classical scale invariance, the model also contains a light pseudo-dilaton in the scalar mass spectrum that is not present in the usual DFSZ axion model. We discussed the cosmology of this light pseudo-dilaton in detail and showed that it does not pose a problem for cosmology within a large range of the parameter space available to the model. Moreover, the axion provides a plausible cold dark matter candidate for $v_s \sim 10^{12}$ GeV.

[19] Although not explicitly mentioned, note that the additional couplings arising from the two Higgs doublets can be chosen to avoid the vacuum instability of the SM at $\Lambda \sim 10^9$–10^{10} GeV [288].

Chapter 5

Summary and outlook

The SM does a remarkably good job in fitting the large collection of experimental results in high energy physics. Moreover, when combined with the standard Big Bang cosmology it provides a compelling picture of processes in the early universe back to at least the era of primordial nucleosynthesis.

Despite its successes, the SM is unable to provide an adequate explanation for several important phenomenological results. It also introduces a number of unanswered theoretical questions. In the former category, the discovery of neutrino oscillations implies that neutrinos are massive with a misalignment of their weak and mass eigenbases. Although a complete description of neutrino masses and mixings has not been determined yet, massive neutrinos are a relatively simple extension of the SM and can easily be accommodated by right-handed neutrinos. The remaining phenomenological shortcomings of the SM are related to cosmology. Dark matter and the baryon asymmetry of the universe are both necessary to our understanding of the cosmological evolution, but they do not have compelling particle candidates or mechanisms within the SM. Similarly, a period of inflation in the early universe may require some particle beyond the SM.

On the theoretical side, the seemingly fine-tuned parameters in the SM corresponding to the gauge hierarchy problem, the strong CP problem, and the cosmological constant problem indicate that some new physics is needed to explain their small values. The pattern of masses and mixing angles in the flavour sector of the SM also hints at the existence of an underlying flavour symmetry. As with the phenomenological shortcomings of the SM, these theoretical shortcomings provide motivation for a number of BSM theories, many of which have significant couplings to the SM sector and observable signatures at the LHC.

The fact that there has been no strong indication of new physics at the LHC so far has led us to pursue an alternative approach to BSM physics in this thesis: consider minimal extensions of the SM required to explain BSM phenomenology and avoid introducing new physics between the EW and Planck scales that couples significantly to the Higgs. In this approach, the lack of an intermediate scale of new physics with significant Higgs couplings avoids the gauge hierarchy problem — at least in the technical sense that the quadratically divergent corrections to the Higgs mass are unphysical and there are no heavy states giving large logarithmic corrections to the Higgs mass. This approach is closely related to the more general principle of technical naturalness, under which small Lagrangian parameters are acceptable so long as they remain small in the presence of radiative or quantum corrections.

Following these ideas, we first considered issues related to an extension of the SM known as the νMSM. This minimal model attempts to explain neutrino oscillations, dark matter, and the baryon asymmetry of the universe using three right-handed neutrinos with masses below the EW scale. In chapter 2, tension between the simplest form of dark matter production in the νMSM and small scale structure bounds from the Lyman-α forest data led us to consider a singlet extension of the model, the νNMSM, in which sterile neutrino dark matter is produced through the decays of the singlet. We showed that the hierarchical pattern of Majorana masses and Yukawa couplings in the νNMSM can arise from flavour symmetries broken at or near the Planck scale for two specific versions of the model: one that stabilizes the EW vacuum of the νMSM and one that provides an alternative model of inflation for the νMSM. Both models require a complex singlet for the flavour symmetry to be realized. We discussed the experimental signatures of the νNMSM that distinguish it from the νMSM and briefly described the possibility that the complex singlet has ultra-weak couplings to the Higgs that are technically natural and hence avoid a hierarchy problem.

Chapter 3 examined the remaining aspect of the νMSM that is important to its minimality: Higgs ξ-inflation. As discussed in the chapter, a large non-minimal coupling $\xi \gg 1$ of the Higgs to gravity causes the SM potential to flatten above $M_{\rm Pl}/\sqrt{\xi}$ and allows slow roll inflation to occur without the need for an additional scalar field. However, a naive estimate for the scale of perturbative unitarity violation in the model is $M_{\rm Pl}/\xi$, thereby bringing into question the self-consistency of Higgs ξ-inflation and its predictions. In chapter 3, we studied whether the running of the Higgs self-coupling λ to very small values near the Planck scale,

which might arise as the boundary condition of some underlying UV physics, allows ξ to be small enough to avoid the unitarity issues with the model. Using a two-loop analysis, we found that values of ξ as small as $\xi \sim 90$ led to successful inflation within the bounds from *Planck* 2013. Although these values of ξ are still too large to address the unitarity problem, a new region of Higgs ξ-inflation with an observable level of the tensor-to-scalar ratio $r \gtrsim 0.15$ was discovered.

Chapter 4 moved away from phenomenological issues related to the νMSM and considered the strong CP problem in a classically scale invariant extension of the SM. Such extensions are motivated by the technical naturalness of a small Higgs mass parameter, for which $m^2 = 0$ is the only intrinsically special value, and from the possibility that an approximate classical scale invariance may arise from the RG flow of mass parameters down to the Planck scale. We showed that a DFSZ-like invisible axion model with an ultra-weakly coupled PQ scalar can solve the strong CP problem and give rise to successful EW symmetry breaking through the CW mechanism. An approximate underlying shift symmetry of the model ensures that the ultra-weak couplings of the PQ scalar are technically natural and therefore that the model does not have a hierarchy problem. Moreover, as a result of the classical scale invariance, the DFSZ-like model contains a light pseudo-Goldstone dilaton. We discussed the cosmology of the light dilaton in detail and showed that it can be consistent with cosmological bounds while the axion can be the dark matter of the universe.

In conclusion, the long-held belief that new physics must be present at the EW scale to solve the gauge hierarchy problem may have to be replaced with the idea that something closely resembling the SM is valid all the way up to the Planck scale. In this regard, the lack of strong evidence for BSM physics at the LHC and the possibility that ultra-weakly coupled physics can solve the phenomenological and theoretical problems with the SM have led some to rethink the usual ideas about fine-tuning. A principle of technical naturalness can instead be adopted to guide BSM physics. According to this principle, there are a number of ways in which the SM can be extended to address its shortcomings. Without providing a complete picture of BSM physics, this thesis has examined several issues with the SM and its extensions, as well as their possible solutions, while attempting to preserve as much of the SM up to the Planck scale as possible.

5.1 Future directions

There are a number of ways the work presented here can be developed further. An obvious direction of future research would be to combine the DFSZ-like invisible axion model from chapter 4 with the νNMSM from chapter 2; the classical scale invariance used in the DFSZ-like axion model forbids the bare Majorana masses of the right-handed neutrinos in the νMSM and forces a singlet extension like the νNMSM. The PQ scalar S, which solves the strong CP problem, could then be identified with the complex singlet scalar ϕ that provides the Majorana masses for the right-handed neutrinos. In a region of parameter space with $v_s \lesssim 7 \times 10^9$ GeV, a significant dilaton population would be produced and the dilaton can be heavy enough to decay to $\mathcal{O}(10$ keV) mass right handed neutrinos N_1^m through $s \to N_1^m N_1^m$. The rate of this decay is comparable to that of the dilaton to two axions, so if a moderate fraction of the dilaton abundance (4.79) is converted into sterile neutrinos, it might provide the correct abundance in N_1^m for dark matter and be consistent with small scale structure bounds from the Lyman-α forest data.

Alternatively, the axion could provide all of the dark matter in this combined model for $v_s \sim 10^{12}$ GeV. In this case, N_1^m is not required for dark matter and may participate in the right-handed neutrino oscillations that produce the baryon asymmetry of the universe. Another direction of research would therefore be to study the more complicated three-body system of neutrino oscillations involving $\{N_1^m, N_2^m, N_3^m\}$ to see if the high mass degeneracy between N_2^m and N_3^m that is required in the νMSM can be avoided — for instance, by considering the original mechanism for baryogenesis through neutrino oscillations as proposed in [44]. If such a scenario is possible and can be realized with all right-handed neutrinos N_I^m at a common mass scale, a much simpler flavour symmetry than those considered in chapter 2 may be sufficient to produce the necessary pattern of Majorana masses and Yukawa couplings in the model.

On a different note, a detailed study of the inflationary possibilities in the DFSZ-like axion model would be worth carrying out. In this regard, a non-minimal coupling of the Higgs doublets and/or the PQ scalar would likely allow for successful inflation with similar predictions as Higgs ξ-inflation from chapter 3. With the additional scalar degrees of freedom, however, the realization of a model of inflation that avoids the violation of perturbative

unitarity at low energies might be possible. Since the running of the SM Higgs self-coupling λ to approximately zero near the Planck scale is spoiled by the couplings of the second Higgs doublet, a tree-level analysis of the inflationary scenarios would likely be sufficient.

As mentioned in chapter 4, a numerical study of the DFSZ-like axion model in which the assumptions $v_2 \ll v_1$ and $\lambda_4 = 0$ can be relaxed would also be a useful direction of future research. In this case, the heavy Higgs states $\{H, A, H^{\pm}\}$ separate from their common mass scale and may exhibit interesting hierarchies. Such a numerical study would be important for determining the range of parameter space in the model that is ruled out by the current LHC data[1] and for determining the experimental signatures of the model. In the latter regard, further exploration of how the light dilaton might be detected directly in fifth-force experiments or cavity search experiments would also be worthwhile.

Another important direction of future research for the models discussed in chapter 4 would be to demonstrate more precisely how an approximate low-energy classical scale invariance can arise from the RG flow of mass parameters above the Planck scale. If successful, such a study would provide a stronger theoretical basis for considering a classical scale invariance and EW symmetry breaking through the CW mechanism.

Finally, although its consideration deviates from the approach taken in this thesis, a supersymmetrization of the DFSZ-like axion model would allow for a stage of Grand Unification without introducing the hierarchy problem. Some preliminary work along these lines has been carried out in [224], but many phenomenological possibilities in a SUSY version of the model remain unexplored.

[1] For instance, a wider range of the parameter R than that considered in chapter 4 might be allowed.

Appendix A

Renormalization group equations for Higgs ξ-inflation

In this appendix we list the (gauge-independent) RG equations for the couplings λ, y_t, g', g, g_s, and ξ in the $\overline{\text{MS}}$ scheme that are used in our analysis of Higgs ξ-inflation. For each coupling we write $dx/dt = \beta_x$, where $t = \ln(\mu/\mu_0)$. The anomalous dimension of the Higgs field γ in the Landau gauge, for use in (3.30), is also given. As described in section 3.3.1, the RG equations contain one suppression factor $s = s(h)$ for each off-shell physical Higgs propagator.[1] Note that the RG equations for the SM can be recovered by setting $s = 1$.

The two-loop RG equations for λ, y_t, g', g, g_s, and ξ are as follows. For the Higgs quartic coupling we have

$$\begin{aligned}
\beta_\lambda = {} & \frac{1}{(4\pi)^2}\left[\left(6+18s^2\right)\lambda^2 - 6y_t^4 + \frac{3}{8}\left(2g^4 + \left(g^2+g'^2\right)^2\right) + \left(-9g^2 - 3g'^2 + 12y_t^2\right)\lambda\right] \\
& + \frac{1}{(4\pi)^4}\left[\frac{1}{48}\left((912+3s)\,g^6 - (290-s)\,g^4g'^2 - (560-s)\,g^2g'^4 - (380-s)\,g'^6\right)\right. \\
& + (38-8s)\,y_t^6 - y_t^4\left(\frac{8}{3}g'^2 + 32g_s^2 + \left(12-117s+108s^2\right)\lambda\right) \\
& + \lambda\left(-\frac{1}{8}\left(181+54s-162s^2\right)g^4 + \frac{1}{4}\left(3-18s+54s^2\right)g^2g'^2 + \frac{1}{24}\left(90+377s+162s^2\right)g'^4\right. \\
& + \left(27+54s+27s^2\right)g^2\lambda + \left(9+18s+9s^2\right)g'^2\lambda - \left(48+288s-324s^2+624s^3-324s^4\right)\lambda^2\Big) \\
& \left. + y_t^2\left(-\frac{9}{4}g^4 + \frac{21}{2}g^2g'^2 - \frac{19}{4}g'^4 + \lambda\left(\frac{45}{2}g^2 + \frac{85}{6}g'^2 + 80g_s^2 - \left(36+108s^2\right)\lambda\right)\right)\right].
\end{aligned} \tag{A.1}$$

[1] The suppression factor $s(h) = s(h(\mu))$ can be written in terms of μ by inverting $\mu = h/\Omega$ or $\mu = h$ for prescriptions I or II, respectively (see section 3.3.2).

For the top quark Yukawa coupling we have

$$\begin{aligned}\beta_{y_t} = &\frac{y_t}{(4\pi)^2}\left[-\frac{9}{4}g^2 - \frac{17}{12}g'^2 - 8g_s^2 + \left(\frac{23}{6} + \frac{2}{3}s\right)y_t^2\right] \\ &+ \frac{y_t}{(4\pi)^4}\left[-\frac{23}{4}g^4 - \frac{3}{4}g^2g'^2 + \frac{1187}{216}g'^4 + 9g^2g_s^2 + \frac{19}{9}g'^2g_s^2 - 108g_s^4\right. \\ &\left. + \left(\frac{225}{16}g^2 + \frac{131}{16}g'^2 + 36g_s^2\right)sy_t^2 + 6\left(-2s^2y_t^4 - 2s^3y_t^2\lambda + s^2\lambda^2\right)\right]. \end{aligned} \tag{A.2}$$

For the gauge couplings g', g, and g_s we have

$$\beta_{g'} = \frac{g'^3}{(4\pi)^2}\left[\frac{81+s}{12}\right] + \frac{g'^3}{(4\pi)^4}\left[\frac{199}{18}g'^2 + \frac{9}{2}g^2 + \frac{44}{3}g_s^2 - \frac{17}{6}sy_t^2\right], \tag{A.3}$$

$$\beta_g = \frac{g^3}{(4\pi)^2}\left[-\frac{39-s}{12}\right] + \frac{g^3}{(4\pi)^4}\left[\frac{3}{2}g'^2 + \frac{35}{6}g^2 + 12g_s^2 - \frac{3}{2}sy_t^2\right], \tag{A.4}$$

$$\beta_{g_s} = \frac{g_s^3}{(4\pi)^2}\left[-7\right] + \frac{g_s^3}{(4\pi)^4}\left[\frac{11}{6}g'^2 + \frac{9}{2}g^2 - 26g_s^2 - 2sy_t^2\right]. \tag{A.5}$$

And for the non-minimal coupling ξ we have

$$\begin{aligned}\beta_\xi = &\frac{1}{(4\pi)^2}\left(\xi + \frac{1}{6}\right)\left[-\frac{3}{2}g'^2 - \frac{9}{2}g^2 + 6y_t^2 + (6+6s)\lambda\right] \\ &+ \frac{1}{(4\pi)^4}\left(\xi + \frac{1}{6}\right)\left[\left(-\frac{199}{16} + \frac{27}{8}s\right)g^4 + \left(-\frac{3}{8} + \frac{9}{4}s\right)g^2g'^2 + \left(\frac{3}{2} + \frac{485}{48}s\right)g'^4\right. \\ &+ \left(\frac{45}{4}g^2 + \frac{85}{12}g'^2 + 40g_s^2\right)y_t^2 + \left(18 - \frac{63}{2}s\right)y_t^4 + \left(36g^2 + 12g'^2 - 36y_t^2\right)(1+s)\lambda \\ &\left. + \left(-108 + 126s - 144s^2 + 66s^3\right)\lambda^2\right]. \end{aligned} \tag{A.6}$$

In addition, the Higgs anomalous dimension $\gamma = -d\ln h/dt$ is given by

$$\begin{aligned}\gamma = &-\frac{1}{(4\pi)^2}\left[\frac{9}{4}g^2 + \frac{3}{4}g'^2 - 3y_t^2\right] \\ &- \frac{1}{(4\pi)^4}\left[\frac{271}{32}g^4 - \frac{9}{16}g^2g'^2 - \frac{431}{96}sg'^4 - \frac{5}{2}\left(\frac{9}{4}g^2 + \frac{17}{12}g'^2 + 8g_s^2\right)y_t^2 + \frac{27}{4}sy_t^4 - 6s^3\lambda^2\right]. \end{aligned} \tag{A.7}$$

The RG equations (A.1)–(A.7) can easily be extended to include (i) the complete three-loop expressions for the gauge coupling beta functions [198] and (ii) the leading three-loop corrections to β_λ, β_{y_t}, and γ [199]. These improvements can be made by adding the following

terms to the beta functions:

$$\Delta\beta_\lambda = \frac{1}{(4\pi)^6}\left[(7176+4032\zeta_3)\,\lambda^4 + 1746 y_t^2\lambda^3 + (1719+1512\zeta_3)\,y_t^4\lambda^2 + \left(\frac{117}{4}-396\zeta_3\right)y_t^6\lambda \right.$$
$$- \left(\frac{1599}{4}+72\zeta_3\right)y_t^8 + (-2448+2304\zeta_3)\,g_s^2 y_t^2\lambda^2 + (1790-2592\zeta_3)\,g_s^2 y_t^4\lambda$$
$$\left. + (-76+480\zeta_3)\,g_s^2 y_t^6 + \left(\frac{2488}{3}-96\zeta_3\right)g_s^4 y_t^2\lambda + \left(-\frac{532}{3}+64\zeta_3\right)g_s^4 y_t^4\right], \qquad \text{(A.8)}$$

$$\Delta\beta_{y_t} = \frac{y_t}{(4\pi)^6}\left[-36\lambda^3 + \frac{15}{4}y_t^2\lambda^2 + 198 y_t^4\lambda + \left(\frac{339}{8}+\frac{27}{2}\zeta_3\right)y_t^6 + 16 g_s^2 y_t^2\lambda \right.$$
$$\left. - 157 g_s^2 y_t^4 + \left(\frac{3827}{6}-228\zeta_3\right)g_s^4 y_t^2 + \left(-\frac{4166}{3}+640\zeta_3\right)g_s^6\right], \qquad \text{(A.9)}$$

$$\Delta\beta_{g'} = \frac{g'^3}{(4\pi)^6}\left[\frac{1315}{64}g^4 + \frac{205}{96}g^2 g'^2 - \frac{388613}{5184}g'^4 - g^2 g_s^2 - \frac{137}{27}g'^2 g_s^2 + 99 g_s^4 \right.$$
$$\left. - y_t^2\left(\frac{785}{32}g^2 + \frac{2827}{288}g'^2 + \frac{29}{3}g_s^2\right) + \frac{315}{16}y_t^4 + \lambda\left(\frac{3}{2}g^2 + \frac{3}{2}g'^2 - 3\lambda\right)\right], \qquad \text{(A.10)}$$

$$\Delta\beta_g = \frac{g^3}{(4\pi)^6}\left[\frac{324953}{1728}g^4 + \frac{291}{32}g^2 g'^2 - \frac{5597}{576}g'^4 + 39 g^2 g_s^2 - \frac{1}{3}g'^2 g_s^2 + 81 g_s^4 \right.$$
$$\left. - y_t^2\left(\frac{729}{32}g^2 + \frac{593}{96}g'^2 + 7 g_s^2\right) + \frac{147}{16}y_t^4 + \lambda\left(\frac{3}{2}g^2 + \frac{1}{2}g'^2 - 3\lambda\right)\right], \qquad \text{(A.11)}$$

$$\Delta\beta_{g_s} = \frac{g_s^3}{(4\pi)^6}\left[\frac{109}{8}g^4 - \frac{1}{8}g^2 g'^2 - \frac{2615}{216}g'^4 + 21 g^2 g_s^2 + \frac{77}{9}g'^2 g_s^2 + \frac{65}{2}g_s^4 \right.$$
$$\left. - y_t^2\left(\frac{93}{8}g^2 + \frac{101}{24}g'^2 + 40 g_s^2\right) + 15 y_t^4\right], \qquad \text{(A.12)}$$

$$\Delta\gamma = -\frac{1}{(4\pi)^6}\left[36\lambda^3 + \frac{135}{2}y_t^2\lambda^2 - 45 y_t^4\lambda - \left(\frac{789}{16}+9\zeta_3\right)y_t^6 \right.$$
$$\left. - \left(\frac{15}{2}-72\zeta_3\right)g_s^2 y_t^4 - \left(\frac{622}{3}-24\zeta_3\right)g_s^4 y_t^2\right], \qquad \text{(A.13)}$$

where $\zeta_3 \equiv \zeta(3) \simeq 1.202$.

Appendix B

Renormalization group equations for the DFSZ axion model

The RG equations for the DFSZ invisible axion model with a classical scale invariance can be found from the results for a general QFT given in [289–291]. For the potential (4.26), the one-loop RG equations for the couplings λ_i are

$$\beta_{\lambda_1} = \frac{1}{16\pi^2}\left[\frac{9}{8}g^4 + \frac{3}{4}g^2g'^2 + \frac{3}{8}g'^4 - 6y_t^4 + \left(-9g^2 - 3g'^2 + 12y_t^2\right)\lambda_1 + 24\lambda_1^2 + 2\lambda_3^2 + 2\lambda_3\lambda_4 + \lambda_4^2 + \zeta_1^2\right], \tag{B.1}$$

$$\beta_{\lambda_2} = \frac{1}{16\pi^2}\left[\frac{9}{8}g^4 + \frac{3}{4}g^2g'^2 + \frac{3}{8}g'^4 - 6y_b^4 + \left(-9g^2 - 3g'^2 + 12y_b^2\right)\lambda_2 + 24\lambda_2^2 + 2\lambda_3^2 + 2\lambda_3\lambda_4 + \lambda_4^2 + \zeta_2^2\right], \tag{B.2}$$

$$\beta_{\lambda_3} = \frac{1}{16\pi^2}\left[\frac{9}{4}g^4 - \frac{3}{2}g^2g'^2 + \frac{3}{4}g'^4 - 12y_t^2y_b^2 + \left(-9g^2 - 3g'^2 + 6y_t^2 + 6y_b^2\right)\lambda_3 + 12\lambda_1\lambda_3 + 12\lambda_2\lambda_3 + 4\lambda_1\lambda_4 + 4\lambda_2\lambda_4 + 4\lambda_3^2 + 2\lambda_4^2 + 2\zeta_1\zeta_2\right], \tag{B.3}$$

$$\beta_{\lambda_4} = \frac{1}{16\pi^2}\left[3g^2g'^2 + 12y_t^2y_b^2 - 9g^2\lambda_4 - 3g'^2\lambda_4 + 6y_t^2\lambda_4 + 6y_b^2\lambda_4 + 4\lambda_1\lambda_4 + 4\lambda_2\lambda_4 + 8\lambda_3\lambda_4 + 4\lambda_4^2 + \zeta_3^2\right] \tag{B.4}$$

where $\beta_x \equiv dx/d\ln\mu$. Note that, up to the contribution $3g^2g'^2 + 12y_t^2y_b^2 + \zeta_3^2$, the coupling λ_4 is multiplicatively renormalized and so typically remains small if it is assumed small to begin with. The one-loop RG equations for the ultra-weak couplings ζ_i are

$$\beta_{\zeta_1} = \frac{1}{16\pi^2}\left[\left(-\frac{9}{2}g^2 - \frac{3}{2}g'^2 + 6y_t^2 + 12\lambda_1\right)\zeta_1 + (4\lambda_3 + 2\lambda_4)\,\zeta_2 + 4\zeta_1^2 + 2\zeta_3^2 + 8\zeta_1\zeta_4\right], \tag{B.5}$$

$$\beta_{\zeta_2} = \frac{1}{16\pi^2}\left[\left(-\frac{9}{2}g^2 - \frac{3}{2}g'^2 + 6y_b^2 + 12\lambda_2\right)\zeta_2 + (4\lambda_3 + 2\lambda_4)\,\zeta_1 + 4\zeta_2^2 + 2\zeta_3^2 + 8\zeta_2\zeta_4\right], \quad \text{(B.6)}$$

$$\beta_{\zeta_3} = \frac{1}{16\pi^2}\left[\left(-\frac{9}{2}g^2 - \frac{3}{2}g'^2 + 3y_t^2 + 3y_b^2 + 2\lambda_3 + 4\lambda_4\right)\zeta_3 + 4\zeta_1\zeta_3 + 4\zeta_2\zeta_3 + 4\zeta_3\zeta_4\right], \quad \text{(B.7)}$$

$$\beta_{\zeta_4} = \frac{1}{16\pi^2}\left[2\zeta_1^2 + 2\zeta_2^2 + \zeta_3^2 + 20\zeta_4^2\right]. \quad \text{(B.8)}$$

Note that the set of ultra-weak couplings is multiplicatively renormalized as a whole. Therefore there is no expectation for the magnitude of their values and small values are technically natural. Finally, for the gauge couplings we have

$$\beta_g = -\frac{3g^3}{16\pi^2}, \qquad \beta_{g'} = \frac{7g'^3}{16\pi^2}, \qquad \beta_{g_s} = -\frac{7g_s^3}{16\pi^2}, \quad \text{(B.9)}$$

and for the Yukawa couplings we have

$$\beta_{y_t} = \frac{y_t}{16\pi^2}\left[-\frac{9}{4}g^2 - \frac{17}{12}g'^2 - 8g_s^2 + \frac{9}{2}y_t^2\right], \quad \text{(B.10)}$$

$$\beta_{y_b} = \frac{y_b}{16\pi^2}\left[-\frac{9}{4}g^2 - \frac{5}{12}g'^2 - 8g_s^2 + \frac{9}{2}y_b^2\right]. \quad \text{(B.11)}$$

Bibliography

[1] **LHCb collaboration** Collaboration, R. Aaij et al., *Measurement of Form-Factor-Independent Observables in the Decay $B^0 \to K^{*0}\mu^+\mu^-$*, *Phys.Rev.Lett.* **111** (2013), no. 19 191801, [arXiv:1308.1707].

[2] Y. Stadnik, B. Roberts, and V. Flambaum, *Tests of CPT and Lorentz symmetry from muon anomalous magnetic dipole moment*, arXiv:1407.5728.

[3] B. Grinstein and C. W. Murphy, *Bottom-Quark Forward-Backward Asymmetry in the Standard Model and Beyond*, *Phys.Rev.Lett.* **111** (2013) 062003, [arXiv:1302.6995].

[4] **Particle Data Group** Collaboration, J. Beringer et al., *Review of Particle Physics (RPP)*, *Phys.Rev.* **D86** (2012) 010001.

[5] S. M. Bilenky, C. Giunti, and W. Grimus, *Phenomenology of neutrino oscillations*, *Prog.Part.Nucl.Phys.* **43** (1999) 1–86, [hep-ph/9812360].

[6] M. Gonzalez-Garcia, M. Maltoni, J. Salvado, and T. Schwetz, *Global fit to three neutrino mixing: critical look at present precision*, *JHEP* **1212** (2012) 123, [arXiv:1209.3023].

[7] A. Boyarsky, O. Ruchayskiy, and M. Shaposhnikov, *The Role of sterile neutrinos in cosmology and astrophysics*, *Ann.Rev.Nucl.Part.Sci.* **59** (2009) 191–214, [arXiv:0901.0011].

[8] A. Del Popolo, *Non-baryonic dark matter in cosmology*, *AIP Conf.Proc.* **1548** (2013) 2–63.

[9] A. Bosma, *21-cm line studies of spiral galaxies. 2. The distribution and kinematics of neutral hydrogen in spiral galaxies of various morphological types.*, *Astron.J.* **86** (1981) 1825.

[10] A. B. Mantz, S. W. Allen, R. G. Morris, D. A. Rapetti, D. E. Applegate, et al., *Cosmology and Astrophysics from Relaxed Galaxy Clusters II: Cosmological Constraints*, *Mon.Not.Roy.Astron.Soc.* **440** (2014) 2077–2098, [arXiv:1402.6212].

[11] **WMAP** Collaboration, G. Hinshaw et al., *Nine-Year Wilkinson Microwave Anisotropy Probe (WMAP) Observations: Cosmological Parameter Results*, *Astrophys.J.Suppl.* **208** (2013) 19, [arXiv:1212.5226].

[12] **Planck Collaboration** Collaboration, P. Ade et al., *Planck 2013 results. XVI. Cosmological parameters*, arXiv:1303.5076.

[13] L. Bergstrom, *Nonbaryonic dark matter: Observational evidence and detection methods*, *Rept.Prog.Phys.* **63** (2000) 793, [hep-ph/0002126].

[14] E. Giusarma, E. Di Valentino, M. Lattanzi, A. Melchiorri, and O. Mena, *Relic Neutrinos, thermal axions and cosmology in early 2014*, arXiv:1403.4852.

[15] H. Baer, K.-Y. Choi, J. E. Kim, and L. Roszkowski, *Non-thermal dark matter: supersymmetric axions and other candidates*, arXiv:1407.0017.

[16] M. Milgrom, *A Modification of the Newtonian dynamics as a possible alternative to the hidden mass hypothesis*, *Astrophys.J.* **270** (1983) 365–370.

[17] D. Gerbal, F. Durret, M. Lachieze-Rey, and G. Lima-Neto, *Analysis of X-ray galaxy clusters in the framework of modified Newtonian dynamics*, *Astron.Astrophys.* **2262** (1992) 395–400.

[18] B. Famaey and S. McGaugh, *Modified Newtonian Dynamics (MOND): Observational Phenomenology and Relativistic Extensions*, *Living Rev.Rel.* **15** (2012) 10, [arXiv:1112.3960].

[19] J. R. Ellis, J. Hagelin, D. V. Nanopoulos, K. A. Olive, and M. Srednicki, *Supersymmetric Relics from the Big Bang*, *Nucl.Phys.* **B238** (1984) 453–476.

[20] H. Goldberg, *Constraint on the Photino Mass from Cosmology*, *Phys.Rev.Lett.* **50** (1983) 1419.

[21] J. McDonald, *Gauge singlet scalars as cold dark matter*, *Phys.Rev.* **D50** (1994) 3637–3649, [hep-ph/0702143].

[22] C. Burgess, M. Pospelov, and T. ter Veldhuis, *The Minimal model of nonbaryonic dark matter: A Singlet scalar*, *Nucl.Phys.* **B619** (2001) 709–728, [hep-ph/0011335].

[23] L. Abbott and P. Sikivie, *A Cosmological Bound on the Invisible Axion*, *Phys.Lett.* **B120** (1983) 133–136.

[24] M. Dine and W. Fischler, *The Not So Harmless Axion*, *Phys.Lett.* **B120** (1983) 137–141.

[25] J. Preskill, M. B. Wise, and F. Wilczek, *Cosmology of the Invisible Axion*, *Phys.Lett.* **B120** (1983) 127–132.

[26] S. Dodelson and L. M. Widrow, *Sterile-neutrinos as dark matter*, *Phys.Rev.Lett.* **72** (1994) 17–20, [hep-ph/9303287].

[27] S. Sarkar, *Big bang nucleosynthesis and physics beyond the standard model*, *Rept.Prog.Phys.* **59** (1996) 1493–1610, [hep-ph/9602260].

[28] A. Sakharov, *Violation of CP Invariance, c Asymmetry, and Baryon Asymmetry of the Universe*, *Pisma Zh.Eksp.Teor.Fiz.* **5** (1967) 32–35.

[29] V. Kuzmin, V. Rubakov, and M. Shaposhnikov, *On the Anomalous Electroweak Baryon Number Nonconservation in the Early Universe*, *Phys.Lett.* **B155** (1985) 36.

[30] M. Shaposhnikov, *Possible Appearance of the Baryon Asymmetry of the Universe in an Electroweak Theory*, *JETP Lett.* **44** (1986) 465–468.

[31] M. Shaposhnikov, *Baryon Asymmetry of the Universe in Standard Electroweak Theory*, *Nucl.Phys.* **B287** (1987) 757–775.

[32] **ATLAS Collaboration** Collaboration, G. Aad et al., *Measurement of the Higgs boson mass from the $H \to \gamma\gamma$ and $H \to ZZ^* \to 4\ell$ channels with the ATLAS detector using 25 fb^{-1} of pp collision data*, arXiv:1406.3827.

[33] **CMS Collaboration** Collaboration, C. Collaboration, *Precise determination of the mass of the Higgs boson and studies of the compatibility of its couplings with the standard model*, .

[34] K. Kajantie, M. Laine, K. Rummukainen, and M. E. Shaposhnikov, *Is there a hot electroweak phase transition at m(H) larger or equal to m(W)?*, *Phys.Rev.Lett.* **77** (1996) 2887–2890, [hep-ph/9605288].

[35] M. Gavela, P. Hernandez, J. Orloff, and O. Pene, *Standard model CP violation and baryon asymmetry*, *Mod.Phys.Lett.* **A9** (1994) 795–810, [hep-ph/9312215].

[36] P. Huet and E. Sather, *Electroweak baryogenesis and standard model CP violation*, *Phys.Rev.* **D51** (1995) 379–394, [hep-ph/9404302].

[37] M. Gavela, P. Hernandez, J. Orloff, O. Pene, and C. Quimbay, *Standard model CP violation and baryon asymmetry. Part 2: Finite temperature*, *Nucl.Phys.* **B430** (1994) 382–426, [hep-ph/9406289].

[38] D. V. Nanopoulos and S. Weinberg, *Mechanisms for Cosmological Baryon Production*, *Phys.Rev.* **D20** (1979) 2484.

[39] J. R. Ellis, J. E. Kim, and D. V. Nanopoulos, *Cosmological Gravitino Regeneration and Decay*, *Phys.Lett.* **B145** (1984) 181.

[40] E. W. Kolb, A. D. Linde, and A. Riotto, *GUT baryogenesis after preheating*, *Phys.Rev.Lett.* **77** (1996) 4290–4293, [hep-ph/9606260].

[41] E. W. Kolb, A. Riotto, and I. I. Tkachev, *GUT baryogenesis after preheating: Numerical study of the production and decay of X bosons*, *Phys.Lett.* **B423** (1998) 348–354, [hep-ph/9801306].

[42] I. Affleck and M. Dine, *A New Mechanism for Baryogenesis*, *Nucl.Phys.* **B249** (1985) 361.

[43] M. Fukugita and T. Yanagida, *Baryogenesis Without Grand Unification*, *Phys.Lett.* **B174** (1986) 45.

[44] E. K. Akhmedov, V. Rubakov, and A. Y. Smirnov, *Baryogenesis via neutrino oscillations*, *Phys.Rev.Lett.* **81** (1998) 1359–1362, [hep-ph/9803255].

[45] A. A. Starobinsky, *A New Type of Isotropic Cosmological Models Without Singularity*, *Phys.Lett.* **B91** (1980) 99–102.

[46] A. H. Guth, *The Inflationary Universe: A Possible Solution to the Horizon and Flatness Problems*, *Phys.Rev.* **D23** (1981) 347–356.

[47] A. D. Linde, *A New Inflationary Universe Scenario: A Possible Solution of the Horizon, Flatness, Homogeneity, Isotropy and Primordial Monopole Problems*, *Phys.Lett.* **B108** (1982) 389–393.

[48] A. Albrecht and P. J. Steinhardt, *Cosmology for Grand Unified Theories with Radiatively Induced Symmetry Breaking*, *Phys.Rev.Lett.* **48** (1982) 1220–1223.

[49] A. D. Linde, *Chaotic Inflation*, *Phys.Lett.* **B129** (1983) 177–181.

[50] **Planck** Collaboration, P. Ade et al., *Planck 2013 results. XXII. Constraints on inflation*, arXiv:1303.5082.

[51] G. Dvali, A. Gruzinov, and M. Zaldarriaga, *A new mechanism for generating density perturbations from inflation*, *Phys.Rev.* **D69** (2004) 023505, [astro-ph/0303591].

[52] D. H. Lyth and A. Riotto, *Particle physics models of inflation and the cosmological density perturbation*, *Phys.Rept.* **314** (1999) 1–146, [hep-ph/9807278].

[53] J. Martin, C. Ringeval, and V. Vennin, *Encyclopaedia Inflationaris*, arXiv:1303.3787.

[54] F. L. Bezrukov and M. Shaposhnikov, *The Standard Model Higgs boson as the inflaton*, *Phys.Lett.* **B659** (2008) 703–706, [arXiv:0710.3755].

[55] G. Isidori, V. S. Rychkov, A. Strumia, and N. Tetradis, *Gravitational corrections to standard model vacuum decay*, *Phys.Rev.* **D77** (2008) 025034, [arXiv:0712.0242].

[56] I. Masina and A. Notari, *Standard Model False Vacuum Inflation: Correlating the Tensor-to-Scalar Ratio to the Top Quark and Higgs Boson masses*, *Phys.Rev.Lett.* **108** (2012) 191302, [arXiv:1112.5430].

[57] I. Masina and A. Notari, *The Higgs mass range from Standard Model false vacuum Inflation in scalar-tensor gravity*, *Phys.Rev.* **D85** (2012) 123506, [arXiv:1112.2659].

[58] I. Masina and A. Notari, *Inflation from the Higgs field false vacuum with hybrid potential*, *JCAP* **1211** (2012) 031, [arXiv:1204.4155].

[59] C. Germani and A. Kehagias, *New Model of Inflation with Non-minimal Derivative Coupling of Standard Model Higgs Boson to Gravity*, *Phys.Rev.Lett.* **105** (2010) 011302, [arXiv:1003.2635].

[60] K. Nakayama and F. Takahashi, *Running Kinetic Inflation*, *JCAP* **1011** (2010) 009, [arXiv:1008.2956].

[61] K. Kamada, T. Kobayashi, M. Yamaguchi, and J. Yokoyama, *Higgs G-inflation*, *Phys.Rev.* **D83** (2011) 083515, [arXiv:1012.4238].

[62] K. Kamada, T. Kobayashi, T. Takahashi, M. Yamaguchi, and J. Yokoyama, *Generalized Higgs inflation*, *Phys.Rev.* **D86** (2012) 023504, [arXiv:1203.4059].

[63] M. P. Hertzberg, *Can Inflation be Connected to Low Energy Particle Physics?*, *JCAP* **1208** (2012) 008, [arXiv:1110.5650].

[64] M. Shaposhnikov and C. Wetterich, *Asymptotic safety of gravity and the Higgs boson mass*, *Phys.Lett.* **B683** (2010) 196–200, [arXiv:0912.0208].

[65] M. Chaichian, R. Gonzalez Felipe, and K. Huitu, *On quadratic divergences and the Higgs mass*, *Phys.Lett.* **B363** (1995) 101–105, [hep-ph/9509223].

[66] M. Veltman, *The Infrared - Ultraviolet Connection*, *Acta Phys.Polon.* **B12** (1981) 437.

[67] R. Peccei, *The Strong CP problem and axions*, *Lect.Notes Phys.* **741** (2008) 3–17, [hep-ph/0607268].

[68] M. S. Turner, *Windows on the Axion*, *Phys.Rept.* **197** (1990) 67–97.

[69] C. Baker, D. Doyle, P. Geltenbort, K. Green, M. van der Grinten, et al., *An Improved experimental limit on the electric dipole moment of the neutron*, *Phys.Rev.Lett.* **97** (2006) 131801, [hep-ex/0602020].

[70] J. Christenson, J. Cronin, V. Fitch, and R. Turlay, *Evidence for the 2 pi Decay of the k(2)0 Meson*, *Phys.Rev.Lett.* **13** (1964) 138–140.

[71] R. Peccei and H. R. Quinn, *CP Conservation in the Presence of Instantons*, *Phys.Rev.Lett.* **38** (1977) 1440–1443.

[72] R. Peccei and H. R. Quinn, *Constraints Imposed by CP Conservation in the Presence of Instantons*, *Phys.Rev.* **D16** (1977) 1791–1797.

[73] L. Wolfenstein, *Parametrization of the Kobayashi-Maskawa Matrix*, *Phys.Rev.Lett.* **51** (1983) 1945.

[74] S. F. King and C. Luhn, *Neutrino Mass and Mixing with Discrete Symmetry*, *Rept.Prog.Phys.* **76** (2013) 056201, [arXiv:1301.1340].

[75] S. Weinberg, *The Cosmological Constant Problem*, *Rev.Mod.Phys.* **61** (1989) 1–23.

[76] H. Georgi and S. Glashow, *Unity of All Elementary Particle Forces*, *Phys.Rev.Lett.* **32** (1974) 438–441.

[77] H. Fritzsch and P. Minkowski, *Unified Interactions of Leptons and Hadrons*, *Annals Phys.* **93** (1975) 193–266.

[78] H. Baer, V. Barger, D. Mickelson, and M. Padeffke-Kirkland, *SUSY models under siege: LHC constraints and electroweak fine-tuning*, *Phys.Rev.* **D89** (2014) 115019, [arXiv:1404.2277].

[79] B. Bellazzini, C. Cski, and J. Serra, *Composite Higgses*, *Eur.Phys.J.* **C74** (2014) 2766, [arXiv:1401.2457].

[80] M. Farina, D. Pappadopulo, and A. Strumia, *A modified naturalness principle and its experimental tests*, *JHEP* **1308** (2013) 022, [arXiv:1303.7244].

[81] G. F. Giudice, *Naturalness after LHC8*, *PoS* **EPS-HEP2013** (2013) 163, [arXiv:1307.7879].

[82] G. Degrassi, S. Di Vita, J. Elias-Miro, J. R. Espinosa, G. F. Giudice, et al., *Higgs mass and vacuum stability in the Standard Model at NNLO*, *JHEP* **1208** (2012) 098, [arXiv:1205.6497].

[83] M. Holthausen, K. S. Lim, and M. Lindner, *Planck scale Boundary Conditions and the Higgs Mass*, *JHEP* **1202** (2012) 037, [arXiv:1112.2415].

[84] M. Shaposhnikov, *Is there a new physics between electroweak and Planck scales?*, arXiv:0708.3550.

[85] S. Y. Khlebnikov and M. Shaposhnikov, *Extra Space-time Dimensions: Towards a Solution to the Strong CP Problem*, *Phys.Lett.* **B203** (1988) 121.

[86] S. Khlebnikov and M. Shaposhnikov, *Brane-worlds and theta-vacua*, *Phys.Rev.* **D71** (2005) 104024, [hep-th/0412306].

[87] T. Asaka, S. Blanchet, and M. Shaposhnikov, *The nuMSM, dark matter and neutrino masses*, *Phys.Lett.* **B631** (2005) 151–156, [hep-ph/0503065].

[88] T. Asaka and M. Shaposhnikov, *The nuMSM, dark matter and baryon asymmetry of the universe*, *Phys.Lett.* **B620** (2005) 17–26, [hep-ph/0505013].

[89] W. A. Bardeen, *On naturalness in the standard model*, .

[90] S. R. Coleman and E. J. Weinberg, *Radiative Corrections as the Origin of Spontaneous Symmetry Breaking*, *Phys.Rev.* **D7** (1973) 1888–1910.

[91] K. Allison, *Dark matter, singlet extensions of the nuMSM, and symmetries*, *JHEP* **1305** (2013) 009, [arXiv:1210.6852].

[92] L. Canetti, M. Drewes, T. Frossard, and M. Shaposhnikov, *Dark Matter, Baryogenesis and Neutrino Oscillations from Right Handed Neutrinos*, *Phys.Rev.* **D87** (2013), no. 9 093006, [arXiv:1208.4607].

[93] A. Boyarsky, J. Lesgourgues, O. Ruchayskiy, and M. Viel, *Lyman-alpha constraints on warm and on warm-plus-cold dark matter models*, *JCAP* **0905** (2009) 012, [arXiv:0812.0010].

[94] M. Miranda and A. Maccio, *Constraining Warm Dark Matter using QSO gravitational lensing*, arXiv:0706.0896.

[95] E. Polisensky and M. Ricotti, *Constraints on the Dark Matter Particle Mass from the Number of Milky Way Satellites*, *Phys.Rev.* **D83** (2011) 043506, [arXiv:1004.1459].

[96] C. R. Watson, Z.-Y. Li, and N. K. Polley, *Constraining Sterile Neutrino Warm Dark Matter with Chandra Observations of the Andromeda Galaxy*, *JCAP* **1203** (2012) 018, [arXiv:1111.4217].

[97] M. Laine and M. Shaposhnikov, *Sterile neutrino dark matter as a consequence of nuMSM-induced lepton asymmetry*, *JCAP* **0806** (2008) 031, [arXiv:0804.4543].

[98] T. Asaka, M. Shaposhnikov, and A. Kusenko, *Opening a new window for warm dark matter*, *Phys.Lett.* **B638** (2006) 401–406, [hep-ph/0602150].

[99] T. Asaka, M. Laine, and M. Shaposhnikov, *Lightest sterile neutrino abundance within the nuMSM*, *JHEP* **0701** (2007) 091, [hep-ph/0612182].

[100] F. Bezrukov, H. Hettmansperger, and M. Lindner, *keV sterile neutrino Dark Matter in gauge extensions of the Standard Model*, *Phys.Rev.* **D81** (2010) 085032, [arXiv:0912.4415].

[101] M. Nemevsek, G. Senjanovic, and Y. Zhang, *Warm Dark Matter in Low Scale Left-Right Theory*, *JCAP* **1207** (2012) 006, [arXiv:1205.0844].

[102] A. Roy and M. Shaposhnikov, *Resonant production of the sterile neutrino dark matter and fine-tunings in the [nu]MSM*, *Phys.Rev.* **D82** (2010) 056014, [arXiv:1006.4008].

[103] M. Shaposhnikov and I. Tkachev, *The nuMSM, inflation, and dark matter*, *Phys.Lett.* **B639** (2006) 414–417, [hep-ph/0604236].

[104] A. Anisimov, Y. Bartocci, and F. L. Bezrukov, *Inflaton mass in the nuMSM inflation*, *Phys.Lett.* **B671** (2009) 211–215, [arXiv:0809.1097].

[105] F. Bezrukov and D. Gorbunov, *Light inflaton Hunter's Guide*, *JHEP* **1005** (2010) 010, [arXiv:0912.0390].

[106] A. Kusenko, *Sterile neutrinos, dark matter, and the pulsar velocities in models with a Higgs singlet*, *Phys.Rev.Lett.* **97** (2006) 241301, [hep-ph/0609081].

[107] K. Petraki and A. Kusenko, *Dark-matter sterile neutrinos in models with a gauge singlet in the Higgs sector*, *Phys.Rev.* **D77** (2008) 065014, [arXiv:0711.4646].

[108] **ATLAS** Collaboration, G. Aad et al., *Observation of a new particle in the search for the Standard Model Higgs boson with the ATLAS detector at the LHC*, *Phys.Lett.* **B716** (2012) 1–29, [arXiv:1207.7214].

[109] **CMS** Collaboration, S. Chatrchyan et al., *Observation of a new boson at a mass of 125 GeV with the CMS experiment at the LHC*, *Phys.Lett.* **B716** (2012) 30–61, [arXiv:1207.7235].

[110] J. Elias-Miro, J. R. Espinosa, G. F. Giudice, G. Isidori, A. Riotto, et al., *Higgs mass implications on the stability of the electroweak vacuum*, *Phys.Lett.* **B709** (2012) 222–228, [arXiv:1112.3022].

[111] C.-S. Chen and Y. Tang, *Vacuum stability, neutrinos, and dark matter*, *JHEP* **1204** (2012) 019, [arXiv:1202.5717].

[112] O. Lebedev, *On Stability of the Electroweak Vacuum and the Higgs Portal*, *Eur.Phys.J.* **C72** (2012) 2058, [arXiv:1203.0156].

[113] J. Elias-Miro, J. R. Espinosa, G. F. Giudice, H. M. Lee, and A. Strumia, *Stabilization of the Electroweak Vacuum by a Scalar Threshold Effect*, *JHEP* **1206** (2012) 031, [arXiv:1203.0237].

[114] F. Bezrukov, A. Magnin, M. Shaposhnikov, and S. Sibiryakov, *Higgs inflation: consistency and generalisations*, *JHEP* **1101** (2011) 016, [arXiv:1008.5157].

[115] G. F. Giudice and H. M. Lee, *Unitarizing Higgs Inflation*, *Phys.Lett.* **B694** (2011) 294–300, [arXiv:1010.1417].

[116] R. N. Lerner and J. McDonald, *A Unitarity-Conserving Higgs Inflation Model*, *Phys.Rev.* **D82** (2010) 103525, [arXiv:1005.2978].

[117] R. N. Lerner and J. McDonald, *Unitarity-Violation in Generalized Higgs Inflation Models*, *JCAP* **1211** (2012) 019, [arXiv:1112.0954].

[118] M. Shaposhnikov, *A Possible symmetry of the nuMSM*, *Nucl.Phys.* **B763** (2007) 49–59, [hep-ph/0605047].

[119] M. Lindner, A. Merle, and V. Niro, *Soft $L_e - L_\mu - L_\tau$ flavour symmetry breaking and sterile neutrino keV Dark Matter*, *JCAP* **1101** (2011) 034, [arXiv:1011.4950].

[120] T. Araki and Y. Li, *Q_6 flavor symmetry model for the extension of the minimal standard model by three right-handed sterile neutrinos*, *Phys.Rev.* **D85** (2012) 065016, [arXiv:1112.5819].

[121] A. Kusenko, F. Takahashi, and T. T. Yanagida, *Dark Matter from Split Seesaw*, *Phys.Lett.* **B693** (2010) 144–148, [arXiv:1006.1731].

[122] A. Adulpravitchai and R. Takahashi, *A4 Flavor Models in Split Seesaw Mechanism*, *JHEP* **1109** (2011) 127, [arXiv:1107.3829].

[123] A. Merle and V. Niro, *Deriving Models for keV sterile Neutrino Dark Matter with the Froggatt-Nielsen mechanism*, *JCAP* **1107** (2011) 023, [arXiv:1105.5136].

[124] J. Barry, W. Rodejohann, and H. Zhang, *Light Sterile Neutrinos: Models and Phenomenology*, *JHEP* **1107** (2011) 091, [arXiv:1105.3911].

[125] J. Barry, W. Rodejohann, and H. Zhang, *Sterile Neutrinos for Warm Dark Matter and the Reactor Anomaly in Flavor Symmetry Models*, *JCAP* **1201** (2012) 052, [arXiv:1110.6382].

[126] L. Canetti and M. Shaposhnikov, *Baryon Asymmetry of the Universe in the NuMSM*, *JCAP* **1009** (2010) 001, [arXiv:1006.0133].

[127] T. Asaka and H. Ishida, *Flavour Mixing of Neutrinos and Baryon Asymmetry of the Universe*, *Phys.Lett.* **B692** (2010) 105–113, [arXiv:1004.5491].

[128] M. Shaposhnikov, *Baryon asymmetry of the universe and neutrinos*, *Prog.Theor.Phys.* **122** (2009) 185–203.

[129] M. Shaposhnikov, *The nuMSM, leptonic asymmetries, and properties of singlet fermions*, *JHEP* **0808** (2008) 008, [arXiv:0804.4542].

[130] O. Ruchayskiy and A. Ivashko, *Experimental bounds on sterile neutrino mixing angles*, *JHEP* **1206** (2012) 100, [arXiv:1112.3319].

[131] V. M. Gorkavenko, I. Rudenok, and S. I. Vilchynskiy, *Leptonic asymmetry of the sterile neutrino hadronic decays in the νMSM*, *Ukr. J. Phys. , Vol. 58, No.* **9** (2013) 811–826, [arXiv:1201.0003].

[132] L. Canetti, M. Drewes, and M. Shaposhnikov, *Sterile Neutrinos as the Origin of Dark and Baryonic Matter*, *Phys.Rev.Lett.* **110** (2013), no. 6 061801, [arXiv:1204.3902].

[133] P. B. Pal and L. Wolfenstein, *Radiative Decays of Massive Neutrinos*, *Phys.Rev.* **D25** (1982) 766.

[134] A. Boyarsky, O. Ruchayskiy, and D. Iakubovskyi, *A Lower bound on the mass of Dark Matter particles*, *JCAP* **0903** (2009) 005, [arXiv:0808.3902].

[135] D. Gorbunov, A. Khmelnitsky, and V. Rubakov, *Constraining sterile neutrino dark matter by phase-space density observations*, *JCAP* **0810** (2008) 041, [arXiv:0808.3910].

[136] A. Boyarsky, J. Lesgourgues, O. Ruchayskiy, and M. Viel, *Realistic sterile neutrino dark matter with keV mass does not contradict cosmological bounds*, *Phys.Rev.Lett.* **102** (2009) 201304, [arXiv:0812.3256].

[137] G. Bertone, W. Buchmuller, L. Covi, and A. Ibarra, *Gamma-Rays from Decaying Dark Matter*, *JCAP* **0711** (2007) 003, [arXiv:0709.2299].

[138] M. Cirelli, E. Moulin, P. Panci, P. D. Serpico, and A. Viana, *Gamma ray constraints on Decaying Dark Matter*, *Phys.Rev.* **D86** (2012) 083506, [arXiv:1205.5283].

[139] T. Asaka, S. Eijima, and H. Ishida, *Kinetic Equations for Baryogenesis via Sterile Neutrino Oscillation*, *JCAP* **1202** (2012) 021, [arXiv:1112.5565].

[140] P. P. Giardino, K. Kannike, M. Raidal, and A. Strumia, *Is the resonance at 125 GeV the Higgs boson?*, *Phys.Lett.* **B718** (2012) 469–474, [arXiv:1207.1347].

[141] K. Abazajian, M. Acero, S. Agarwalla, A. Aguilar-Arevalo, C. Albright, et al., *Light Sterile Neutrinos: A White Paper*, arXiv:1204.5379.

[142] C. Boehm, M. J. Dolan, and C. McCabe, *Increasing Neff with particles in thermal equilibrium with neutrinos*, *JCAP* **1212** (2012) 027, [arXiv:1207.0497].

[143] S. Galli, M. Martinelli, A. Melchiorri, L. Pagano, B. D. Sherwin, et al., *Constraining Fundamental Physics with Future CMB Experiments*, *Phys.Rev.* **D82** (2010) 123504, [arXiv:1005.3808].

[144] K. A. Meissner and H. Nicolai, *Conformal Symmetry and the Standard Model*, *Phys.Lett.* **B648** (2007) 312–317, [hep-th/0612165].

[145] R. Foot, A. Kobakhidze, K. McDonald, and R. Volkas, *Neutrino mass in radiatively-broken scale-invariant models*, *Phys.Rev.* **D76** (2007) 075014, [arXiv:0706.1829].

[146] K. A. Meissner and H. Nicolai, *Neutrinos, Axions and Conformal Symmetry*, *Eur.Phys.J.* **C57** (2008) 493–498, [arXiv:0803.2814].

[147] W. Buchmuller and N. Dragon, *Scale Invariance and Spontaneous Symmetry Breaking*, *Phys.Lett.* **B195** (1987) 417.

[148] W. Buchmuller and C. Busch, *Symmetry breaking and mass bounds in the standard model with hidden scale invariance*, *Nucl.Phys.* **B349** (1991) 71–90.

[149] L. E. Ibanez and G. G. Ross, *Discrete gauge symmetry anomalies*, *Phys.Lett.* **B260** (1991) 291–295.

[150] C. Burgess, J. Conlon, L.-Y. Hung, C. Kom, A. Maharana, et al., *Continuous Global Symmetries and Hyperweak Interactions in String Compactifications*, *JHEP* **0807** (2008) 073, [arXiv:0805.4037].

[151] L. E. Ibanez, F. Marchesano, and R. Rabadan, *Getting just the standard model at intersecting branes*, *JHEP* **0111** (2001) 002, [hep-th/0105155].

[152] I. Antoniadis, E. Kiritsis, and J. Rizos, *Anomalous U(1)s in type 1 superstring vacua*, *Nucl.Phys.* **B637** (2002) 92–118, [hep-th/0204153].

[153] L. M. Krauss and F. Wilczek, *Discrete Gauge Symmetry in Continuum Theories*, *Phys.Rev.Lett.* **62** (1989) 1221.

[154] T. Araki, T. Kobayashi, J. Kubo, S. Ramos-Sanchez, M. Ratz, et al., *(Non-)Abelian discrete anomalies*, *Nucl.Phys.* **B805** (2008) 124–147, [arXiv:0805.0207].

[155] T. Araki, *Anomaly of Discrete Symmetries and Gauge Coupling Unification*, *Prog.Theor.Phys.* **117** (2007) 1119–1138, [hep-ph/0612306].

[156] L. E. Ibanez, *More about discrete gauge anomalies*, *Nucl.Phys.* **B398** (1993) 301–318, [hep-ph/9210211].

[157] H. K. Dreiner, C. Luhn, and M. Thormeier, *What is the discrete gauge symmetry of the MSSM?*, *Phys.Rev.* **D73** (2006) 075007, [hep-ph/0512163].

[158] Y. Zeldovich, I. Y. Kobzarev, and L. Okun, *Cosmological Consequences of the Spontaneous Breakdown of Discrete Symmetry*, *Zh.Eksp.Teor.Fiz.* **67** (1974) 3–11.

[159] H. Casini and S. Sarkar, *No cosmological domain wall problem for weakly coupled fields*, *Phys.Rev.* **D65** (2002) 025002, [hep-ph/0106272].

[160] C. Froggatt and H. B. Nielsen, *Hierarchy of Quark Masses, Cabibbo Angles and CP Violation*, *Nucl.Phys.* **B147** (1979) 277.

[161] A. Datta, L. Everett, and P. Ramond, *Cabibbo haze in lepton mixing*, *Phys.Lett.* **B620** (2005) 42–51, [hep-ph/0503222].

[162] L. B. Anderson, J. Gray, A. Lukas, and E. Palti, *Heterotic Line Bundle Standard Models*, *JHEP* **1206** (2012) 113, [arXiv:1202.1757].

[163] L. B. Anderson, J. Gray, A. Lukas, and B. Ovrut, *Stabilizing All Geometric Moduli in Heterotic Calabi-Yau Vacua*, *Phys.Rev.* **D83** (2011) 106011, [arXiv:1102.0011].

[164] A. Denner, S. Heinemeyer, I. Puljak, D. Rebuzzi, and M. Spira, *Standard Model Higgs-Boson Branching Ratios with Uncertainties*, *Eur.Phys.J.* **C71** (2011) 1753, [arXiv:1107.5909].

[165] O. Lebedev and H. M. Lee, *Higgs Portal Inflation*, *Eur.Phys.J.* **C71** (2011) 1821, [arXiv:1105.2284].

[166] B. W. Lynn, G. D. Starkman, K. Freese, and D. I. Podolsky, *The 'Goldstone Exception' II: Absence of a Higgs Fine-Tuning Problem in the Spontaneously Broken Limit of the Gell Mann Levy Linear Sigma Model: O(4) with PCAC and $SU(2)_L$ with PCAC and Standard Model Quarks and Leptons*, arXiv:1112.2150.

[167] G. Kane, S. King, I. Peddie, and L. Velasco-Sevilla, *Study of theory and phenomenology of some classes of family symmetry and unification models*, *JHEP* **0508** (2005) 083, [hep-ph/0504038].

[168] **WMAP** Collaboration, E. Komatsu et al., *Seven-Year Wilkinson Microwave Anisotropy Probe (WMAP) Observations: Cosmological Interpretation*, *Astrophys.J.Suppl.* **192** (2011) 18, [arXiv:1001.4538].

[169] A. Linde, M. Noorbala, and A. Westphal, *Observational consequences of chaotic inflation with nonminimal coupling to gravity*, *JCAP* **1103** (2011) 013, [arXiv:1101.2652].

[170] E. Bulbul, M. Markevitch, A. Foster, R. K. Smith, M. Loewenstein, et al., *Detection of An Unidentified Emission Line in the Stacked X-ray spectrum of Galaxy Clusters*, *Astrophys.J.* **789** (2014) 13, [arXiv:1402.2301].

[171] A. Boyarsky, O. Ruchayskiy, D. Iakubovskyi, and J. Franse, *An unidentified line in X-ray spectra of the Andromeda galaxy and Perseus galaxy cluster*, arXiv:1402.4119.

[172] M. Loewenstein and A. Kusenko, *Dark Matter Search Using Chandra Observations of Willman 1, and a Spectral Feature Consistent with a Decay Line of a 5 keV Sterile Neutrino*, *Astrophys.J.* **714** (2010) 652–662, [arXiv:0912.0552].

[173] M. Loewenstein and A. Kusenko, *Dark Matter Search Using XMM-Newton Observations of Willman 1*, *Astrophys.J.* **751** (2012) 82, [arXiv:1203.5229].

[174] T. E. Jeltema and S. Profumo, *Dark matter searches going bananas: the contribution of Potassium (and Chlorine) to the 3.5 keV line*, arXiv:1408.1699.

[175] A. Boyarsky, J. Franse, D. Iakubovskyi, and O. Ruchayskiy, *Checking the dark matter origin of 3.53 keV line with the Milky Way center*, arXiv:1408.2503.

[176] A. Boyarsky, J. Franse, D. Iakubovskyi, and O. Ruchayskiy, *Comment on the paper "Dark matter searches going bananas: the contribution of Potassium (and Chlorine) to the 3.5 keV line" by T. Jeltema and S. Profumo*, arXiv:1408.4388.

[177] K. Cheung, J. S. Lee, and P.-Y. Tseng, *Higgcision Updates 2014*, arXiv:1407.8236.

[178] K. Allison, *Higgs xi-inflation for the 125-126 GeV Higgs: a two-loop analysis*, *JHEP* **1402** (2014) 040, [arXiv:1306.6931].

[179] A. R. Liddle and D. H. Lyth, *The Cold dark matter density perturbation*, *Phys.Rept.* **231** (1993) 1–105, [astro-ph/9303019].

[180] D. Salopek, J. Bond, and J. M. Bardeen, *Designing Density Fluctuation Spectra in Inflation*, *Phys.Rev.* **D40** (1989) 1753.

[181] R. Fakir and W. Unruh, *Improvement on cosmological chaotic inflation through nonminimal coupling*, *Phys.Rev.* **D41** (1990) 1783–1791.

[182] D. I. Kaiser, *Primordial spectral indices from generalized Einstein theories*, *Phys.Rev.* **D52** (1995) 4295–4306, [astro-ph/9408044].

[183] E. Komatsu and T. Futamase, *Complete constraints on a nonminimally coupled chaotic inflationary scenario from the cosmic microwave background*, *Phys.Rev.* **D59** (1999) 064029, [astro-ph/9901127].

[184] P. P. Giardino, K. Kannike, I. Masina, M. Raidal, and A. Strumia, *The universal Higgs fit*, *JHEP* **1405** (2014) 046, [arXiv:1303.3570].

[185] C. Burgess, H. M. Lee, and M. Trott, *Power-counting and the Validity of the Classical Approximation During Inflation*, *JHEP* **0909** (2009) 103, [arXiv:0902.4465].

[186] J. Barbon and J. Espinosa, *On the Naturalness of Higgs Inflation*, *Phys.Rev.* **D79** (2009) 081302, [arXiv:0903.0355].

[187] C. Burgess, H. M. Lee, and M. Trott, *Comment on Higgs Inflation and Naturalness*, *JHEP* **1007** (2010) 007, [arXiv:1002.2730].

[188] M. P. Hertzberg, *On Inflation with Non-minimal Coupling*, *JHEP* **1011** (2010) 023, [arXiv:1002.2995].

[189] F. Bezrukov and M. Shaposhnikov, *Standard Model Higgs boson mass from inflation: Two loop analysis*, *JHEP* **0907** (2009) 089, [arXiv:0904.1537].

[190] S. Ferrara, R. Kallosh, A. Linde, A. Marrani, and A. Van Proeyen, *Superconformal Symmetry, NMSSM, and Inflation*, *Phys.Rev.* **D83** (2011) 025008, [arXiv:1008.2942].

[191] A. De Simone, M. P. Hertzberg, and F. Wilczek, *Running Inflation in the Standard Model*, *Phys.Lett.* **B678** (2009) 1–8, [arXiv:0812.4946].

[192] F. Bezrukov, D. Gorbunov, and M. Shaposhnikov, *Late and early time phenomenology of Higgs-dependent cutoff*, *JCAP* **1110** (2011) 001, [arXiv:1106.5019].

[193] F. Bezrukov, M. Y. Kalmykov, B. A. Kniehl, and M. Shaposhnikov, *Higgs Boson Mass and New Physics*, *JHEP* **1210** (2012) 140, [arXiv:1205.2893].

[194] F. L. Bezrukov, A. Magnin, and M. Shaposhnikov, *Standard Model Higgs boson mass from inflation*, *Phys.Lett.* **B675** (2009) 88–92, [arXiv:0812.4950].

[195] T. Clark, B. Liu, S. Love, and T. ter Veldhuis, *The Standard Model Higgs Boson-Inflaton and Dark Matter*, *Phys.Rev.* **D80** (2009) 075019, [arXiv:0906.5595].

[196] R. N. Lerner and J. McDonald, *Gauge singlet scalar as inflaton and thermal relic dark matter*, *Phys.Rev.* **D80** (2009) 123507, [arXiv:0909.0520].

[197] R. N. Lerner and J. McDonald, *Distinguishing Higgs inflation and its variants*, *Phys.Rev.* **D83** (2011) 123522, [arXiv:1104.2468].

[198] L. N. Mihaila, J. Salomon, and M. Steinhauser, *Gauge Coupling Beta Functions in the Standard Model to Three Loops*, *Phys.Rev.Lett.* **108** (2012) 151602, [arXiv:1201.5868].

[199] K. Chetyrkin and M. Zoller, *Three-loop β-functions for top-Yukawa and the Higgs self-interaction in the Standard Model*, *JHEP* **1206** (2012) 033, [arXiv:1205.2892].

[200] D. I. Kaiser, *Conformal Transformations with Multiple Scalar Fields*, *Phys.Rev.* **D81** (2010) 084044, [arXiv:1003.1159].

[201] F. Bezrukov, *The Standard model Higgs as the inflaton*, arXiv:0805.2236.

[202] F. Bezrukov, D. Gorbunov, and M. Shaposhnikov, *On initial conditions for the Hot Big Bang*, *JCAP* **0906** (2009) 029, [arXiv:0812.3622].

[203] J. Garcia-Bellido, D. G. Figueroa, and J. Rubio, *Preheating in the Standard Model with the Higgs-Inflaton coupled to gravity*, *Phys.Rev.* **D79** (2009) 063531, [arXiv:0812.4624].

[204] S. Dutta, K. Hagiwara, Q.-S. Yan, and K. Yoshida, *Constraints on the electroweak chiral Lagrangian from the precision data*, *Nucl.Phys.* **B790** (2008) 111–137, [arXiv:0705.2277].

[205] W. Buchmuller and O. Philipsen, *Phase structure and phase transition of the SU(2) Higgs model in three-dimensions*, *Nucl.Phys.* **B443** (1995) 47–69, [hep-ph/9411334].

[206] H. Arason, D. Castano, B. Keszthelyi, S. Mikaelian, E. Piard, et al., *Renormalization group study of the standard model and its extensions. 1. The Standard model*, *Phys.Rev.* **D46** (1992) 3945–3965.

[207] M. Baak and R. Kogler, *The global electroweak Standard Model fit after the Higgs discovery*, arXiv:1306.0571.

[208] C. Ford, I. Jack, and D. Jones, *The Standard model effective potential at two loops*, *Nucl.Phys.* **B387** (1992) 373–390, [hep-ph/0111190].

[209] A. Barvinsky, A. Y. Kamenshchik, and A. Starobinsky, *Inflation scenario via the Standard Model Higgs boson and LHC*, *JCAP* **0811** (2008) 021, [arXiv:0809.2104].

[210] M. Shaposhnikov and D. Zenhausern, *Scale invariance, unimodular gravity and dark energy*, *Phys.Lett.* **B671** (2009) 187–192, [arXiv:0809.3395].

[211] M. Shaposhnikov and D. Zenhausern, *Quantum scale invariance, cosmological constant and hierarchy problem*, *Phys.Lett.* **B671** (2009) 162–166, [arXiv:0809.3406].

[212] F. Bezrukov, G. K. Karananas, J. Rubio, and M. Shaposhnikov, *Higgs-Dilaton Cosmology: an effective field theory approach*, *Phys.Rev.* **D87** (2013) 096001, [arXiv:1212.4148].

[213] S. Mooij and M. Postma, *Goldstone bosons and a dynamical Higgs field*, *JCAP* **1109** (2011) 006, [arXiv:1104.4897].

[214] D. P. George, S. Mooij, and M. Postma, *Effective action for the Abelian Higgs model in FLRW*, *JCAP* **1211** (2012) 043, [arXiv:1207.6963].

[215] A. Salvio, *Higgs Inflation at NNLO after the Boson Discovery*, *Phys.Lett.* **B727** (2013) 234–239, [arXiv:1308.2244].

[216] C. Ford, D. Jones, P. Stephenson, and M. Einhorn, *The Effective potential and the renormalization group*, *Nucl.Phys.* **B395** (1993) 17–34, [hep-lat/9210033].

[217] C. Burigana, C. Destri, H. de Vega, A. Gruppuso, N. Mandolesi, et al., *Forecast for the Planck precision on the tensor to scalar ratio and other cosmological parameters*, *Astrophys.J.* **724** (2010) 588–607, [arXiv:1003.6108].

[218] **BICEP2 Collaboration** Collaboration, P. Ade et al., *BICEP2 I: Detection Of B-mode Polarization at Degree Angular Scales*, arXiv:1403.3985.

[219] J. L. Cook, L. M. Krauss, A. J. Long, and S. Sabharwal, *Is Higgs Inflation Dead?*, *Phys.Rev.* **D89** (2014) 103525, [arXiv:1403.4971].

[220] Y. Hamada, H. Kawai, K.-y. Oda, and S. C. Park, *Higgs inflation still alive*, *Phys.Rev.Lett.* **112** (2014) 241301, [arXiv:1403.5043].

[221] F. Bezrukov and M. Shaposhnikov, *Higgs inflation at the critical point*, arXiv:1403.6078.

[222] R. Flauger, J. C. Hill, and D. N. Spergel, *Toward an Understanding of Foreground Emission in the BICEP2 Region*, arXiv:1405.7351.

[223] K. Allison, C. T. Hill, and G. G. Ross, *Ultra-weak sector, Higgs boson mass, and the dilaton*, *Phys.Lett.* **B738** (2014) 191–195, [arXiv:1404.6268].

[224] K. Allison, C. T. Hill, and G. G. Ross, *An ultra-weak sector, the strong CP problem and the pseudo-Goldstone dilaton*, *Nucl.Phys.* **B891** (2014) 613–626, [arXiv:1409.4029].

[225] V. Elias, R. B. Mann, D. McKeon, and T. G. Steele, *Radiative electroweak symmetry breaking revisited*, *Phys.Rev.Lett.* **91** (2003) 251601, [hep-ph/0304153].

[226] V. Elias, R. B. Mann, D. McKeon, and T. G. Steele, *Optimal renormalization group improvement of two radiatively broken gauge theories*, *Nucl.Phys.* **B678** (2004) 147–196, [hep-ph/0308301].

[227] L. Alexander-Nunneley and A. Pilaftsis, *The Minimal Scale Invariant Extension of the Standard Model*, *JHEP* **1009** (2010) 021, [arXiv:1006.5916].

[228] J. S. Lee and A. Pilaftsis, *Radiative Corrections to Scalar Masses and Mixing in a Scale Invariant Two Higgs Doublet Model*, *Phys.Rev.* **D86** (2012) 035004, [arXiv:1201.4891].

[229] T. Hambye and A. Strumia, *Dynamical generation of the weak and Dark Matter scale*, *Phys.Rev.* **D88** (2013) 055022, [arXiv:1306.2329].

[230] T. Hambye and M. H. Tytgat, *Electroweak symmetry breaking induced by dark matter*, *Phys.Lett.* **B659** (2008) 651–655, [arXiv:0707.0633].

[231] R. Dermisek, T. H. Jung, and H. D. Kim, *Coleman-Weinberg Higgs*, arXiv:1308.0891.

[232] R. Barbieri, L. J. Hall, and V. S. Rychkov, *Improved naturalness with a heavy Higgs: An Alternative road to LHC physics*, *Phys.Rev.* **D74** (2006) 015007, [hep-ph/0603188].

[233] L. Lopez Honorez, E. Nezri, J. F. Oliver, and M. H. Tytgat, *The Inert Doublet Model: An Archetype for Dark Matter*, *JCAP* **0702** (2007) 028, [hep-ph/0612275].

[234] J. R. Espinosa and M. Quiros, *Novel Effects in Electroweak Breaking from a Hidden Sector*, *Phys.Rev.* **D76** (2007) 076004, [hep-ph/0701145].

[235] R. Foot, A. Kobakhidze, K. L. McDonald, and R. R. Volkas, *A Solution to the hierarchy problem from an almost decoupled hidden sector within a classically scale invariant theory*, *Phys.Rev.* **D77** (2008) 035006, [arXiv:0709.2750].

[236] A. Arhrib, R. Benbrik, and N. Gaur, $H \to \gamma\gamma$ *in Inert Higgs Doublet Model*, *Phys.Rev.* **D85** (2012) 095021, [arXiv:1201.2644].

[237] K. Ishiwata, *Dark Matter in Classically Scale-Invariant Two Singlets Standard Model*, *Phys.Lett.* **B710** (2012) 134–138, [arXiv:1112.2696].

[238] C. D. Carone and R. Ramos, *Classical scale-invariance, the electroweak scale and vector dark matter*, *Phys.Rev.* **D88** (2013), no. 5 055020, [arXiv:1307.8428].

[239] T. Steele and Z.-W. Wang, *Is Radiative Electroweak Symmetry Breaking Consistent with a 125 GeV Higgs Mass?*, *Phys.Rev.Lett.* **110** (2013), no. 15 151601, [arXiv:1209.5416].

[240] T. Steele, Z.-W. Wang, D. Contreras, and R. Mann, *Viable dark matter via radiative symmetry breaking in a scalar singlet Higgs portal extension of the standard model*, arXiv:1310.1960.

[241] F. Chishtie, D. McKeon, and T. Steele, *A Unique determination of the effective potential in terms of renormalization group functions*, *Phys.Rev.* **D77** (2008) 065007, [arXiv:0706.1760].

[242] F. Chishtie, T. Hanif, J. Jia, R. B. Mann, D. McKeon, et al., *Can the Renormalization Group Improved Effective Potential be used to estimate the Higgs Mass in the Conformal Limit of the Standard Model?*, *Phys.Rev.* **D83** (2011) 105009, [arXiv:1006.5887].

[243] A. Farzinnia, H.-J. He, and J. Ren, *Natural Electroweak Symmetry Breaking from Scale Invariant Higgs Mechanism*, *Phys.Lett.* **B727** (2013) 141–150, [arXiv:1308.0295].

[244] C. Englert, J. Jaeckel, V. Khoze, and M. Spannowsky, *Emergence of the Electroweak Scale through the Higgs Portal*, *JHEP* **1304** (2013) 060, [arXiv:1301.4224].

[245] V. V. Khoze and G. Ro, *Leptogenesis and Neutrino Oscillations in the Classically Conformal Standard Model with the Higgs Portal*, *JHEP* **1310** (2013) 075, [arXiv:1307.3764].

[246] V. V. Khoze, *Inflation and Dark Matter in the Higgs Portal of Classically Scale Invariant Standard Model*, *JHEP* **1311** (2013) 215, [arXiv:1308.6338].

[247] M. Holthausen, J. Kubo, K. S. Lim, and M. Lindner, *Electroweak and Conformal Symmetry Breaking by a Strongly Coupled Hidden Sector*, *JHEP* **1312** (2013) 076, [arXiv:1310.4423].

[248] R. Foot, A. Kobakhidze, K. L. McDonald, and R. R. Volkas, *Poincare Protection for a Natural Electroweak Scale*, arXiv:1310.0223.

[249] E. Gabrielli, M. Heikinheimo, K. Kannike, A. Racioppi, M. Raidal, et al., *Towards Completing the Standard Model: Vacuum Stability, EWSB and Dark Matter*, *Phys.Rev.* **D89** (2014) 015017, [arXiv:1309.6632].

[250] M. Aoki, S. Kanemura, and H. Yokoya, *Reconstruction of Inert Doublet Scalars at the International Linear Collider*, *Phys.Lett.* **B725** (2013) 302–309, [arXiv:1303.6191].

[251] D.-W. Jung and P. Ko, *Higgs-dilaton(radion) system confronting the LHC Higgs data*, *Phys.Lett.* **B732** (2014) 364–372, [arXiv:1401.5586].

[252] C. T. Hill, *Is the Higgs Boson Associated with Coleman-Weinberg Dynamical Symmetry Breaking?*, *Phys.Rev.* **D89** (2014) 073003, [arXiv:1401.4185].

[253] M. Dine, W. Fischler, and M. Srednicki, *A Simple Solution to the Strong CP Problem with a Harmless Axion*, *Phys.Lett.* **B104** (1981) 199.

[254] A. Zhitnitsky, *On Possible Suppression of the Axion Hadron Interactions. (In Russian)*, *Sov.J.Nucl.Phys.* **31** (1980) 260.

[255] J. E. Kim, *Weak Interaction Singlet and Strong CP Invariance*, *Phys.Rev.Lett.* **43** (1979) 103.

[256] M. A. Shifman, A. Vainshtein, and V. I. Zakharov, *Can Confinement Ensure Natural CP Invariance of Strong Interactions?*, *Nucl.Phys.* **B166** (1980) 493.

[257] G. 't Hooft, *Naturalness, chiral symmetry, and spontaneous chiral symmetry breaking*, *NATO Adv.Study Inst.Ser.B Phys.* **59** (1980) 135.

[258] A. Djouadi, M. Spira, and P. Zerwas, *Two photon decay widths of Higgs particles*, *Phys.Lett.* **B311** (1993) 255–260, [hep-ph/9305335].

[259] C. Vafa and E. Witten, *Parity Conservation in QCD*, *Phys.Rev.Lett.* **53** (1984) 535.

[260] R. Peccei, *Particle physics footprints of the invisible axion*, *Phys.Scripta* **T36** (1991) 218–221.

[261] G. G. Raffelt, *Astrophysical axion bounds*, *Lect.Notes Phys.* **741** (2008) 51–71, [hep-ph/0611350].

[262] G. Branco, P. Ferreira, L. Lavoura, M. Rebelo, M. Sher, et al., *Theory and phenomenology of two-Higgs-doublet models*, *Phys.Rept.* **516** (2012) 1–102, [arXiv:1106.0034].

[263] K. S. Jeong, M. Kawasaki, and F. Takahashi, *Axions as Hot and Cold Dark Matter*, *JCAP* **1402** (2014) 046, [arXiv:1310.1774].

[264] B. Coleppa, F. Kling, and S. Su, *Constraining Type II 2HDM in Light of LHC Higgs Searches*, *JHEP* **1401** (2014) 161, [arXiv:1305.0002].

[265] N. Chakrabarty, U. K. Dey, and B. Mukhopadhyaya, *High-scale validity of a two-Higgs doublet scenario: a study including LHC data*, arXiv:1407.2145.

[266] B. Dumont, J. F. Gunion, Y. Jiang, and S. Kraml, *Constraints on and future prospects for Two-Higgs-Doublet Models in light of the LHC Higgs signal*, arXiv:1405.3584.

[267] V. Barger, L. L. Everett, C. B. Jackson, A. D. Peterson, and G. Shaughnessy, *Measuring the 2HDM Scalar Potential at LHC14*, arXiv:1408.2525.

[268] E. Salumbides, W. Ubachs, and V. Korobov, *Bounds on fifth forces at the sub-Angstrom length scale*, arXiv:1308.1711.

[269] G. Coughlan, W. Fischler, E. W. Kolb, S. Raby, and G. G. Ross, *Cosmological Problems for the Polonyi Potential*, *Phys.Lett.* **B131** (1983) 59.

[270] K. Mukaida, K. Nakayama, and M. Takimoto, *Fate of Z_2 Symmetric Scalar Field*, *JHEP* **1312** (2013) 053, [arXiv:1308.4394].

[271] K. Mukaida and K. Nakayama, *Dynamics of oscillating scalar field in thermal environment*, *JCAP* **1301** (2013) 017, [arXiv:1208.3399].

[272] M. Bastero-Gil, A. Berera, and R. O. Ramos, *Dissipation coefficients from scalar and fermion quantum field interactions*, *JCAP* **1109** (2011) 033, [arXiv:1008.1929].

[273] G. Bellini, I. I. Bigi, and P. Dornan, *Lifetimes of charm and beauty hadrons*, *Phys.Rept.* **289** (1997) 1–155.

[274] M. Viel, G. D. Becker, J. S. Bolton, and M. G. Haehnelt, *Warm dark matter as a solution to the small scale crisis: New constraints from high redshift Lyman- forest data*, *Phys.Rev.* **D88** (2013) 043502, [arXiv:1306.2314].

[275] K. Ichiki, M. Oguri, and K. Takahashi, *WMAP constraints on decaying cold dark matter*, *Phys.Rev.Lett.* **93** (2004) 071302, [astro-ph/0403164].

[276] Y. Gong and X. Chen, *Cosmological Constraints on Invisible Decay of Dark Matter*, *Phys.Rev.* **D77** (2008) 103511, [arXiv:0802.2296].

[277] S. De Lope Amigo, W. M.-Y. Cheung, Z. Huang, and S.-P. Ng, *Cosmological Constraints on Decaying Dark Matter*, *JCAP* **0906** (2009) 005, [arXiv:0812.4016].

[278] M.-Y. Wang and A. R. Zentner, *Weak Gravitational Lensing as a Method to Constrain Unstable Dark Matter*, *Phys.Rev.* **D82** (2010) 123507, [arXiv:1011.2774].

[279] A. H. Peter, C. E. Moody, A. J. Benson, and M. Kamionkowski, *Constraints on Decaying Dark Matter*, *PoS* **IDM2010** (2011) 084, [arXiv:1011.4970].

[280] O. E. Bjaelde, S. Das, and A. Moss, *Origin of ΔN_eff as a Result of an Interaction between Dark Radiation and Dark Matter*, *JCAP* **1210** (2012) 017, [arXiv:1205.0553].

[281] S. Aoyama, T. Sekiguchi, K. Ichiki, and N. Sugiyama, *Evolution of perturbations and cosmological constraints in decaying dark matter models with arbitrary decay mass products*, *JCAP* **1407** (2014) 021, [arXiv:1402.2972].

[282] L. Visinelli and P. Gondolo, *Axion cold dark matter in view of BICEP2 results*, *Phys.Rev.Lett.* **113** (2014) 011802, [arXiv:1403.4594].

[283] L. D. Duffy and K. van Bibber, *Axions as Dark Matter Particles*, *New J.Phys.* **11** (2009) 105008, [arXiv:0904.3346].

[284] P. Sikivie, *Axion theory*, .

[285] P. Sikivie, *Axion Cosmology*, *Lect.Notes Phys.* **741** (2008) 19–50, [astro-ph/0610440].

[286] A. Vilenkin and A. Everett, *Cosmic Strings and Domain Walls in Models with Goldstone and PseudoGoldstone Bosons*, *Phys.Rev.Lett.* **48** (1982) 1867–1870.

[287] P. Sikivie, *Of Axions, Domain Walls and the Early Universe*, *Phys.Rev.Lett.* **48** (1982) 1156–1159.

[288] D. Buttazzo, G. Degrassi, P. P. Giardino, G. F. Giudice, F. Sala, et al., *Investigating the near-criticality of the Higgs boson*, *JHEP* **1312** (2013) 089, [arXiv:1307.3536].

[289] M. E. Machacek and M. T. Vaughn, *Two Loop Renormalization Group Equations in a General Quantum Field Theory. 1. Wave Function Renormalization*, *Nucl.Phys.* **B222** (1983) 83.

[290] M. E. Machacek and M. T. Vaughn, *Two Loop Renormalization Group Equations in a General Quantum Field Theory. 2. Yukawa Couplings*, *Nucl.Phys.* **B236** (1984) 221.

[291] M. E. Machacek and M. T. Vaughn, *Two Loop Renormalization Group Equations in a General Quantum Field Theory. 3. Scalar Quartic Couplings*, *Nucl.Phys.* **B249** (1985) 70.